Thesis defended by

Malik Atik

For the degree of doctorate

University of Lille 1- Science and Technology

Discipline:

Civil Engineering

SEISMIC EVALUATION OF TALL BUILDING STRUCTURES USING NONLINEAR STATIC PROCEDURES

---

10 December 2013

Jury:

M.	Marwan	Alheib	Prof., INERIS, Ecole des Mines de Nancy
M.	Yasin	Fahjan	Prof., Gebze Institute of Technology, Turkey
M.	Mohammed	Hjiaj	Prof. INSA de Rennes
M.	Mhamed	Souli	Prof., Université Lille1 - sciences et technologies
M.	Isam	Shahrour	Prof., Université Lille1 - sciences et technologies
M.	Marwan	Sadek	Ass. Prof., Université Lille1-sciences et technologies

Remerciements

Merci Dieu, Tu nous as donné l'ouïe, les yeux et les cœurs.

Merci maman, sans tes invocations je ne pourrais rien faire.

Je tiens à remercier mon père qui m'a appris comment penser d'une manière libre et avoir une vision critique malgré leur absence dans mon entourage, là où j'ai grandi.

Je remercie ma femme qui était toujours là pendant trois ans pour moi mais aussi auprès de nos enfants pour leur éducation, Mohammed et Ibraham. Avec tous ses efforts j'estime qu'elle mérite mon diplôme de doctorat bien plus que moi.

A vous tous, surtout en France et en Syrie, merci.

Dieu exalté dit :

Ô hommes! Nous vous avons créés d'un mâle et d'une femelle, et Nous avons fait de vous des nations et des tribus, pour que vous vous entre-connaissiez. Le plus noble d'entre vous, auprès d'Allah, est le plus pieux. (49:13)

شكراً لله الذي جعل لنا السمع و الأبصار و الأفئدة .
شكراً أمي لولا دعاؤك ما استطعت إنجاز أي عمل.
أشكر أبي الذي علمني كيفة التفكير بحرية بالرغم من غيابها في ثقافة المجتمع الذي نشأت فيه.
أشكر زوجتي التي شاركتني هذا العمل طوال ثلاث سنوات ولو منحت شهادة الدكتوراة حسب الجهد لاستحقتها أكثر مني.
أشكر أهلي أهل زوجتي الذين كانوا لنا كل سند.
أشكركم جميعاً خصوصا من التقيت في فرنسا ومع من عشت في سوريا.
قال الله تعالى:
يَا أَيُّهَا النَّاسُ إِنَّا خَلَقْنَاكُمْ مِنْ ذَكَرٍ وَأُنْثَىٰ وَجَعَلْنَاكُمْ شُعُوبًا وَقَبَائِلَ لِتَعَارَفُوا ۚ إِنَّ أَكْرَمَكُمْ عِنْدَ اللَّهِ أَتْقَاكُمْ ۚ إِنَّ اللَّهَ عَلِيمٌ خَبِيرٌ.
(الحجرات 13)

Remerciements

Je remercie vivement le professeur Isam Shahrour de m'avoir guidé, conseillé et soutenu tout au long de la thèse. Je le remercie car il m'a apprit comment être non seulement un ingénieur mais aussi un chercheur.

Je remercie également monsieur Marwan Sadek pour ses nombreux conseils et son grand soutien. Grâce à lui j'ai réalisé cette thèse, je lui en suis très reconnaissant.

Je tiens à remercier les professeurs Marwan Alheib et Yasin Fahjan pour avoir accepté d'être les rapporteurs de mon mémoire de thèse. Je remercie vivement les professeurs Mohammed Hjiaj et Mhamed Souli pour avoir accepté d'être membre du jury de ma thèse.

Je remercie aussi l'ensemble des membres du LGCgE, doctorants, chercheurs et personnels administratifs et tout particulièrement mes collègues de bureau, Ramzi Messahel et Mohammed Amdi pour leurs soutiens scientifique et moral.

Abstract

Non linear dynamic analysis constitutes the most powerful method for the assessment of the non linear seismic response of structures subjected to strong earthquake motions. Considering the complexity associated to time history analysis, the use of nonlinear static techniques, or pushover analysis constitutes an efficient and easy to use alternative to dynamic analysis. The conventional pushover procedures implemented in the international codes assumes that the seismic response is mainly controlled by the fundamental mode which is not suitable for tall buildings that have significant responses in higher modes. This thesis develops innovative static nonlinear method to assess the seismic behavior of high-rise buildings. It is composed of three parts:

In the first part, the continuum model which constitutes a simple and efficient tool to analyze high-rise wall-frame buildings is revisited. The influence of calculation precision in specifying the optimum level of wall curtailment is discussed. The relationship between the curtailment level and the resulting internal forces is investigated. The linear analysis discussed in this chapter constituted a strong base for the use of nonlinear static procedures.

The second part proposes a new single-run adaptive pushover method for the seismic assessment of shear wall structures. This method has two main advantages: It is practical tool to integrate the effect of higher modes with full interaction between them and it overcomes the criticisms forwarded against the previous single-run adaptive pushover analyses. The proposed method is presented as well as its numerical implementation. The predictions of this method are compared to those of other recent adaptive pushover methods and to the rigorous non-linear time history analysis. Analyses show the efficiency of the proposed method.

The third part presents an innovative method to specifying the seismic peak response quantities of the tall structures. The principle of the single-run adaptive pushover procedures is integrated with the capacity spectrum method proposed by ATC-40 (1996). Where, this latter is limited for structures that vibrate primarily in the fundamental mode. The rigorous analytical base of the proposed method can be considered as a consequence of avoiding the pitfall inherent to single-run adaptive pushover procedures available in the literature.

Keywords: Wall-Frame Structures, continuum model, Adaptive pushover analysis, Non-linear analysis, Seismic analysis, Higher modes, Plastic hinges, Capacity spectrum, Performance point.

Résumé

L'Analyse dynamique non linéaire constitue la méthode la plus efficace pour l'évaluation de la réponse non linéaire des structures soumises à de fortes sollicitations sismiques. Compte tenu de la complexité associée à l'analyse non linéaire temporelle, l'utilisation de l'analyse statique équivalente ou analyse en poussée progressive «Push-over » constitue une alternative simple et efficace à l'analyse dynamique temporelle. Les procédures conventionnelles de l'analyse Push-over disponibles dans les règlements internationaux supposent que la réponse sismique est principalement contrôlée par le mode fondamental. Cette hypothèse n'est pas pertinente dans le cas des immeubles de grande hauteur où les modes supérieurs jouent un rôle significatif. Cette thèse développe une méthode statique non linéaire innovante pour évaluer le comportement sismique des immeubles de grande hauteur. Elle est composée de trois parties:

Dans la première partie, le modèle "continuum" qui est un outil simple et efficace de l'analyse des immeubles de grande hauteur à contreventement mixte (voile-portique) est revisité. L'influence de la précision de calcul dans la détermination de la hauteur optimale d'interruption des voiles est examinée tout en analysant la relation entre la hauteur optimale et les sollicitations induites. L'analyse linéaire abordée dans ce chapitre est une étape primordiale qui doit précéder toute analyse non linéaire.

La deuxième partie propose une nouvelle procédure Push-over adaptative à exécution unique "single-run" pour l'évaluation sismique des structures à contreventement par voiles. Cette méthode possède deux avantages principaux : elle représente un outil pratique intégrant l'effet des modes supérieurs avec une interaction complète entre eux. D'un autre côté, elle permet d'éviter les critiques relatives aux analyses adaptatives à exécution unique "single-run".

La troisième partie présente une méthode innovante permettant la détermination du point de fonctionnement des immeubles de grande hauteur. Le principe des méthodes adaptatives Push-over à exécution unique est intégré à la méthode du spectre de capacité proposé par le règlement ATC -40 dont l'application est limitée aux structures oscillant au mode fondamental. Cette approche rigoureuse et efficace permet d'éviter les incohérences relatives aux analyses Push-over adaptatives disponibles dans la littérature.

Mots clés : Structures mixte voile-portique, modèle continuum, Analyses Push-over adaptatives, Analyse non linéaire, Analyse sismique, Modes supérieurs, Rotules plastiques, Spectre de capacité, Point de fonctionnement.

Table of contents

Table of contents

List of figures

List of figures

List of tables

Chapter 1: General introduction

1.1 Seismic design challenges

The seismic design of structures concerns large areas in the world with an increasing demand for the development of reliable design methods for the assessment of the seismic response of structures. Especially after recent major earthquakes (e.g. Loma prieta 1989, Northridge 1994, Kobe 1995, Kocaeli 1999, Haiti 2012), the necessity for using ever more accurate methods, which explicitly account for geometrical nonlinearities and material inelasticity, for evaluating seismic demand on structures, became evident. These requirements should be considered in both the new building design and the evaluation of the existing buildings.

Generally, the design codes propose simplified methods which are not time consuming and could be simply integrated to engineering design practice. These equivalent static methods are well adapted for specific type of structures. An important research effort has been carried out for the generalization of these methods in order to overcome their limitations maintaining the simple implementation. The non linear analysis of high rise buildings is considered as one of the most important issue in seismic design since it concerns a complex multi-degree of freedom system where the higher modes could play a significant role. Recently, an important development of tall buildings is observed for both their high-density accommodation and their important role in urban sustainability (Gonçalzves, 2010).

1.2 Reinforced concrete tall building structures

"Tall" is a relative term: in New York City, 30 stories are rather average, while in Paris, they may be considered tall. From the structural engineer's point of view, the most common types of reinforced concrete tall building structures could be classified upon their bracing systems (Stafford Smith and Coull 1991):

- *Rigid-frame structures*
- *Shear wall structures*
- *Wall-Frame Structures*

The Rigid-frame structures consist of columns and beams jointed by moment-resistant connections. Rigid framing is economic only for building up to about 25 stories. Above 25 stories, the relatively high lateral flexibility of the frame calls for uneconomically large members in order to control the drift.

The shear wall structures consist of vertical walls that carry both gravity and lateral loading. Their high in-plane stiffness makes them ideally suited for bracing tall building. Because they are much stiffer horizontally than rigid frames, they could be economical up to about 35 stories. On the other hand, shear walls are easy to construct so they are a popular choice in many earthquake countries even for low-rise buildings (4 stories).

Wall-Frame structures consist of a combination of shear walls and rigid frames. The walls tend to deflect in a flexural configuration, while the frames tend to deflect in a shear mode as depicted in Fig. 1-1. Consequently, they are constrained to adopt a common deflected shape by the horizontal rigidity of the beams and slabs. As a consequence, the walls and the frames interact horizontally to produce a stiffer structure. The interacting wall-frame combination is appropriate for buildings in the 40- to60-story range, well beyond that of rigid frames and shear walls alone. The lower part of the structure deflects in a flexural configuration, i.e., concavity downwind, and the upper part in a shear configuration, i.e., concavity upwind, with a point of inflection at the transition (Fig. 1-1). Consequently, the upper part of the shear wall could play a negative role and may lead to unreasonable design by introducing additional internal forces to the system (Paulay and Priestley 1992; Stafford Smith and Coull 1991). Nollet and Stafford Smith (1993) developed a continuum model to analyze the effect of the wall curtailment on the performance of the structure. In this model, the wall is represented by a flexural column, the frame by a shear column, and the connecting links by distributed horizontally rigid connecting beams. They showed that curtailment of the walls is not necessarily detrimental to the performance of the structure. The deflection at the top of the structure is minimized to provide guidance for the optimum level of wall curtailment. But they did not discuss the relationship between the optimum level of curtailment and the resulting internal forces. Also note that they utilized a linear model in their investigation.

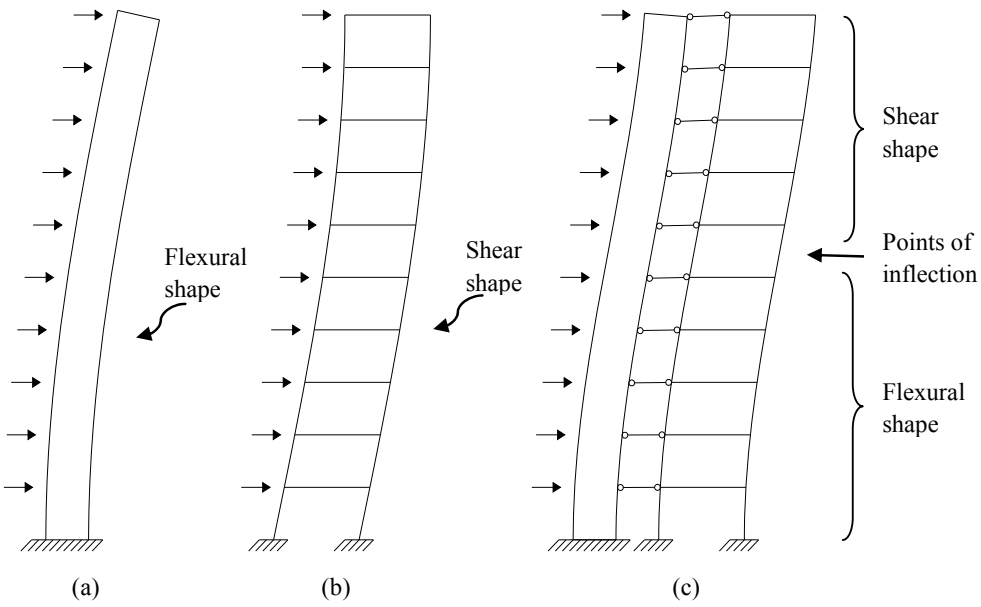

Fig. 1-1 Deflected Configurations of: (a) Shear Wall; (b) Rigid Frame; and (c) Wall-Frame

1.3 Seismic Analysis Methods

Various analysis methods, based on both elastic (linear) and inelastic (nonlinear) approaches, have been developed for the seismic analysis of buildings (e. g., Eurocode 8; ATC-40; FEMA-273; ASCE-41).

1.3.1 *Linear methods*

The use of the linear approach in buildings design includes mainly the following methods:

- *Lateral force method of analysis*
- *Modal response spectrum analysis*
- *Linear Time History Method*

The lateral force method is used for buildings where the response is not significantly affected by the contribution of high vibration modes in each principal direction. In addition, the building should satisfy the Criteria for regularity in elevation.

The modal response spectrum analysis is used for buildings that do not respect the conditions of the “lateral force method”. The response of vibration modes affecting significantly to the global response should be taken into account. Peak member forces,

floor displacements, story forces, story shears, and base reactions for each mode of response should be combined by either the SRSS (square root sum of squares) rule or the CQC (complete quadratic combination) rule.

The "Linear Time History Method" consists in determination of the building seismic response at discrete time steps using discretized recorded or synthetic time histories as base motion. Although this method gives more accurate results than the response spectrum analysis, it produces a large amount of output information that can require a significant amount of computational effort to conduct required design checks. However, this method could be limited by the availability of time record for a specific site. Where these records are unavailable, artificial ground motions need to be generated for the analysis which is not always a very simple task.

1.3.2 *Non-linear methods*

The use of the non linear approach in buildings design includes mainly the following methods:

- *Non-linear time-history analysis*
- *Non-linear static (pushover) analysis*

The non-linear dynamic analysis is based on a mathematical model incorporating the nonlinear load deformation characteristics of individual elements as part of a time domain analysis. This approach is rigorous, but time consuming. and need the seismic ground motion records which are not always available especially in developing countries.

The pushover analysis is a non-linear static analysis carried out by monotonically increasing the horizontal loads. It may be applied to verify the structural performance of newly designed or existing buildings where it can estimate expected plastic mechanisms and the distribution of damage. The method is adapted in international codes for structures that vibrate primarily in the fundamental mode.

Fig. 1-2 summarizes the advantages and inconveniences of each method. The nonlinear static procedures or pushover analyses constitute a reliable alternative of nonlinear time-history analysis of structures. But for tall buildings, the effect of high modes is not negligible, that's why ignoring their effect is one of the main limitations

of the pushover analysis. Furthermore, the modes of vibration of the structure can significantly change during strong seismic motion.

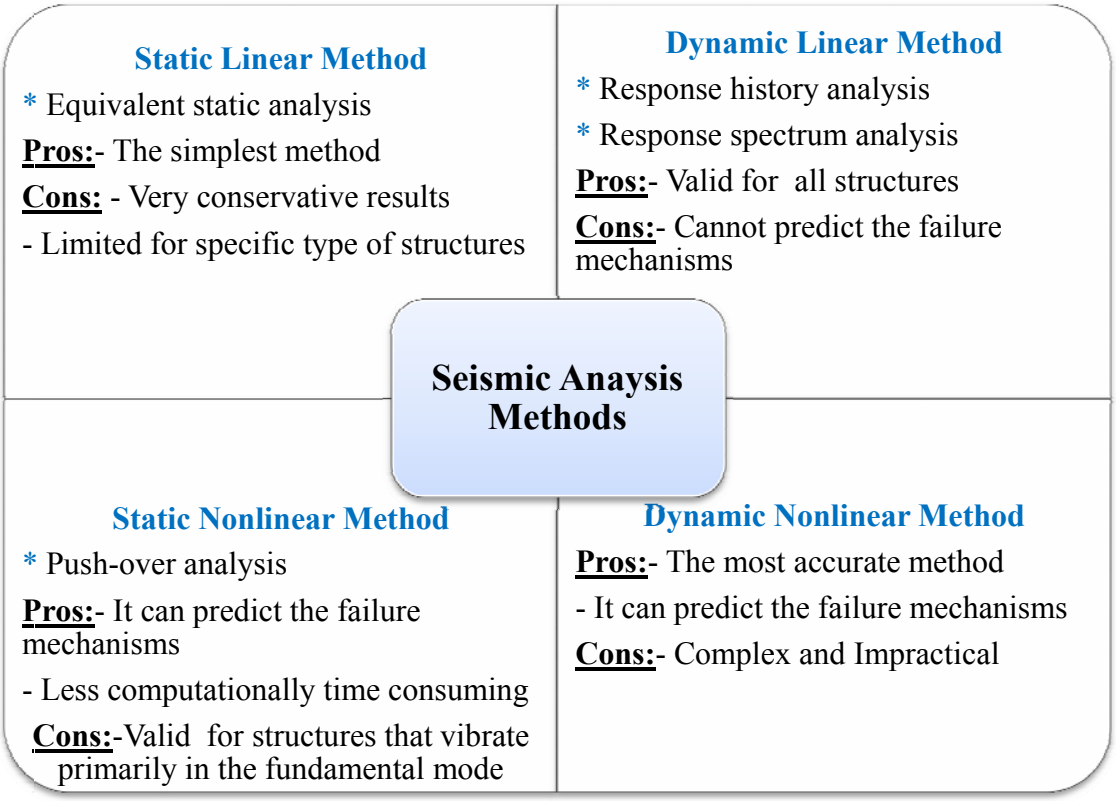

Fig. 1-2 Advantages and limitations of the seismic analysis methods

In recent years, several techniques have been proposed to integrate the effect of higher modes in pushover analyses and to incorporate the variation in their dynamic properties associated to structural damages. Three basic approaches could be distinguished:

a) The adaptive Modal Combination Procedure (AMC) (Kalkan and Kunnath, 2006)
b) The adaptive Response Spectrum Analyses (Gupta and Kunnath 2000; Aydinoğlu 2003, 2004,2007)
c) The single-run adaptive pushover procedures (Elnashai 2001; Antoniou and Pinho 2004a, 2004b; Casarotti and Pinho 2007; Shakeri et al 2010).

The Adaptive Modal Combination Procedure (AMC) (Kalkan and Kunnath, 2006) procedure accounts for higher mode effects by combining the response of individual modal pushover analyses and incorporates the effects of varying dynamic characteristics

during the inelastic response via its adaptive feature. The applied lateral forces used in the progressive pushover analysis are based on instantaneous inertia force distributions across the height of the building for each mode. But these multi-run methods do not reflect the yielding effect of one mode on other modes and on the interaction between modes in the nonlinear range.

In *the Adaptive Response Spectrum Analyses* (Gupta and Kunnath 2000; Aydinoğlu 2003, 2004, 2007) the load is updated at each increment. Eigenvalue analysis is conducted, then a static analysis is carried out for each mode. The calculated effects are combined with SRSS and added to the corresponding values from the previous step. This method takes into account the interaction between the different modes at the end of each step, but it is considered impractical for the following reasons:

- A routine application has to be made in order to impose the stiffness of the structure at the beginning of each step because of the absence of a structural equilibrium at the end of each step as the result of using SRSS to combine the responses (Antoniou and Pinho 2004a; Chopra and Goel 2002; Baros and Anagnastopoulos 2008).
- Small step should be chosen to avoid overshooting of element yield forces, where the interaction between the modes occurs at the end of each step (Gupta and Kunnath 2000; Aydinoğlu 2003).

The single-run adaptive pushover procedures (Elnashai 2001; Antoniou and Pinho 2004a, 2004b; Casarotti and Pinho 2007; Shakeri et al 2010) consist in the application of equivalent seismic loads, where one of the modal components is chosen to be combined by one of the modal combination rules and used as a base to the equivalent seismic loads. Although this method is practical with full interaction between the modes, it presents two main critical points:

- It is a pitfall to use the modal combination in defining the applied loads instead of combining the response quantities induced by those loads in individual modes (Chopra 2007, Aydinoğlu 2003, 2007).
- It is not possible to specify the performance point because of the absence of the pushover curve for each mode.

Other remarks can be oriented to these methods:

- There is no possibility to assign different damping ratios to different modes.

- All the previous methods were mainly applied to estimate the seismic performance of frame structures; that's why it is an important task to investigate their efficiency in the case of shear wall structures.

1.4 Thesis objectives and developments

Analyses presented in the previous sections reveal two major issues. The first one is related to the method of the analysis "Improving the single-run adaptive pushover procedures in order to overcome their actual limitations", while the second issue is related with the type of structures "The effect of the wall curtailment on the performance of tall buildings in nonlinear domain"

In the design of tall building structures, a preliminary analysis should be carried out in order to define the bracing system. When we revisited the linear model proposed by Nollet and Stafford Smith (1993) concerning the effect of the wall curtailment on the performance of the structure, some results of their study showed that, in spite of existing negative moments and shear forces in the shear wall, there is no need to curtail the wall. This result seems inconsistent from the physicial point of view and requires a thorough review of analyses, that's why ***the second chapter*** is devoted to an overview of the continuum model and the principle of determination of the optimum level. Analyses showed the influence of calculation precision on the determination of the optimum level of wall curtailment by utilizing the continuum model. The recommendations proposed for the practical use of continuum model is very important because of its wide use in the literature. Indeed, both static and dynamic applications are available (Bozdogan and Ozturk 2012, Bozdogan 2011, Miranda and Akkar 2006, Miranda and Taghavi 2005, Miranda and Reyes 2002, Miranda 1999,..). Problems of interaction soil-structure can also be incoporated (Houssam and Toutanji 1997). The second part of this chapter investigates the relationship between the curtailment level and the resulting internal forces. Finally, curves for optimum level of wall curtailment are given. These curves are very useful in the preliminary stages of the design of tall buildings subject to lateral loading.

The linear analysis discussed in the first chapter constituted a strong base for the use of nonlinear static procedures. Results showed a relationship between the type of structures and the base utilized in single-run adaptive pushover procedures.

Because of the previous mentioned pitfall related to the single-run adaptive pushover methods, it can be noted the absence of any application of these methods for shear wall structures. So in ***the third chapter***, a new single-run adaptive pushover method for the seismic assessment of shear wall structures is proposed. It is based on the modal overturning moment story. This method offers two main advantages: it does not require decomposing the structure in nonlinear domain and it avoids the pitfall of previous single-run adaptive pushover analyses in utilizing the modal combination in the determination of the applied loads instead of combining the response quantities induced by those loads in individual modes. The comparison between the non-adaptive form and the adaptive form of the proposed method emphasizes the importance of the adaptive feature to incorporate the progressive variation in dynamic and modal properties. The proposed procedure is implemented in a Visual Fortran program. The subroutines are linked to the SAP2000 computer program which is considered as common tool in structural engineering practice.

The fourth chapter proposes an innovative method to specifying the peak response quantities using the single-run adaptive pushover procedures. Where, although a single-run adaptive pushover analysis is performed, the modal quantities are picked out at each increment. As a result, using an equivalent single degree of freedom system for estimating the peak response quantities becomes available. At the same time, the proposed method developed a new technique to convert the capacity curve to a capacity spectrum. This technique does not only have conceptual superiority over the conventional formulation but it also has easier numerical implementation. The results of the proposed method have been compared to the non linear time history analysis. They indicate that this method predict the results of the nonlinear time history analysis appropriately.

1.5 References

Antoniou, S., Pinho, R. (2004a). Advantages and limitations of adaptive and non adaptive force-based pushover Procedures. Journal of Earthquake Engineering, Vol. 8, No 4, pp. 497-522.

Antoniou, S., Pinho, R. (2004b). Development and verification of a displacement-based adaptive pushover Procedure. Journal of Earthquake Engineering, Vol. 8, No. 5, pp. 643-661.

ASCE/SEI Standard 41-06. Seismic Rehabilitation of Existing Buildings. prepublication edition. Structural Engineering Institute, American Society of Civil Engineers; 2006.

ATC. Seismic evaluation and retrofit of concrete buildings. Report ATC-40. Redwood City (CA): Applied Technology Council; 1996.

Aydinoğlu, M. N. (2003). An incremental response spectrum analysis procedure based on inelastic spectral displacements for multi-mode seismic performance evaluation. Bull Earthquake Eng, 1:3_36.

Aydinoğlu, M. N. (2004). An improved pushover procedure for engineering practice: Incremental response spectrum analysis procedure (IRSA). In: International workshop on performance-based seismic design: concept and implementation. Bled, Slovenia. PEER Report 2004/05, pp. 345-356.

Aydinoğlu, M. N. (2007). A response spectrum-based nonlinear assessment tool for practice: incremental response spectrum analysis (IRSA). ISET Journal of Earthquake Technology, Paper No. 481, Vol. 44, No. 1, pp. 169–192.

Bozdogan, K. B. (2011). "Free Vibration Analysis of Wall-Frame Structures By Differential Quadrature Method." *International Journal of Engineering and Applied Sciences* (IJEAS), 3(4), 7-20

Bozdogan, K. B., and Ozturk, D. (2012). "Vibration Analysis of Asymmetric Shear Wall- Frame Structures Using The Transfer Matrix Method." *IJST, Transactions of Civil Engineering*, 36(C1), 1-12

Building Seismic Safety Council (BSSC), NEHRP guidelines for the seismic rehabilitation of buildings, FEMA-273, developed by ATC for FEMA, Washington, D.C., 1997.

Casarotti, C., Pinho, R. (2007). An adaptive capacity spectrum method for assessment of bridges subjected to earthquake action. Bull Earthquake Eng, 5, pp. 377–390.

CEN. Eurocode 8: design of structures for earthquake resistance. Part 1: general rules seismic actions and rules for buildings. EN 1998-1, CEN, Brussels, December 2004.

Chopra A.K. (2007). Dynamics of Structures, third edition, Prentice Hall, New Jersey.

Chopra, A. K., and Goel, R. K. (2002). A modal pushover analysis procedure for estimating seismic demands for buildings. Earthquake Eng. Struct. Dyn., 31(3), pp. 561-582.

Elnashai, A. S. (2001). Advanced inelastic static (pushover) analysis for earthquake applications. Structural Engineering and Mechanics 12(1), pp. 51-69.

Gupta, B., and Kunnath, S. K. (2000). Adaptive spectra-based pushover procedure for seismic evaluation of structures. Earthquake Spectra, 16(2), pp. 367-391.

Joana Carla Soares Gonçalves J. C. S. (2010). The Environmental Performance of Tall Buildings, Taylor & Francis.

Kalkan, E. and Kunnath, SK. (2006). Adaptive modal combination procedure for nonlinear static analysis of building structures. J Struct Eng ASCE, 132(11), pp. 1721-1731.

Miranda, E. (1999). "Approximate Seismic Lateral Deformation Demands in Multistory Buildings". ASCE Journal of Structural Division, Vol. 125, No. 4, pp. 417-425.

Miranda, E., and Akkar,S. (2006). "Generalized Interstory Drift Spectrum." *Journal of Structural Engineering*, ASCE, 132 (6), 840-852.

Miranda, E., and Reyes, J. C. (2002). "Approximate lateral drift demands in multistory buildings with nonuniform stiffness." *J. Struct. Div.*, ASCE, 128(7), 840-849.

Miranda, E., and Taghavi, S. (2005). "Approximate floor acceleration demands in multistory buildings I formulation." *J. Struct. Div.*, ASCE, 131(2), 203-211.

Nollet, M. J., and Stafford Smith, B. (1993). "Behavior of Curtailed Wall-Frame Structures." *Journal of Structural Engineering*, ASCE, 119(10), 2835-2854.

Paulay, T., and Priestley, M. J. N. (1992). *Seismic Design of Reinforced Concrete and Masonry Buildings*, Chapter: 6 Dual Systems, JOHN WILEY& SONS, INC. New York.

Shakeri, K., Shayanfar, MA. and Kabeyasawa, T. (2010). A storey shear-based adaptive pushover for estimating seismic demands of buildings. Eng Struct,32, pp. 174–83.

Stafford Smith, B., and Coull, A. (1991). *Tall Building Structure: Analysis and Design*, JOHN WILEY& SONS, INC. New York.

Chapter 2: Optimum level of shear wall curtailment in Wall-Frame buildings: the continuum model revisited

The main content of this chapter was published in the Journal of Structral Engineering: Atik, M., Badawi, M., Shahrour, I., and Sadek, M. (2013). "Optimum Level of Shear Wall Curtailment in Wall-Frame Buildings: The Continuum Model Revisited." J. Struct. Eng. , 10.1061/(ASCE)ST.1943-541X.0000901 , 06013005.

2.1 Abstract

The continuum model constitutes a simple and efficient tool to analyze high-rise wall frame buildings. It has been commonly used in last decades to analyze the behaviour of these structures. The related equations are revisited in order to study the effect of the calculation precision on the determination of the optimum level of wall curtailment. The results obtained illustrate the influence of calculation precision in specifying the optimum level of wall curtailment. The relationship between the curtailment level and the resulting internal forces is investigated. The level of curtailment which results in the minimum top deflection of the structure eliminates at the same time the negative moments and negative shear forces in the wall.

Keywords: Wall-Frame, continuum model, Optimum level, wall curtailment, minimum top deflection, internal forces, calculation precision

2.2 Introduction

Wall-Frame Structures are widely used to resist lateral loads in tall buildings up to 60 storeys (Stafford Smith and Coull 1991). Under lateral load, the shear wall deflects essentially in flexural shape and the frame deflects in shear shape. That's why these components are forced to interact horizontally through the floor slabs as illustrated in Fig. 1-1. Consequently, the upper part of the shear wall could play a negative role and may lead to unreasonable design by introducing additional internal forces to the system (Paulay and Priestley 1992, Atik 2010).

Optimum level of shear wall curtailment

A solution for such a uniform wall-frame structure has been developed using an equivalent continuous medium or "continuum model" (Heidebrecht and Stafford Smith 1973). This simple model is very useful in the preliminary stages of the design of tall building structures subject to lateral loading. It has been widely used in the literature for both static and dynamic application of shear wall-frame structures (Bozdogan and Ozturk 2012, Bozdogan 2011, Miranda and Akkar 2006, Miranda and Taghavi 2005, Miranda and Reyes 2002, Miranda 1999..).

A generalized theory for tall building structures, allowing for axial deformation of the columns was firstly proposed by Stafford Smith et al. (1984). Then Nollet and Stafford Smith (1993) developed a generalized theory for the deflection of wall frame buildings on the basis of continuum model. Their model has been used to analyze the effect of the wall curtailment on the performance of the structure. The deflection at the top of the structure is minimized to provide guidance for the optimum level of wall curtailment. They found that the optimum level is generally situated between the points of inflection and zero shear in the corresponding full-height wall structure. On the other hand, some results of their study showed that in spite of existing negative moments and shear forces in the shear wall, there is no need to curtail the wall. Such a result seems inconsistent and requires a thorough review of calculation which is carried out in the present chapter.

This chapter is organized in three parts: The first part gives an overview of the continuum model and the principle of determination of optimum level. The second part presents a thorough analysis of the continuum model proposed by Nollet and Stafford Smith (1993). It emphasizes the importance of calculation precision on the corresponding optimum level of wall curtailment. The last part discusses the effect of curtailment height on the resulting internal forces. The results of two case studies are presented: the first one illustrates the relationship between the optimum level and the induced internal forces in the structure. The second shows the influence of calculation precision in specifying the optimum level of curtailment.

2.3 Curtailed wall-frame structure - Reviewing the continuum model

The plan-symmetric wall frame structures subjected to symmetric loading do not twist and therefore can be represented by a planar model. Indeed, the high in-plane stiffness of the floor slabs causes the lateral deflection of the walls and frames to be effectively identical. For such structures with uniform properties over the height, an equivalent continuous medium, or "continuum model" can be used. In this model, the wall is represented by a flexural column, the frame by a shear column, and the connecting links by distributed horizontally rigid connecting beams.

2.3.1 *Top deflection*

Using the continuum model and considering the axial deformation in the columns, Nollet and Stafford Smith (1993) developed a generalized theory for the deflection of curtailed wall frame structure as follows:

A curtailed wall-frame structure of total height H, subjected to a uniformly distributed horizontal load w (see Fig. 2-1a), is considered as a superposition of two substructures (Fig. 2-1b):

- The lower part (substructure 1), is a wall-frame structure of height H_1 subjected to an external uniformly distributed lateral load (w) superposed to a top concentrated shear force S_1 and a top moment M_1. S_1 and M_1 denote the accumulated shear and the moment from the upper part acting on the lower one respectively;

- The upper part (substructure 2), is a moment-resisting frame of height H_2, subjected only to the external uniformly distributed load (w).

Optimum level of shear wall curtailment

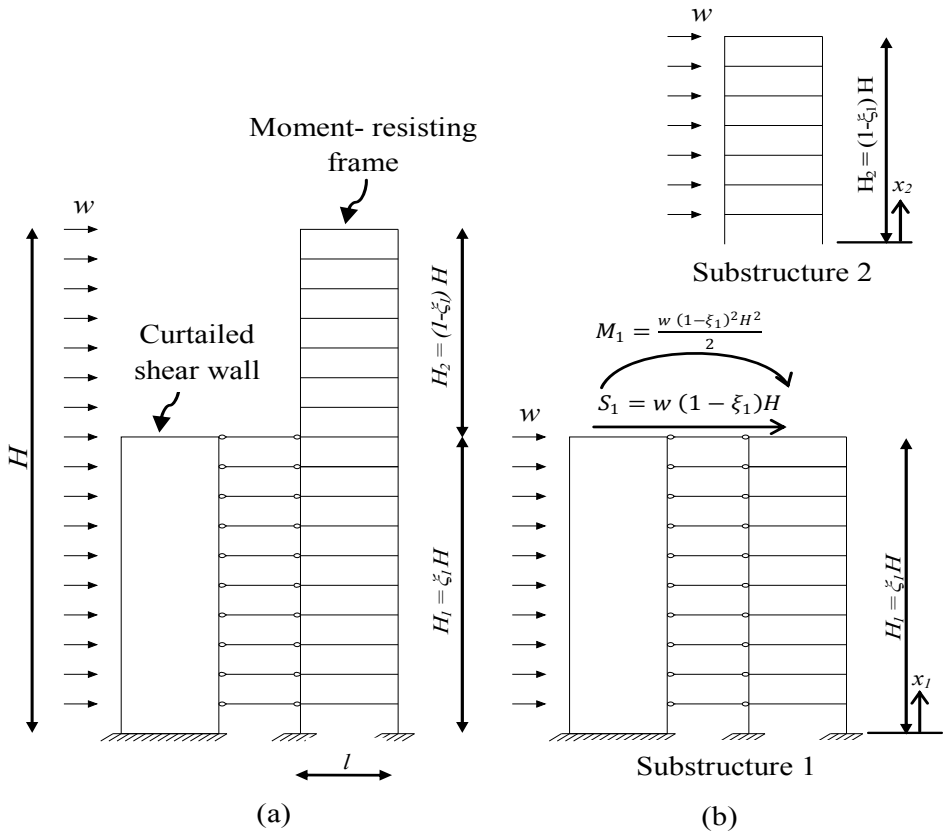

Fig. 2-1 Continuum model: (a) Curtailed Wall-Frame Structure; (b) Substructures of Curtailed Wall-Frame Structure (Nollet and Stafford Smith 1993)

Considering zero displacement/rotation boundary condition at the base, the top deflection of substructure 1 can be expressed by:

$$y_1(H_1) = \frac{wH^4}{EI}\frac{(k^2-1)}{k^2}\left[\frac{\xi_1^2}{4} - \frac{\xi_1^3}{6} + \frac{\xi_1^4}{24} - \frac{(1-\xi_1)^2}{2}\frac{(\cosh \xi_1 k\alpha H - 1)}{(k\alpha H)^2 \cosh \xi_1 k\alpha H}\right]$$

$$+\frac{wH^4}{EI}\frac{1}{k^2}\left[\frac{(2\xi_1-\xi_1^2)}{2(k\alpha H)^2} - \frac{\tanh \xi_1 k\alpha H}{(K\alpha H)^3} + \frac{(\cosh \xi_1 k\alpha H - 1)}{(k\alpha H)^4 \cosh \xi_1 k\alpha H}\right] \quad (1)$$

Where:

$\xi_1 = \frac{H1}{H}$; $\alpha H = \sqrt{\frac{(GA)}{EI}}$ H ; (GA) is the total racking shear rigidity of the set of frames. For a single uniform frame n° "i", this rigidity is given by (Stafford Smith et al. 1981):

$$(GA)_i = \frac{12E}{h\left(\frac{1}{\Sigma\frac{I_c}{h}} + \frac{1}{\Sigma\frac{I_b}{l}}\right)_i} \quad (2)$$

Where E is the modulus of elasticity; h is the storey height; $\sum I_c$ represents the sum of the columns inertias in a storey of the frame "i", I_b is the inertia of a beam and l its span, $\sum \frac{I_b}{l}$ being summed for all the beams in a single floor of the frame "i".

$$EI = E\sum I_c + E\sum I_w \tag{3}$$

In which $\sum I_w$ denotes the sum of the inertias of walls.

$$k^2 = \frac{EI + E\sum Ac^2}{E\sum Ac^2} \tag{4}$$

In which $\sum Ac^2$ is the second moment of area of the column sectional areas about their common center of area.

The drift over the height of substructure 2 is given by:

$$y_2(H_2) = \frac{wH^4}{EI}\left[\frac{(1-\xi_1)^2}{2(\alpha H)^2} + (k^2-1)\frac{(1-\xi_1)^4}{8}\right] + \emptyset_{H_1}(1-\xi_1)H \tag{5}$$

Where:

$$\emptyset_{H_1} = \frac{wH^3}{EI}\frac{(k^2-1)}{6}\left(3\xi_1 - 3{\xi_1}^2 + {\xi_1}^3\right) - (k^2-1)y'(H_1) \tag{6}$$

and

$$y_1'(H_1) = \frac{wH^3}{EI}\frac{(K^2-1)}{K^2}\left[\frac{\xi_1}{2} - \frac{\xi_1^2}{2} + \frac{\xi_1^3}{6} - \frac{(1-\xi_1)^2}{2}\frac{\tanh \xi_1 k\alpha H}{(k\alpha H)}\right] + \frac{WH^3}{EI}\frac{1}{K^2}\left[\frac{(1-\xi_1)}{(k\alpha H)^2} - \frac{1}{(k\alpha H)^2 \cosh \xi_1 k\alpha H} + \frac{\tanh \xi_1 k\alpha H}{(k\alpha H)^3}\right] \tag{7}$$

Where $\emptyset_{H_1}$ represents the slope at the top of substructure 1 resulting from the axial deformation of the columns. Note that the slope of the frame at any level (equal to that of the wall) is the sum of two components: the first one is due to racking at the corresponding level, while the second is due to axial deformation of the columns accumulating from the base (Fig. 2-2).

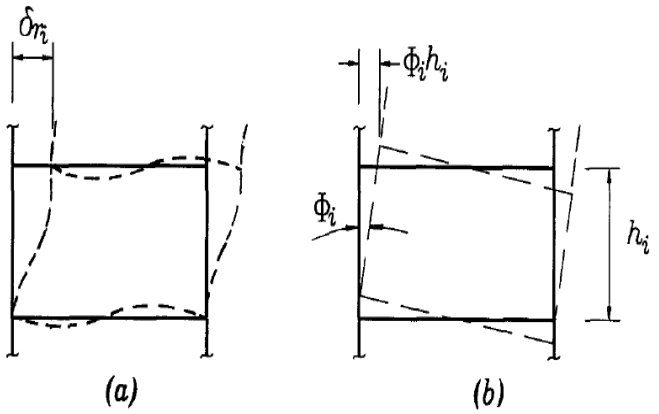

Fig. 2-2 Components of Drift: (a) Storey Drift of Frame due to Racking; (b) Storey Drift of the Frame due to Axial Deformation of the Columns

Finally, the lateral deflection at the top of the curtailed structure is (the equations contained in Nollet and Stafford Smith (1993) have been utilized after some typographical corrections in the equations: 20, 23, 30 and 36, see appendix I):

$$y(H) = y_1(H_1) + y_2(H_2) \tag{8}$$

$$y(H) = \frac{wH^4}{EI}\frac{{\xi_1}^4}{k^2}\left[\frac{k^2-1}{8} + \frac{1}{2(\xi_1 k\alpha H)^2} + \frac{(\cosh \xi_1 k\alpha H - 1)}{(\xi_1 k\alpha H)^4 \cosh \xi_1 k\alpha H} - \frac{\tanh \xi_1 k\alpha H}{(\xi_1 k\alpha H)^3}\right]$$

$$+\frac{wH^4}{EI}\frac{{\xi_1}^3(1-\xi_1)}{k^2}\left[\frac{k^2-1}{3} + \frac{1}{(\xi_1 k\alpha H)^2} - \frac{\tanh \xi_1 k\alpha H}{(\xi_1 k\alpha H)^3}\right]$$

$$+\frac{wH^4}{EI}\frac{{\xi_1}^2(1-\xi_1)^2}{2}\frac{(k^2-1)}{K^2}\left[\frac{1}{2} - \frac{(\cosh \xi_1 K\alpha H - 1)}{(\xi_1 K\alpha H)^2 \cosh \xi_1 k\alpha H}\right] + \frac{wH^4}{EI}\left[\frac{(1-\xi_1)^2}{2(\alpha H)^2} + (k^2-1)\frac{(1-\xi_1)^4}{8}\right]$$

$$+\frac{wH^4}{EI}\frac{(k^2-1)}{6}\left[(1-\xi_1)\left(3\xi_1 - 3{\xi_1}^2 + {\xi_1}^3\right)\right]$$

$$-\frac{wH^4}{EI}\frac{(k^2-1)^2}{k^2}(1-\xi_1)\left[\frac{\xi_1}{2} - \frac{\xi_1^2}{2} + \frac{\xi_1^3}{6} - \frac{(1-\xi_1)^2}{2}\frac{\tanh \xi_1 k\alpha H}{(k\alpha H)}\right] - \frac{wH^4}{EI}\frac{(k^2-1)}{K^2}(1-$$

$$\xi_1)\left[\frac{(\cosh \xi_1 k\alpha H - 1)}{(K\alpha H)^2 \cosh \xi_1 k\alpha H} - \frac{(\xi_1)}{(k\alpha H)^2} + \frac{\tanh \xi_1 k\alpha H}{(k\alpha H)^3}\right] \tag{9}$$

2.3.2 *Optimum level of wall curtailment*

In order to determine the optimum level of curtailment corresponding to the minimum top deflection, the aforementioned expression of y(H) should be minimized. Note that the top deflection can also be expressed as a function $F(\xi_1)$. Its minimum corresponds to a first derivative equal zero:

$$F'(\xi_1) = 0 \tag{10}$$

This equation is an implicit function of ξ_1 that could be solved by iterative process. Nollet and Stafford Smith (1993) used the Newton-Raphson algorithm to obtain the optimal value ξ_{opt} corresponding to a minimum top deflection of the curtailed wall-frame structure. Fig. 2-3 shows the results of Nollet and Stafford Smith that gives the curves of $\xi_{\text{opt}}$with respect to the characteristic parameter αH for different values of k² between 1 and 1.2 which cover wide ranges of wall- frame structures.

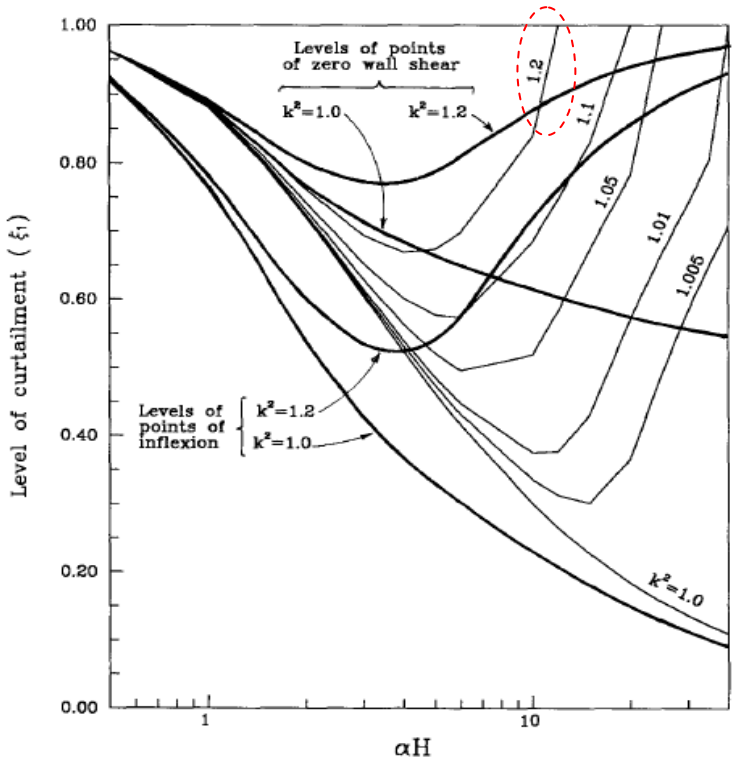

Fig. 2-3 Location of Optimum Level for Curtailment (Nollet and Stafford Smith 1993)

2.4 Optimum Level based on continuum model - Influence of calculation precision

It can be seen from Fig. 2-3 that for most of the range of values of αH, the optimum level of curtailment generally lies between the points of inflection and zero wall shear in the corresponding full-height wall structure, regardless of the value of k².

Optimum level of shear wall curtailment

A closer look at the figure reveals that this rule is not respected for some values. For example, in case of $k^2=1.2$ and for $\alpha H \geq 12$, it can be noted that in spite of existing negative moment and negative shear force in the wall, the optimum level corresponds to the full height wall ($\xi_{opt} = 1$): this anomaly requires verification. Fig. 2-4 shows another result of Nollet (1991) relative to the method of calculation of the optimum level of curtailment. He considers the possibility that the function $F'(\xi_1)$ equals zero at two different points (Fig. 2-4b). He attempts to explain this result as follows: for values of αH higher than 15, if a curtailment is made at a level very close to the top, the resulting top deflection is some times greater than the top deflection of the full-height-wall structure (Fig. 2-4a). This interpretation is misleading and not compatible with the physical behavior of the wall-frame structures which will be discussed in the following section considering the calculation precision.

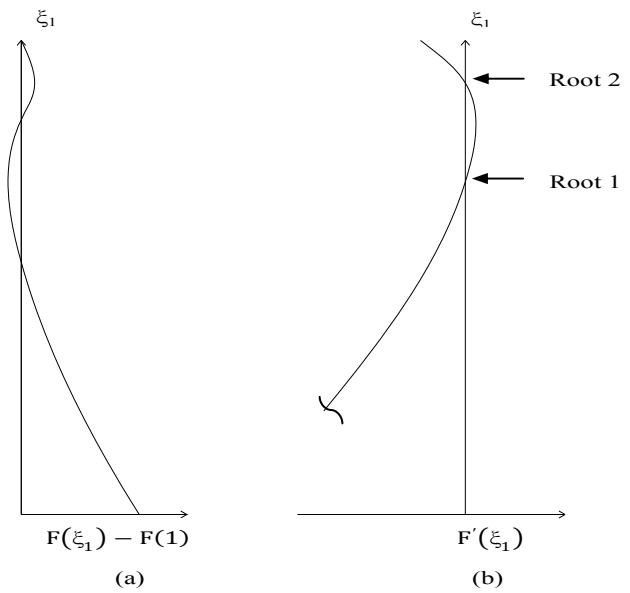

Fig. 2-4 Possibility of having $\mathbf{F'(\xi_1) = 0}$ at two different points (Nollet, M. J. ,1991)

The determination of top deflection and the optimum level of curtailment involve the use of hyperbolic functions that may be very sensitive to the calculation precision. Fig. 2-5 gives an example of such cases where the chosen function is g(x) = Cosh(x) + 1 - Cosh(x). It shows that the normal precision is not sufficient to estimate the values of the g(x) for $x \geq 10$. For $x \geq 30$, even a double precision calculation becomes insufficient.

The influence of precision on the function $F(\xi_1)$ used in the continuum model for high values of αH is presented in Fig. 2-6. It shows the effect of the precision in specifying the optimum level of curtailment:

- Adequate precision: the optimum level of curtailment which gives the minimum deflection at the top of the structure for $\alpha H = 20$ and $\alpha H = 40$ is 0.9 and 0.95, respectively.

- Insufficient precision: the optimum level is 1 in the both cases of $\alpha H = 20$ and $\alpha H = 40$.

Therefore the equation $F'(\xi_1) = 0$ has been resolved using high precision with the software Mathematica. The new curves of ξ_{opt} are depicted in Fig. 2-7. The optimum level of curtailment always lies between the point of inflection and zero wall shear in the corresponding full-height wall structure, regardless of the value of k^2. This result is more consistent than those presented in Fig. 2-3 for the high values of αH.

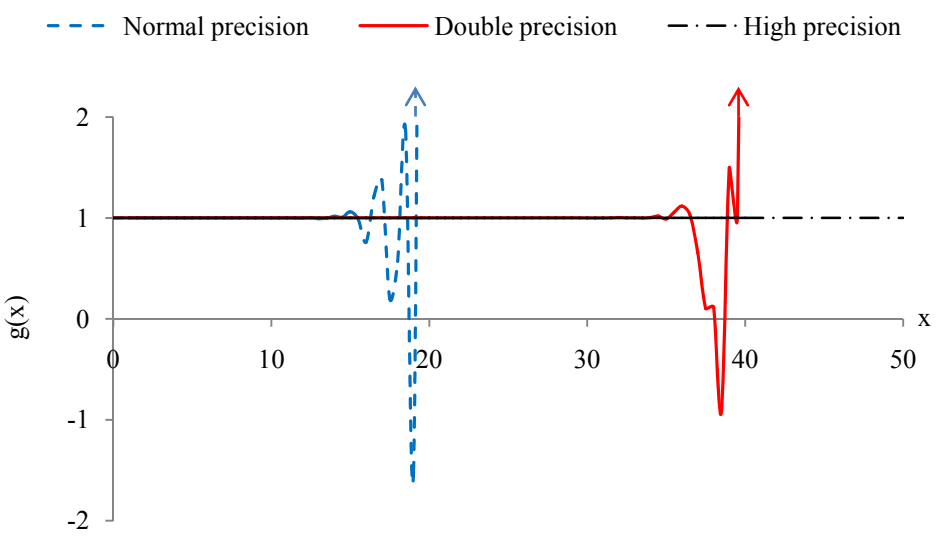

(Fortran, compiled by Silverfrost FTN95)

Fig. 2-5 Effect of the precision on the function g(x) = Cosh(x) + 1 - Cosh(x)

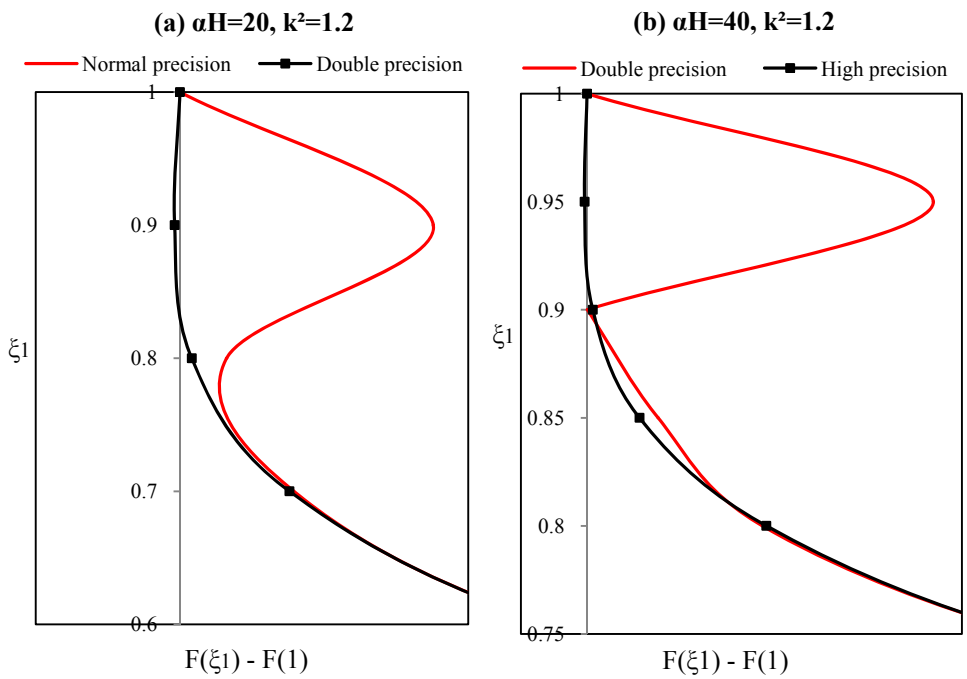

Fig. 2-6 Influence of the precision on the optimum level of curtailment

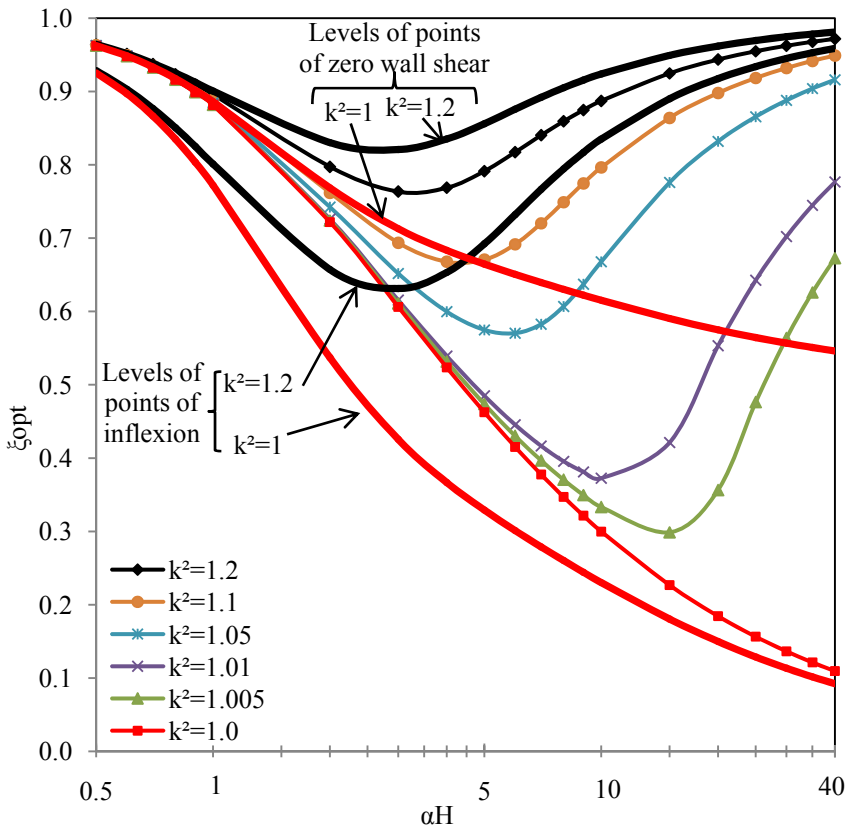

Fig. 2-7 Location of Corrected Optimum Level for Curtailment

2.5 Relationship between the axial deformations, racking shear deformations and the optimum level for curtailment

Figure 3 reveals a noticeable relationship between the axial deformations, the racking shear deformations and the optimum level for curtailment:

a- For a specific value of αH

When the value of k^2 increases the optimum level for curtailment increases. Indeed, the value of k² factor can be expressed as follows: $k^2 = \frac{EI+E\sum AC^2}{E\sum AC^2} = \frac{EI}{E\sum AC^2} + 1$. It can be noticed that the increase in the value of k^2 is associated to a decrease in the axial stiffness of the columns, as a result the story drift of frame due to axial deformation of columns increases. Thus the difference in the free deflected forms of the wall and the frame decreases, so the optimum level for curtailment rises.

b- For a specific value of k^2 and H

i) For $k^2 = 1$ (The axial deformations of the columns are **neglected**); The increase of α is related to the increase of the racking shear rigidity of the frame (GA) which results in higher interaction between the frame and the wall. In this case the optimum level of curtailment is reduced.

ii) For $k^2 > 1$ (the axial deformations of the columns are **not neglected**). As in the previous case, when α increases the optimum level for curtailment is reduced but this reduction continues until a certain value of αH and then it starts increasing. This change is attributed to relative higher value of GA which reduces the racking shear deformations in the frame. In this case, the axial deformations will be dominant and the interaction between the frame and the wall will decrease and consequently the optimum level of curtailment rises.

2.6 Optimum Level and resulting internal forces

In this section, the relationship between the optimum level of curtailment and the resulting internal forces is discussed. It is well known that the maximum positive

or negative moment (mathematically, the local maxima or minima) corresponds to the zero shear point (mathematically, the zero point of the first derivative). Figures 9a and b gives the general trends of the shear force and the corresponding induced bending moment in the wall for different curtailment levels. If the level of curtailment leads to removing the negative shear in the wall by making it equal to zero at the top of the wall, the minimum moment (local minima) will be also at the top of the wall. According to boundary conditions, the moment at the top of the wall is equal to zero, and consequently the moment over the entire height of the wall remains positive. In other terms, the level of curtailment that leads to eliminate the negative shear in the wall by making it equal to zero at the top, leads at the same time to remove the negative moment. As a result, the interruption of the shear wall at this level eliminates the reverse force applied by the wall on the frame and consequently the top deflection of the structure will be minimum (see Fig. 2-8). In summary, the optimum level of curtailment resulting in a minimum top deflection of the structure eliminates at the same time the negative moment and negative shear forces in the wall.

From Fig. 2-8, two zones of wall curtailment can be identified:

i) ($\xi_{opt} < \xi_1 < 1$) : The curtailment of the shear wall at a level greater than the optimum level results in a top deflection less than the top deflection of the full-height-wall structure since the negative effect of the wall on the frame decreases. Returning to section 3, exactly the part reported by Nollet (1991) "*if a curtailment is made at a level very close to the top, the resulting top deflection is some times greater than the top deflection of the full-height-wall structure*", this misleading result has occurred because of the insufficient calculation precision.

ii) ($\xi_1 < \xi_{opt}$): The curtailment of the shear wall at a level less than the optimum level remove the contribution of a useful part of the wall situated between the optimum level and the chosen level of curtailment.

2.7 Numerical applications

This section presents the results of two examples: the first one corresponds to a low value of αH where the calculation precision does not affect the result. This example clearly shows the relationship between the optimum level and the induced internal

forces in the structure. The second example corresponds to a high value of αH; it aims at showing the influence of calculation precision in specifying the optimum level of curtailment.

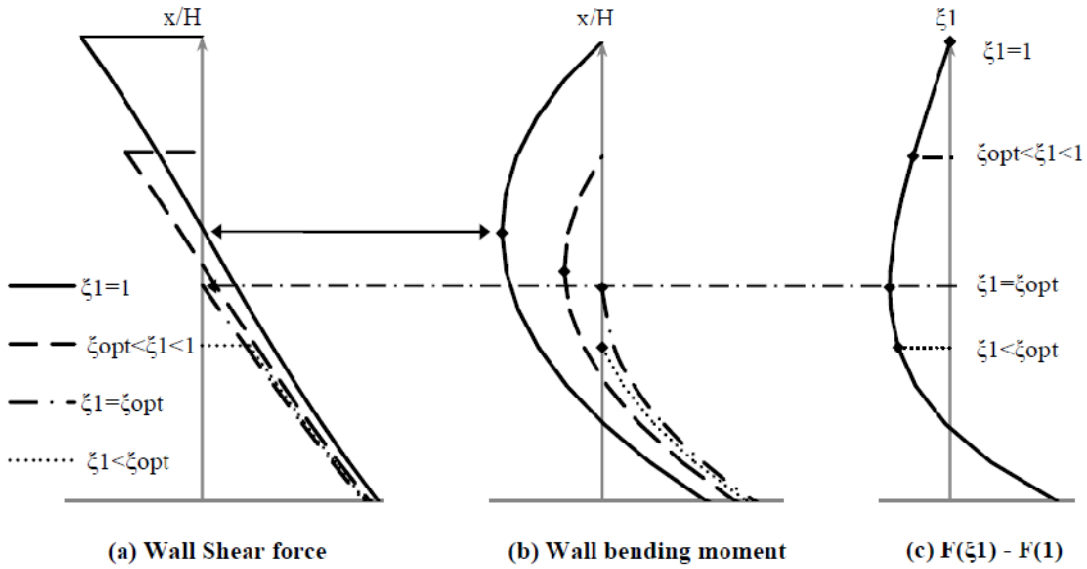

Fig. 2-8 Relationship between the level for curtailment and the resulting internal forces

2.7.1 *Example 1 - Low value of αH*

This example consists of a twenty-storey wall-frame structure, with a storey's height of 3.5 m. The structure's plan consists of one reinforced concrete core (t=25 cm) and six reinforced concrete frames. The plan is symmetrical about the axis of loading (Y) as depicted in Fig. 2-9. The structure is subjected to a uniformly distributed lateral load of 1.5 kN/m². Table 2-1 summarizes the dimensions of the columns and the beams of frames. The Modulus of Elasticity of the concrete is equal to2.6×10^4 MPa. Mechanical characteristics give the following parameters: αH=2.55 and k²=1.077. The calculation precision is not important in this case, the optimum level of curtailment can be obtained using figure 4 or figure 8: $\xi_{opt} = 0.68 \Leftrightarrow \mathrm{H}_1 = 47.6$ m. Consequently, the optimum storey of curtailment equals to $\frac{47.6}{3.5} = 13.6 \approx 14$ as practical value, therefore the practical value of $\xi_{opt} = \frac{14}{20} = 0.7$.

Fig. 2-10 illustrates the resulting internal forces in frame and wall for both cases of curtailed and full-height wall structures. It can be noted that the curtailment

of the wall at the storey 14 eliminates the negative moments and the negative shear forces in the wall as explained above. As a result, the internal shear force and bending moment in the upper part of the frame are reduced to be equal to the external load shear and the external load moment, respectively. Fig. 2-11 shows that the optimum level for curtailment reduces about 4% the top deflection of curtailed wall structure comparatively to full height wall structure.

Table 2-1 Columns and beams dimensions

	Interior columns	Exterior columns	Beams
Interior frames (2→5)	1.00×1.00 m	0.90×0.90 m	0.75×0.30* m
Exterior frames (1 and 6)	0.90×0.90 m	0.80×0.80 m	0.60×0.30* m

*: Height × Width.

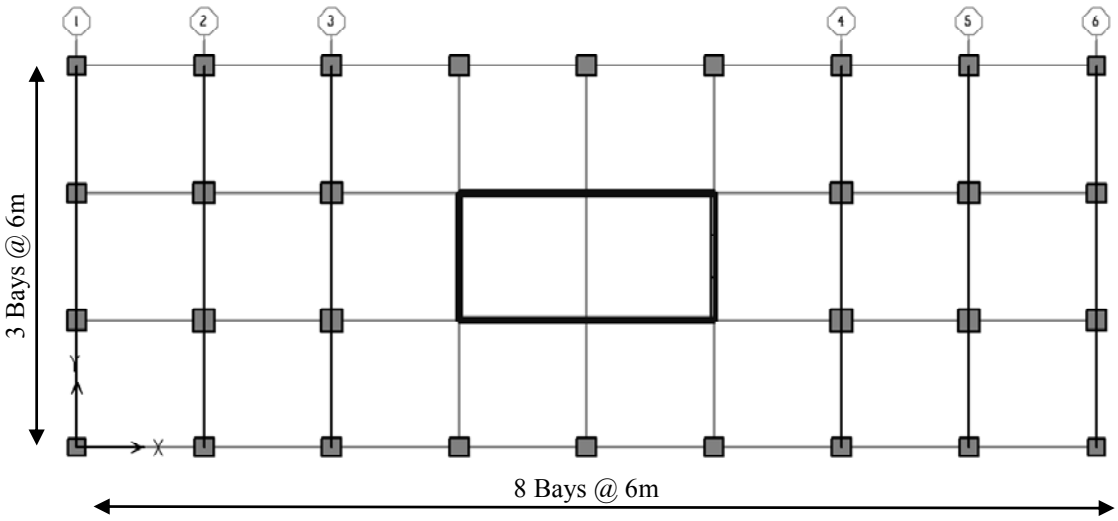

Fig. 2-9 Plan view: Wall-frame Structure - example 1

2.7.2 *Example 2 - High value of αH*

In order to illustrate the importance of the calculation precision, the previous example is modified to obtain a value of $\alpha H > 10$ as follows:

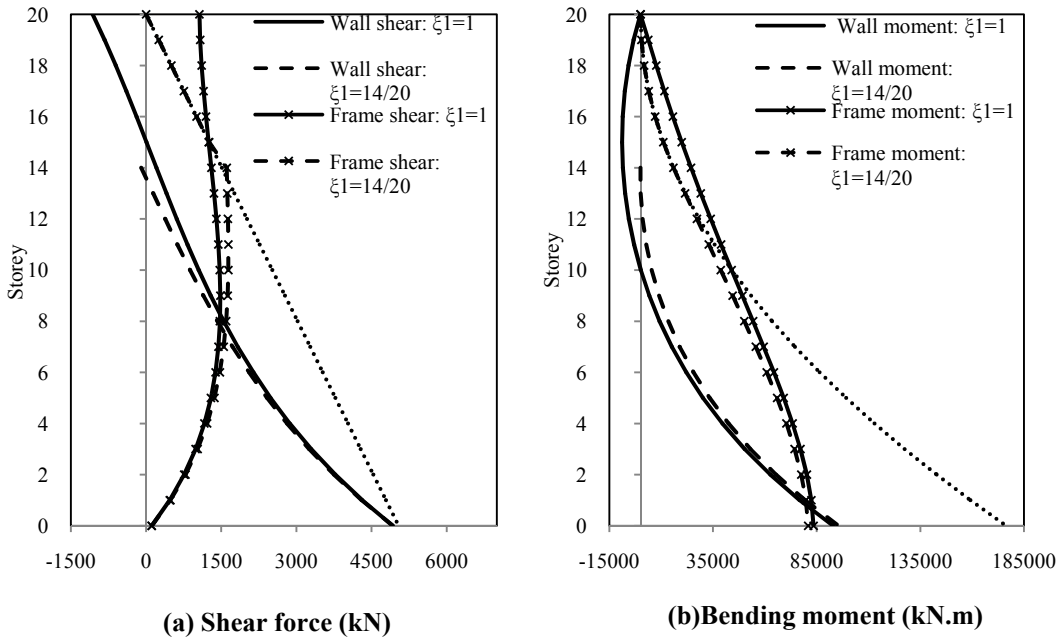

Fig. 2-10 Internal forces for full-height and curtailed-wall frame structures

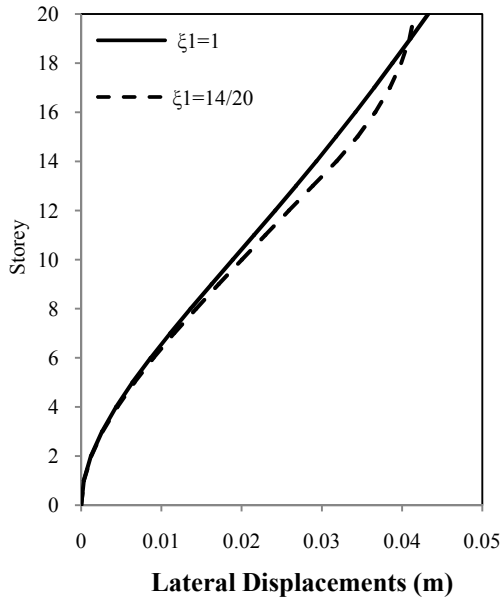

Fig. 2-11 Comparison of Deflections - Curtailed and full height wall structures

The number of stories is changed to 65 storeys and the new thickness of the reinforced concrete core equals to 1.15 m. The new dimensions of the frames elements are summarized in Table 2-2:

Optimum level of shear wall curtailment

Table 2-2 Modified dimensions of the columns and beams

	Interior columns	Exterior columns	Beams
Interior frames	1.50×1.50 m	1.20×1.20 m	1.25×0.60* m
Exterior frames	1.20×1.20 m	1.00×1.00 m	1.25×0.60* m

* Height × Width.

The new characteristics give the following parameters: $\alpha H=12$ and $k^2=1.2$.

According to Nollet and Stafford Smith curves (Fig. 2-3), it can be noted that despite the existence of a negative moment and a negative shear in the wall for a full height wall structure, the optimum level corresponds to the full height wall (see Table 2-3).

Table 2-3 Levels of $Q_w=0^a$, $M_w=0^b$ and ξ_{opt} - Continuum model with normal calculation precision (see Fig. 2-3)

Point	Level / H
$Q_w=0$	0.89
$M_w=0$	0.77
ξ_{opt}	1

a : The point of zero wall shear in the corresponding full-height wall structure.

b : The point of inflection in the corresponding full-height wall structure.

According to the high precision curves (Fig. 2-7), the optimum level of curtailment lies between the point of inflection and zero wall shear (see Table 2-4).

Table 2-4 Levels of $Q_w=0$, $M_w=0$ and ξ_{opt} - continuum model with high calculation precision (see Fig. 2-7)

Point	Level / H
$Q_w=0$	0.89
$M_w=0$	0.77
ξ_{opt}	0.83

Simultaneously, the result of a finite element modeling shows that the optimum level of curtailment is located at the 53th storey. Table 2-5 summarizes the results of this modeling. They confirm the results obtained with the continuum model with high precision calculation.

Table 2-5 Levels of $Q_w=0$, $M_w=0$ and ξ_{opt} - Finite element modeling

Point	Storey	Level / H
$Q_w=0$	59	0.91
$M_w=0$	50	0.77
ξ_{opt}	53	0.82

2.8 Conclusion

This chapter included a thorough analysis of the continuum model used to determine the optimum level of wall curtailment in wall-frame structures. The continuum model is a simple and efficient tool but should be used carefully. It is highly sensitive to the calculation precision because of the use of hyperbolic functions that need high calculation precision for high values of the variables. The optimum level of curtailment lies always between the point of inflection and the zero wall shear in the corresponding full-height wall structure. This result is very useful when searching for the optimum level of curtailment. The optimum level of curtailment which results in the minimum top deflection of the structure eliminates at the same time the negative moments and negative shear forces in the wall. It corresponds to a zero shear force at the top of the wall which represents a simpler alternative to determine the optimum level of curtailment.

2.9 Appendix I : Correction of the typographical errors

$$y_1'(H_1) = \frac{wH^3}{EI}\frac{(k^2-1)}{k^2}\left[\frac{\xi_1}{2} - \frac{\xi_1^2}{2} + \frac{\xi_1^3}{6} - \frac{(1-\xi_1)^2}{2}\frac{\tanh \xi_1 k\alpha H}{(k\alpha H)}\right] + \frac{wH^3}{EI}\frac{1}{k^2}\left[\frac{(1-\xi_1)}{(k\alpha H)^2} - \frac{1}{(k\alpha H)^2 \cosh \xi_1 k\alpha H} + \frac{\tanh \xi_1 k\alpha H}{(k\alpha H)^3}\right] \quad (20)$$

$$\emptyset_{H_1} = \frac{wH^3}{EI}\frac{(k^2-1)}{6}\left(3\xi_1 - 3{\xi_1}^2 + {\xi_1}^3\right)^2 - (k^2-1)y_1'(H_1) \quad (23)$$

$$y(x) = \frac{wH_1^4}{EI}\left\{\frac{(k^2-1)}{k^2}\left[\frac{1}{4}\left(\frac{x}{H_1}\right)^2 - \frac{1}{6}\left(\frac{x}{H_1}\right)^3 + \frac{1}{24}\left(\frac{x}{H_1}\right)^4\right] + \frac{1}{k^2}\left[\frac{2\left(\frac{x}{H_1}\right)-\left(\frac{x}{H_1}\right)^2}{2(k\alpha H_1)^2}\right]\right\} + \frac{wH_1^4}{EI}\frac{1}{k^2}\left[\frac{(\cosh k\alpha x-1)(k\alpha H \sinh k\alpha H_1+1)}{(k\alpha H_1)^4 \cosh k\alpha H_1} - \frac{\sinh k\alpha x}{(k\alpha H_1)^3}\right] \quad (30)$$

$$y_2(x_2) = \frac{wH^4}{EI}\left[\frac{\left(\frac{2x_2}{H_2}-\left(\frac{x_2}{H_2}\right)^2\right)}{2(\alpha H)^2}(1-\xi_1)^2\right] + \frac{wH^4}{EI}(k^2-1)\left\{(1-\xi_1)^4\left[\frac{\left(\frac{x_2}{H_2}\right)^4}{24} - \frac{\left(\frac{x_2}{H_2}\right)^3}{6} + \frac{\left(\frac{x_2}{H_2}\right)^2}{4}\right]\right\} + \emptyset_{H_1}x_2 \quad (36)$$

2.10 References

Atik, M. (2010). *The Effect of Curtailed Walls in Wall-Frame Structures to Resist Lateral Loads*, Master thesis, University of Aleppo, Aleppo, Syria.

Bozdogan, K. B. (2011). "Free Vibration Analysis of Wall-Frame Structures By Differential Quadrature Method." *International Journal of Engineering and Applied Sciences* (IJEAS), 3(4), 7-20

Bozdogan, K. B., and Ozturk, D. (2012). "Vibration Analysis of Asymmetric Shear Wall- Frame Structures Using The Transfer Matrix Method." *IJST, Transactions of Civil Engineering*, 36(C1), 1-12

Heidebrecht, A. C., and Stafford Smith, B. (1973). "Approximate analysis of tall wall-frame structures." *J. Struct. Div.*, ASCE, 99(2), 199-221.

Miranda, E. (1999). "Approximate Seismic Lateral Deformation Demands in Multistory Buildings". ASCE Journal of Structural Division, Vol. 125, No. 4, pp. 417-425.

Miranda, E., and Akkar,S. (2006). "Generalized Interstory Drift Spectrum." *Journal of Structural Engineering*, ASCE, 132 (6), 840-852.

Miranda, E., and Reyes, J. C. (2002). "Approximate lateral drift demands in multistory buildings with nonuniform stiffness." *J. Struct. Div.*, ASCE, 128(7), 840-849.

Miranda, E., and Taghavi, S. (2005). "Approximate floor acceleration demands in multistory buildings I formulation." *J. Struct. Div.*, ASCE, 131(2), 203-211.

Nollet, M. J. (1991). *Behavior of wall-frame structures: a study of the interactive behavior of continuous and discontinuous wall-frame structures*, Ph.D. thesis, McGill University, Montreal, Canada.

Nollet, M. J., and Stafford Smith, B. (1993). "Behavior of Curtailed Wall-Frame Structures." *Journal of Structural Engineering*, ASCE, 119(10), 2835-2854.

Paulay, T., and Priestley, M. J. N. (1992). *Seismic Design of Reinforced Concrete and Masonry Buildings*, Chapter: 6 Dual Systems, JOHN WILEY& SONS, INC. New York.

Stafford Smith, B., Kuster, M., and Hoenderkamp, J. C. D. (1981). "A generalized approach to the deflection analysis of braced-frame, rigid frame and coupled wall structures." *Can. J. Civ. Eng.*, 8(2), 230-240.

Stafford Smith, B., Kuster, M., and Hoenderkamp, J. C. D. (1984). "Generalized method for estimating drift in high rise structures." *J. Struct. Div.*, ASCE,110(7), 1549-1562.

Stafford Smith, B., and Coull, A. (1991). *Tall Building Structure: Analysis and Design*, JOHN WILEY& SONS, INC. New York.

Chapter 3: Single-Run Adaptive Pushover Procedure for Shear Wall Structures

The contents of this chapter submitted to Bulletin of Earthquake Engineering Journal for review on July 2013.

3.1 Abstract

This chapter proposes a new single-run adaptive pushover method for the seismic assessment of shear wall structures. This method offers two main advantages: it does not require decomposing the structure in nonlinear domain and it avoids the pitfall of previous single-run adaptive pushover analyses in utilizing the modal combination in the determination of the applied loads instead of combining the response quantities induced by those loads in individual modes.

After a brief review of the main adaptive pushover procedures, the proposed method is presented as well as its numerical implementation. The predictions of this method are compared to those of other recent adaptive pushover methods and as well as to the rigorous non-linear time history analysis. Analyses show the efficiency of the proposed method.

Keywords: Adaptive pushover, Overturning moment-based, Single-run, Shear wall, Plastic hinges

3.2 Introduction

Nonlinear static procedures or pushover analyses constitute an efficient tool to assess the seismic demand of structures. They constitute a reliable alternative of nonlinear time-history analysis of structures. For tall buildings, the effect of higher modes is not negligible, that's why ignoring their effect is one of the main limitations of pushover analyses. Furthermore, the modes of vibration of the structure can significantly change during strong seismic motion.

In recent years, several techniques have been proposed to integrate the effect of higher modes in pushover analyses and to incorporate the variation in dynamic properties associated to structural damages. Gupta and Kunnath (2000) updated the applied load at each increment. The eigenvalue analysis is carried out at each load increment, then a static analysis is carried out for each mode independently. The calculated effects are combined with SRSS and added to the corresponding values from the previous step. Similarly, Aydinoğlu (2003, 2004, 2007) developed and extended this method to estimate the peak demand quantities. These adaptive procedures provide good estimates of seismic demands, however:

(a) They are computationally complicated (Chopra and Goel 2002; Baros and Anagnastopoulos 2008). This is mainly due to the absence of a structural equilibrium at the end of each step as the result of using SRSS to combine the responses (Antoniou and Pinho 2004a), so a routine application has to be made to impose the stiffness of the structure at the beginning of each step.

(b) In the inelastic domain, the structural system could not be decomposed into several independent systems (corresponding to the desirable number of modes), consequently the application of the modal combination rule in the inelastic domain is no longer valid. To overcome this difficulty, small steps should be taken where the system can be considered linear (Gupta and Kunnath 2000) or the modal response increments in each mode must be scaled in such a way that the response spectrum analysis (RSA) is implemented in a piecewise linear fashion at each pushover step (Aydinoğlu 2003), but it increases the computational demands.

In an attempt to avoid the previous computational complexity (the absence of structural equilibrium) and based on the work of Chopra and Goel (2002), Kalkan and Kunnath (2006) developed an adaptive modal combination procedure that accounts for higher mode effects. They combine the response of individual modal pushover analyses and incorporate the effects of progressive variation in dynamic characteristics during the inelastic response via its adaptive feature. The lateral load distribution used in the progressive pushover analysis is based on instantaneous inertia force distribution across the height of the building for each mode. However, these multi-run methods do not reflect the yielding effect of one mode on other modes and on the interaction between modes in the nonlinear range. On the other hand, this

method, as the method of Chopra and Goel (2002), is not applicable to estimating member forces because forces computed by this procedure may exceed the specified member capacity. Therefore, there is a need to recompute the member force from the member deformation(s) determined by this procedure to have member forces consistent with their specified capacity (Goel and Chopra 2005). That needs additional computational effort.

In order to combine the advantages of previous methods, single-run adaptive pushover procedures have been proposed. Instead of decomposing the structure into several independent structures, equivalent seismic loads are combined and applied to the structure, where one of the modal components is chosen to be combined by one of the modal combination rules and to be as the base to define the equivalent seismic loads. The main critic of these methods consists in the use of the modal combination in defining the applied loads instead of combining the response quantities induced by those loads in individual modes (Chopra 2007, p. 569; Aydinoğlu 2003, 2007).

After a brief description of the single run adaptive pushover procedures, an innovative new single-run adaptive pushover method based on the modal overturning moment story is developed in this paper. This method does not require decomposing the structure and at the same time it avoids the previous pitfall.

3.3 Overview and principle of single-run adaptive pushover procedures

Antoniou and Pinho (2004a) explored the accuracy of force-based adaptive pushover analysis in predicting the horizontal capacity of reinforced concrete buildings. They proposed a force-based adaptive pushover (FAP) which is an extended version of the fully adaptive pushover algorithm proposed by Elnashai (2001). The lateral load distribution is continuously updated during the process, according to modal shapes and participation factors derived by eigenvalue analysis carried out at each analysis step. The modal floor forces for the desirable modes are evaluated at each step according to the instantaneous stiffness matrix and the corresponding elastic spectral accelerations. Then the lateral load pattern is determined by combining the floor forces of each vibration mode. The loads from all modes are combined using the SRSS rule. It was concluded that, despite its apparent conceptual superiority, current force-based adaptive pushover shows a relatively

minor advantage over its traditional non-adaptive counterpart, mainly for the estimation of deformation patterns of buildings, which are poorly predicted by both types of analysis.

Another variant of the method proposed by Antoniou and Pinho (2004b) is the displacement-based adaptive pushover procedure (DAP), whereby a set of laterally applied displacements, rather than forces, is monotonically applied to the structure. In their paper, the authors proposed again the interstory drift as a base instead of the displacement and it has been adopted as the standard DAP variant. The DAP procedure improved the response predictions, throughout the entire deformation range, in comparison to those obtained by force-based methods. Contrary, Casarotti and Pinho (2007) re-adopted the displacement as a base instead of the interstory drift for estimating seismic demands on bridges.

In order to adjust the drawbacks of the FAP procedure, Shakeri et al (2010) proposed a story shear-based adaptive pushover method (SSAP), where the load pattern is derived from the modal story shear profile. They referred the superiority of the SSAP method over the FAP because it takes into account the change in the sign of the story components along the structure height for higher modes.

From the above, it can be noted that all of these methods have made the previous mentioned pitfall in computing the combined peak value of one response quantity from the combined peak values of other response quantities. However, we do not deny that the results were sometimes satisfactory; the present chapter shows that these methods are not valid for shear wall structures. An innovative new single-run adaptive pushover method is proposed. It is based on the modal overturning moment story, which avoids the previous pitfall and it is valid for shear wall structures.

3.4 Description of the Overturning Moment-Based Adaptive Pushover Procedure (OMAP)

3.4.1 *Theoretical base of OMAP method:*

The idea behind the single-run pushover procedures is that in the inelastic domain, the structural system could not be decomposed into several independent systems. Instead of decomposing the structure into several independent structures, combined equivalent seismic loads are applied to the structure, where one of the

modal components (Inertial force, displacement, drift story, shear force,…) is chosen to be combined by one of the modal combination rules and to be as a base to define the equivalent seismic loads. It is clear that each base gives different equivalent lateral loads, this leads to the question which base should be chosen in pushover analysis?

In shear wall structures, the moments and the axial force are generally responsible of plasticity. But under horizontal earthquake, the axial forces in the shear wall structure remain constant (induced by vertical loads), so the prediction of plastic hinges requires only the determination of the bending moments in the shear wall. Therefore in shear wall structures, the equivalent lateral forces are derived from the combined modal flexural moments, which allow the analysis of the plastic behavior of the structure. In other words, the equivalent lateral forces in the OMAP are utilized to modify the stiffness of the structure instead of using a routine application in order to impose this stiffness as in the adaptive response spectrum analysis (Gupta and Kunnath 2000; Aydinoğlu 2003, 2004, 2007). Note that imposing the stiffness of the structure during the analysis is not possible in practical structural engineering software. So the main advantage of the OMAP method consists in its easy implementation maintaining the principle of the adaptive response spectrum analysis for shear wall structures.

On the other hand, it should be emphasized that the equivalent lateral forces are valid for calculating the overturning moments and the corresponding rotations in the structure. These equivalent lateral forces serve to predict the plastic hinge, but they are not valid for estimating other quantities. That’s why the other quantities are estimated by combining the peak response quantities in individual modes at each increment. Consequently, it can be noted that if the proposed method (OMAP) is applied to linearly elastic systems, it reduces to the standard response spectrum analysis. This is not the case for the conventional single-run adaptive pushover procedures.

This is the theoretical base of this chapter and that's why the overturning moments are chosen as the analysis base. In addition, these forces are constantly updated using eigenvalue analysis at each step, which allows consideration of the progressive variation in dynamic properties associated to structural damages.

3.4.2 ***Algorithm of OMAP method:***

The key-elements of the nonlinear static pushover analysis are: the external applied loads and the target displacement. The present chapter is concerned with the first purpose. The second purpose will be discussed in the next chapter.

The algorithm of OMAP method offers two improvements:

a- The possibility of choosing different damping values for the modes. It allows incorporating different approaches of modeling damping in nonlinear time history analysis (Charney 2008, Smyrou et al 2011).

b- The possibility of calculating the incremental applied loads depending on an incremental roof displacement: at each iteration, the corresponding incremental roof displacement is specified then the incremental applied loads are scaled to give this corresponding incremental roof displacement. Note that specifying an incremental target displacement is more relevant than an incremental base shear as in the SSAP method.

The adaptation at each incremental step in single-run adaptive pushover procedures is just to consider the progressive variation in dynamic properties but in multi-run adaptive procedures where the static analyses are done for each mode separately (Gupta and Kunnath 2000 and Aydinoğlu2003, 2004), it is not only for this reason but also to avoid overshooting of element yield forces when a modal combination rule is applied. So, a non-adaptive version of single-run adaptive pushover procedures can be performed but this is not the case for the methods proposed by Gupta and Kunnath (2000) and Aydinoğlu (2003, 2004). Consequently, the application of the non-adaptive version of the proposed method allows investigating the effect of neglecting the variation in dynamic properties associated to the structural damage.

The OMAP algorithm includes the following basic steps:

1. Specifying the desirable number of iteration (N) and the corresponding incremental floor displacement (D_{roof}) for each iteration.
2. Defining the elastic response spectrum (Pseudo-accelerations vs. Periods) with the corresponding damping ratio.

3. Performing an eigenvalue analysis of the structure to compute periods (T_j), mode shapes (Φ_{ij}) and modal participation factors (Γ_j) for the (n) desirable modes, where "i" is the story number and "j" is the mode number.
4. Choosing the modal damping ratio of the structure ξ_j , ($1 \leq j \leq n$)
5. Computing the pseudo-spectral acceleration for each considered mode (Sa_j); if the damping ratio of the jth mode is different from that of the used response spectrum, this latter is adjusted using the following formula (Newmark and Hall, 1982):

$$A_2 = A_1 \frac{(2.31 - 0.41 * \ln \beta_2)}{(2.31 - 0.41 * \ln \beta_1)} \quad (1)$$

where:

A_1 = Acceleration corresponding to damping ratio β_1;

A_2 = Acceleration corresponding to damping ratio β_2;

$0 < \beta_1 < 100$ (percentage);

$0 < \beta_2 < 100$ (percentage); and

ln = natural logarithm (base e).

6. Computing the load factor (λ) for this iteration as follows:
   a) Determine the roof displacement before the scaling (D_r) by quadratic combination rule to the peak modal floor displacements

$$D_r = \sqrt{\sum_{j=1}^{n} {D_{rj}}^2} \quad (2)$$

$$D_{rj} = \Gamma_j \Phi_{rj} \frac{Sa_j}{{\omega_j}^2} \quad (3)$$

where,

D_{rj} is the peak modal floor displacement at the roof for j^{th} mode before the scaling.

ω_j is the jth natural frequency

   b) Determine the load factor (λ)

$$\lambda = \frac{D_{roof}}{D_r} \quad (4)$$

Where, D_{roof} is the desirable incremental floor displacement for this iteration.

7. Computing the peak modal responses for the (n) modes as follows:

$$F_{ij} = \lambda \Gamma_j \Phi_{ij} m_i Sa_j \quad (5)$$

$$SS_{ij} = \sum_{k=i}^{ns} F_{kj} \quad (6)$$

$$OM_{ij} = \sum_{k=i}^{ns} SS_{kj} * h_k \quad (7)$$

$$D_{ij} = \lambda \Gamma_j \Phi_{ij} \frac{Sa_j}{\omega_j{}^2} \quad (8)$$

$$\Delta_{ij} = D_{ij} - D_{(i-1)j} \quad (9)$$

where:

m_i is the mass of ith story

F_{ij} is the lateral floor force at i^{th} floor for j^{th} mode

SS_{ij} is the modal story shear at i^{th} story for j^{th} mode

OM_{ij} is the modal overturning moment at i^{th} floor for j^{th} mode

h_i is the height of the ith story

ns is the number of stories or floors.

D_{ij} is the floor displacement at i^{th} floor for j^{th} mode

Δ_{ij} is the story drift at i^{th} story for j^{th} mode

8. Calculating the desirable combined peak responses by quadratic combination rule for this iteration and add these to the same from the previous iteration:

$$r_i = \sqrt{\sum_{j=1}^{n} r_{ij}{}^2} \quad (10)$$

For example, the combined overturning moment at i^{th} floor is given as follow:

$$OM_i = \sqrt{\sum_{j=1}^{mn} OM_{ij}{}^2}$$

9. Calculating the equivalent lateral forces which give the combined overturning moment:

$$F_i = \frac{OM_i - OM_{i+1}}{h_i} - \frac{OM_{i+1} - OM_{i+2}}{h_{i+1}}; i = 1,2, \dots, (ns - 1)$$

$$F_{ns} = \frac{OM_{ns}}{h_{ns}}; i = ns \tag{11}$$

10. Performing the pushover analysis by using the equivalent lateral forces computed in the step (9) and starting from state at end of the previous iteration.
11. Returning to step 3 and continuing the process N time.

The steps (9) and (10) are the responsible of modifying the structure stiffness, so it can be noted that if the system is elastic, these steps do not modify the eigenvalues. Consequently, for a summation of incremental floor displacements equals to Dr, the method reduces to the standard response spectrum analysis. Noting that the Eq.1 is utilized for simplifying the computing of the pseudo-spectral acceleration but that does not prevent using the exact pseudo-spectral acceleration.

Note (1): The square-root-of-sum of squares (SRSS) rule appears to be the obvious choice for modal combination, although complete quadratic combination (CQC) rule may be more appropriate when close modes are present as in the case of coupled lateral-torsional response of three-dimensional systems (Chopra 2007, 13.7.2 Modal Combination rules).

Note (2): Overturning moments and plastic hinge rotations can be picked up directly from the structure subjected to pushover analysis.

3.5 Illustrative example:

The proposed method (OMAP) as well as the methods proposed by Gupta and Kunnath (2000) and Aydinoğlu (2003, 2004) are based on the principle of the adaptive response spectrum analysis. It was demonstrated that these procedures are able to reasonably estimate the response quantities. The objective of this paragraph is not to validate the proposed OMAP method, but to illustrate the methodology of the use of a single-run adaptive pushover analysis depending on the principle of the adaptive response spectrum analysis. The OMAP procedure has been implemented in a Visual Fortran program. The subroutines are linked to the nonlinear version of SAP2000 program in order to calculate and apply equivalent lateral forces at each increment.

3.5.1 *Case study*

The case study consists of a shear wall designed for 20 story buildings. The length of the wall is 6 m and the thickness is variable with the height. Table 3-1 summarizes the shear wall properties. The thickness of the wall varies with height. Also note a capacity ratio taken as a result of a vertical load of 420 kN/Story. The yield strength of the steel is f_y= 345 MPa and the concrete compressive strength is f'c = 28 MPa.

Table 3-1 Shear wall properties for 20–storey

Story ID	Thickness (cm)	Longitudinal Reinforcement	Capacity Ratio* (Vertical Load)
1→5	28	2φ18/20cm	0.37
6→9	25	2φ14/20cm	0.33
10→11	20	2φ12/20cm	0.35
12→15	18	2φ12/20cm	0.35
16→18	15	2φ10/20cm	0.26
19→20	10	2φ10/20cm	0.33

* The capacity ratio concerns the first story of each group

3.5.2 *Ground motions*

The Imperial Valley (1940) is selected in the present study. This record is available in the Pacific Earthquake Engineering Research (PEER) website. Fig. 3-1 shows the seismic record, its response spectrum (5% damping) and frequency content. It has been selected with a frequency content allowing the higher modes to be excited (period less than 1 s in general in tall building structures).The ground motion is scaled by a factor of 2.5 in order to obtain an advanced plasticity state in the structure.

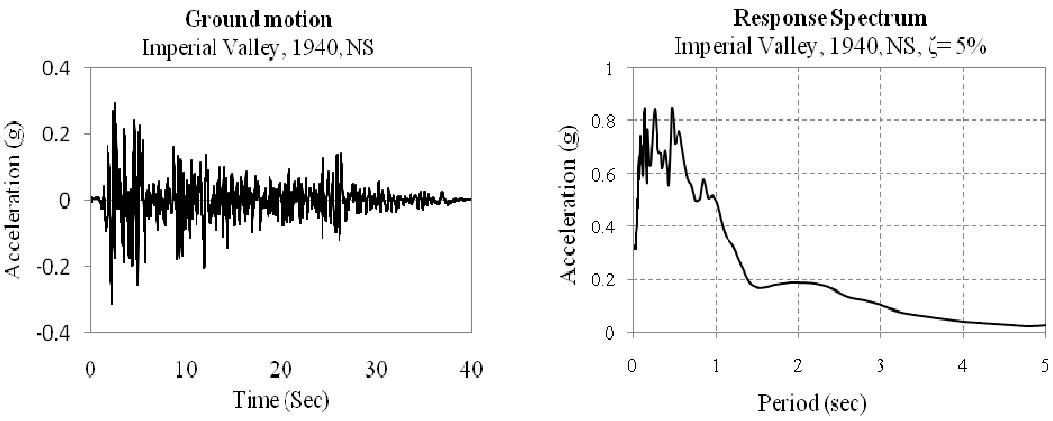

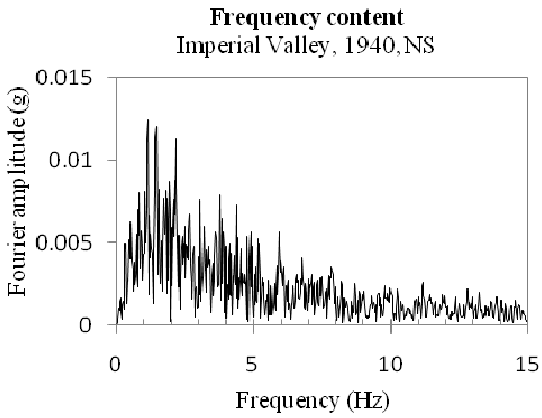

Fig. 3-1 Ground motion characteristics - Imperial Valley 1940, NS

3.5.3 *Modeling*

The walls are modeled as beam elements. The nonlinear behavior of the structure is considered via discrete hinges defined in the wall at the ends of each story. The plasticity criterion is based on the interaction of the axial force and the bending moment. Fig. 3-2 shows the load-deformation curve of the hinges. The hinge properties and the modeling parameters a, b, and c (Fig. 3-2) are specified according to FEMA-356. Note that Q and Q_y are the generalized and yield component loads, respectively. However, in recent years, sophisticated modeling for the nonlinear behavior of shear walls became prevalent simple modeling is adopted in this survey where the objective is principally to compare the proposed method (OMAP) with the NTHA.

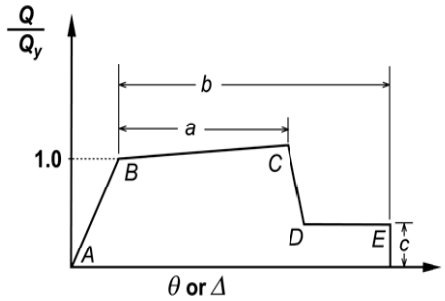

Fig. 3-2 Load-Deformation curve for hinges (FEMA 356)

The time history analysis is performed using the numerical implicit Newmark time integration method (SAP 2000). A damping ratio of 5% is considered for the first and third mode of vibrations in order to specify the Rayleigh damping coefficients c_M and c_K :

$$C = c_M M + c_K K_t \quad (14)$$

M is the mass matrix and K_t is the matrix of the tangent stiffness of the structure at each time step.

The pushover analyses were performed until obtaining a moment (or a plastic rotation) at a reference point (the base of the building in this example) equals to that resulted by NTHA.

3.5.4 *Results and Discussion*

The pushover analysis is performed using six first modes. Table 3-2 shows the natural period T, the modal participation factor Γ, the damping ratio ξ and the spectral acceleration Sa of each mode. Note that the values of Γ are related to the mode shapes which are normalized with respect to the mass matrix such that: $\sum_{i=1}^{ns} \Phi_{ij}^T m_i \Phi_{ij} = 1$. On the other hand, the zero value of Γ corresponds to vertical mode, which does not play any role in the computation of the lateral load vector. The proposed "OMAP" procedure is compared with the conventional pushover approach "Mode 1", and the above-mentioned FAP, DAP and SSAP procedures.

Table 3-2 Modal properties for 20-storey shear wall

Mode	T (sec)	Γ	ξ%	Sa (g)
1	2.98	23.00	5	0.10
2	0.54	12.87	2.6	0.87
3	0.20	7.86	5	0.64
4	0.17	0.00	5.9	0.70
5	0.11	5.69	8.8	0.51
6	0.07	4.44	13.5	0.44

As mentioned before, the main difference between adaptive methods consists in the manner used to construct the shape of the applied load. In order to distinguish the effect of the base from that of the adaptation process, results of two analyses are presented: without adaptation and with adaptation. In the first analysis, the comparison with the DAP method is avoided where the non-adaptive displacement-base pushover could conceal important structural characteristics and leads to misleading results (Antoniou and Pinho, 2004b).

3.5.4.1 Without adaptation:

a- Floor forces:

Fig. 3-3 shows the normalized load patterns obtained by different procedures. Note that the shape is more important than the value itself since the pushover analysis is performed as displacement- controlled. It can be seen that both SSAP and OMAP methods take into account the sign changes of the floor forces relative to higher modes. That's why Shakeri et al (2010) have referred the superiority of the SSAP method over the FAP. In fact this explanation is questionable because, any base in which the floor force is one of the derivatives of this base can result in a reverse in the sign of the floor forces.

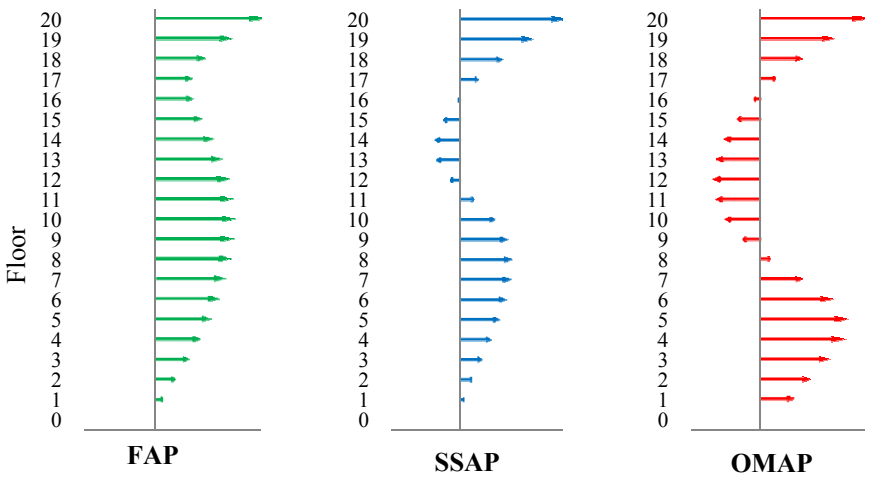

Fig. 3-3 Floor forces patterns

b- Plastic Hinge locations:

The locations of plastic hinges are depicted for each method and for the first mode (Mode 1) in the Fig. 3-4. It can be noted that only the "OMAP" procedure predicted some of the plastic hinges due to the higher modes.

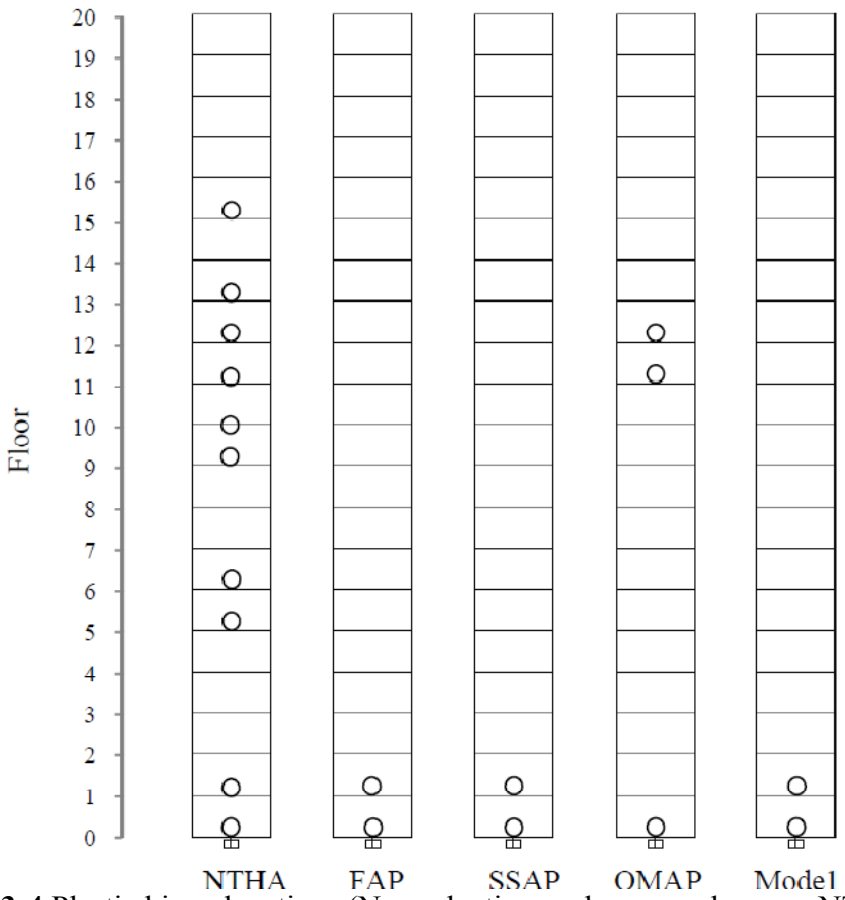

Fig. 3-4 Plastic hinge locations (Non-adaptive pushover analyses vs NTHA)

c- Flexure moments:

Flexure hinge properties involve axial force-bending moment interaction as failure envelope. In the present case of shear wall structure, the axial forces remain constant that's why the difference in the plastic hinge locations between the different methods is referred to the bending moments. Fig. 3-5 shows the bending moment diagrams obtained by different methods compared to that of NTHA where a significant difference can be seen for different methods.

In order to interpret this result, elastic structure is used. The resulting elastic moments are presented in term of scaled values where the maximum moment at the base is equal to that obtained by the linear time history analysis (LTHA), since the prediction of the hinges formation overall the shear wall is governed by the shape of the moment diagram. The obtained result is illustrated in Fig. 3-6. The large difference between the FAP, SSAP and LTHA is due to the previous mentioned pitfall in computing the combined peak value of one response quantity from the combined

peak values of other response quantities, while the little difference between the OMAP and LTHA is due to using the SRSS combination in predicting the moment.

Fig. 3-7 shows the scaled moment diagrams for LTHA, NTHA and OMAP analyses. Despite the presence of plasticity, the change in moment shape does not occur in the OMAP analysis since the adaptation has not been applied. This result emphasizes the importance of integrating the adaptive feature to the proposed method in order to incorporate the variation in modal properties. This issue is developed in the next section.

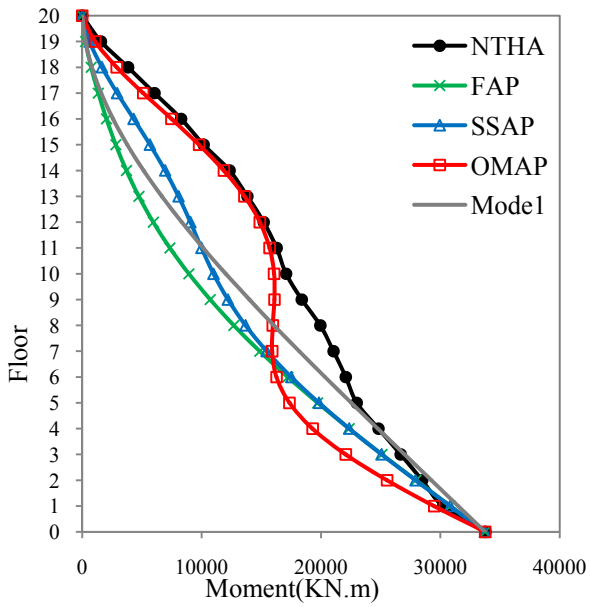

Fig. 3-5 Moment diagrams (Non-adaptive pushover analyses vs NTHA)

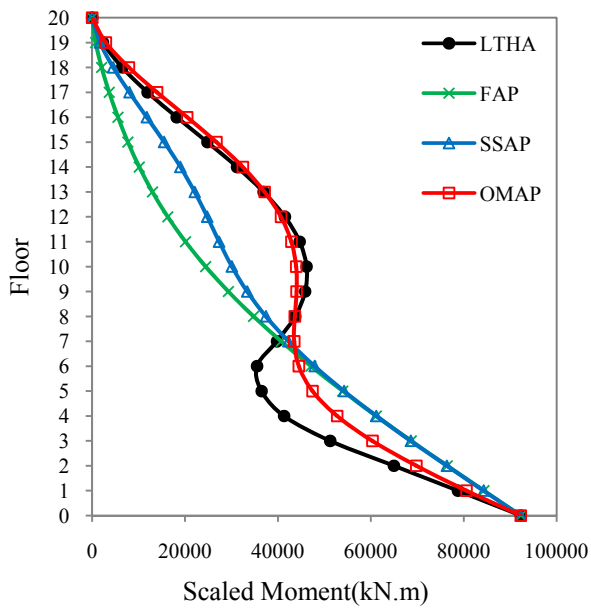

Fig. 3-6 Moment diagrams for an elastic structure (Non-adaptive pushover analyses vs LTHA)

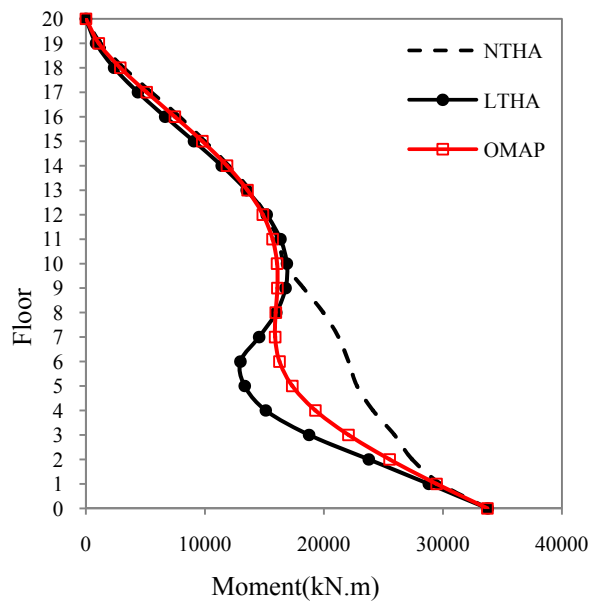

Fig. 3-7 Moment diagrams - Linear vs Nonlinear Analyses

3.5.4.2 With adaptation:

As previously mentioned, the incremental applied loads depend on the specified incremental target displacements. Table 3-3 shows the target displacements for each adaptation (iteration). The first iteration target displacements have been specified in order to initiate the plasticity in the structure. The incremental progressive variation in dynamic properties (Modal shapes, Period, Damping ratio, Modal participating mass ratios and Spectral accelerations) is detailed in Appendix A.

Table 3-3 Target displacements for each iteration (m)

Number of iteration	FAP	SSAP	DAP	OMAP	Mode 1
1	0.4	0.4	0.35	0.30	0.4
2	0.1	0.1	0.05	0.05	0.1
3 → End	0.1	0.1	0.1	0.05	0.1

a- Floor forces:

Fig. 3-8 shows the variation in the incremental applied load pattern and the corresponding plastic hinge locations at different steps during the OMAP analysis. The huge difference between the load patterns in each step requires in-depth research about the adaptation's technique, e.g. the number of iteration. Another work will discuss this issue.

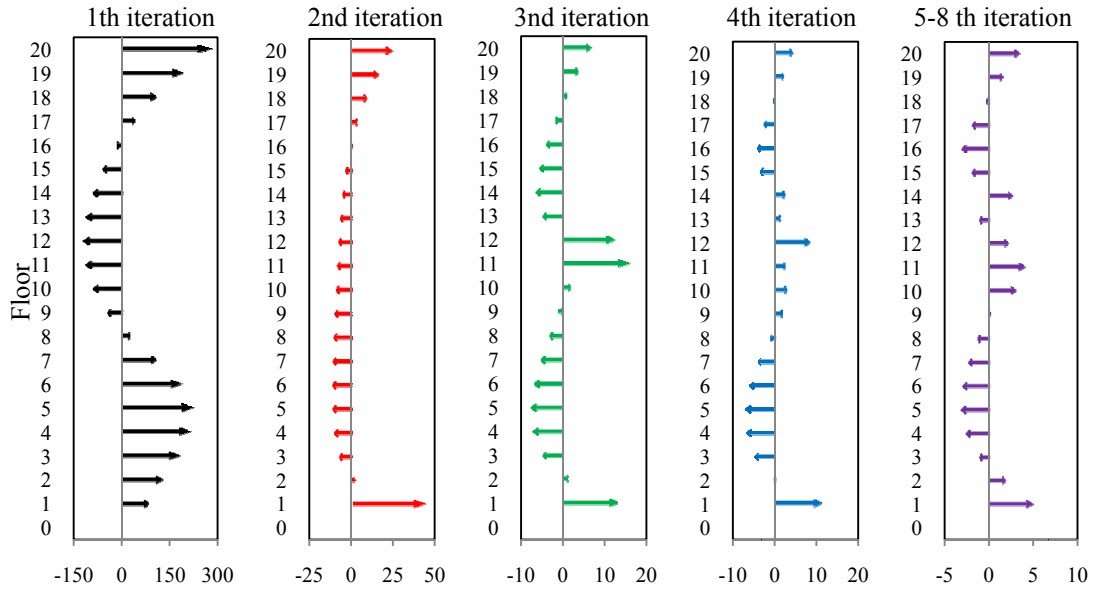

(a) Floor forces (kN)

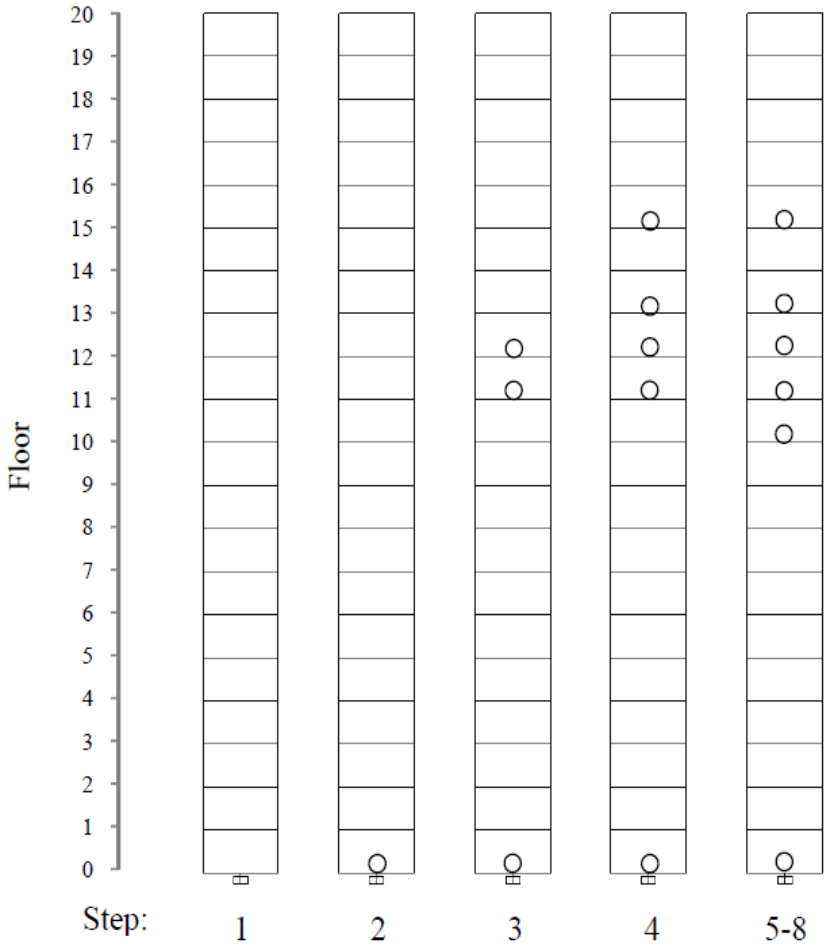

(b) Plastic hinge locations

Fig. 3-8 Variation of the incremental applied load and the corresponding plastic hinges during the OMAP procedure

b- Plastic Hinge locations and corresponding moments:

Fig. 3-9 shows the plastic hinges resulting from the adaptive form of the previous analyses. In comparison with the non-adaptive form, see figure 4, it can be noted that the adaptation only improves the results of the OMAP method. On the other hand, the DAP method succeeded in predicting a plastic hinge resulting from the higher modes because of the shape of corresponding moment diagram (Fig. 3-10).

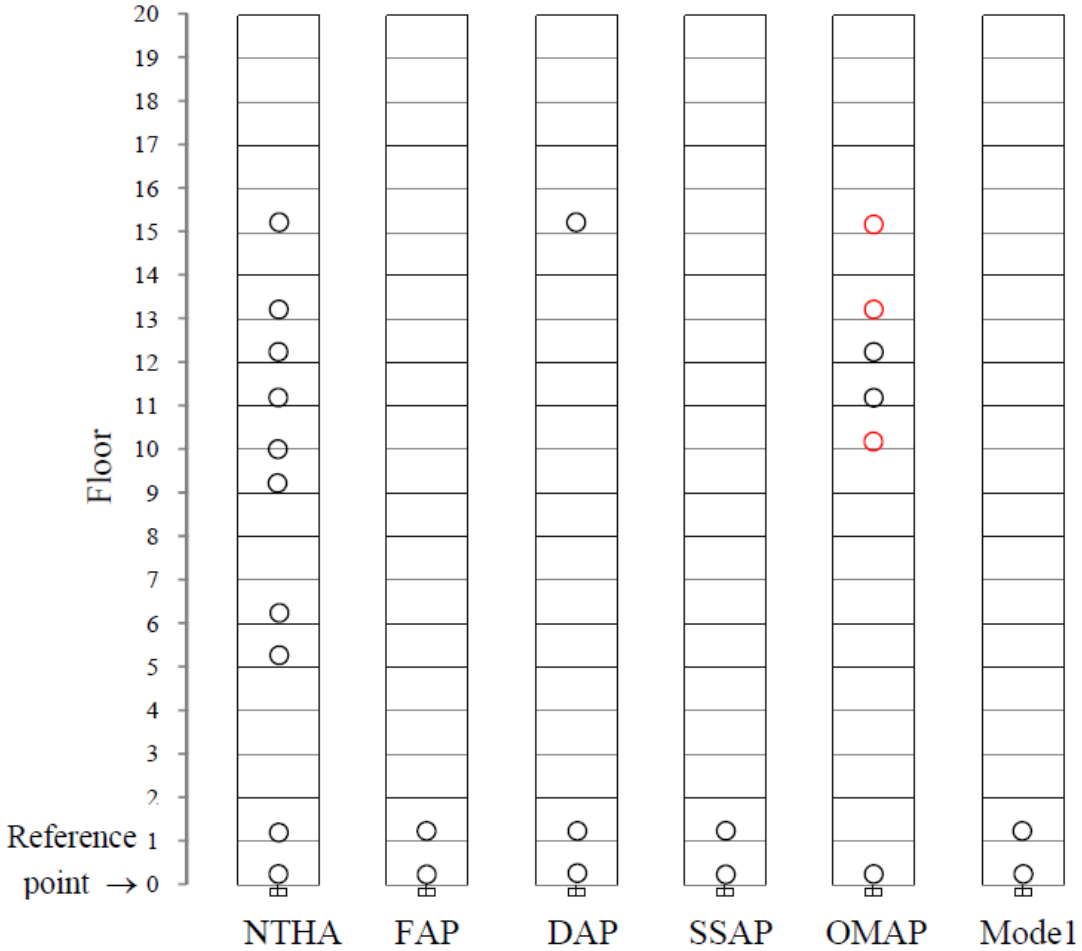

Fig. 3-9 Plastic hinge locations (Adaptive pushover analyses vs NTHA)

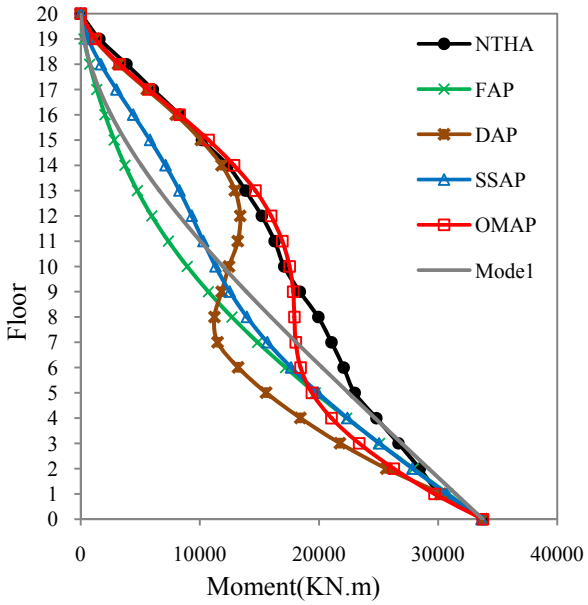

Fig. 3-10 Moment diagrams (Adaptive pushover analyses vs NTHA)

c- Other response quantities:

Fig. 3-11 indicates that OMAP procedure estimates the shear forces, displacement and story drift with a reasonable accuracy. Contrariwise, Fig. 3-12 shows the plastic hinge rotation at the bottom of each story, it can be noted the large errors in plastic hinge rotations estimated by the OMAP procedure. In fact, all Pushover analyses seem to be inherently limited in computing accurately plastic hinge rotations, because the plastic hinge rotation is very small and a little difference in the bending moment induces huge difference in the plastic hinge rotation (see Fig. 3-2). This finding led to a questionable suggestion that story drifts could be considered instead of the plastic hinge rotations as the representative demand parameter in the acceptance criteria of Nonlinear Static Procedure (Chopra and Goel, 2001).

On the other hand, it should be mentioned that in SAP2000 the hysteretic backbone is not identical with the monotonic backbone (See Fig. 3-13) when simplified multilinear curves is used. So for comparing plastic hinge rotations, the pushover analyses were performed until obtaining a plastic rotation (not a moment) at the base of the building equals to maximum one resulted by NTHA. In the next chapter, more sophisticated model (inelastic fibers) will be adopted in order to omit this drawback.

In order to give an idea about the deformation of the structure in the inelastic range, the obtained pushover curve is depicted in Fig. 3-14 that reveals an advanced plasticity state.

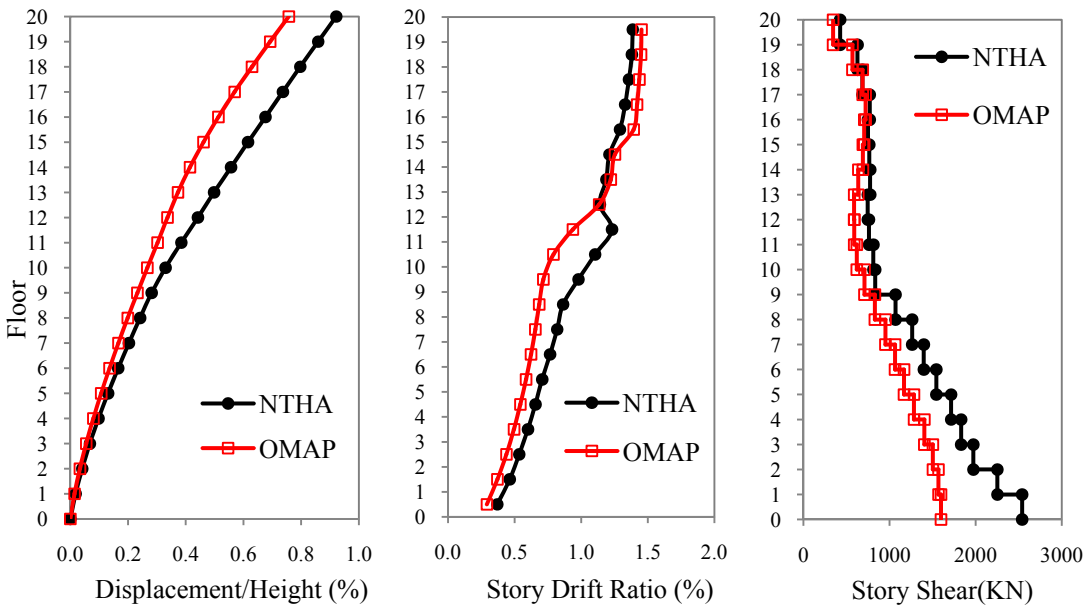

Fig. 3-11 Displacement, Story drift, and Story shear (OMAP vs NTHA)

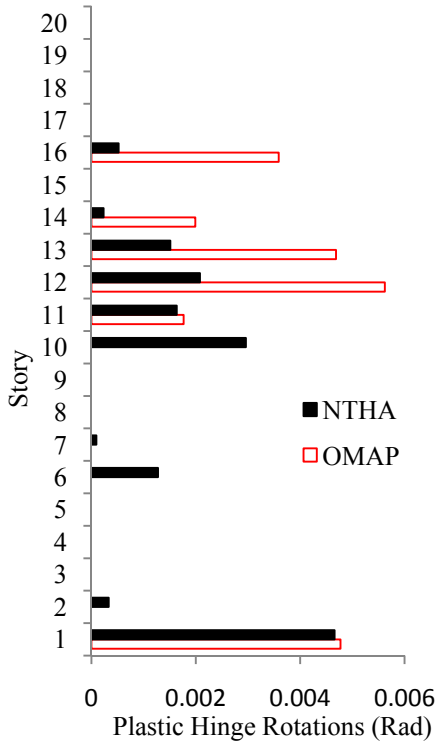

Fig. 3-12 Plastic Hinge Rotations (OMAP vs NTHA)

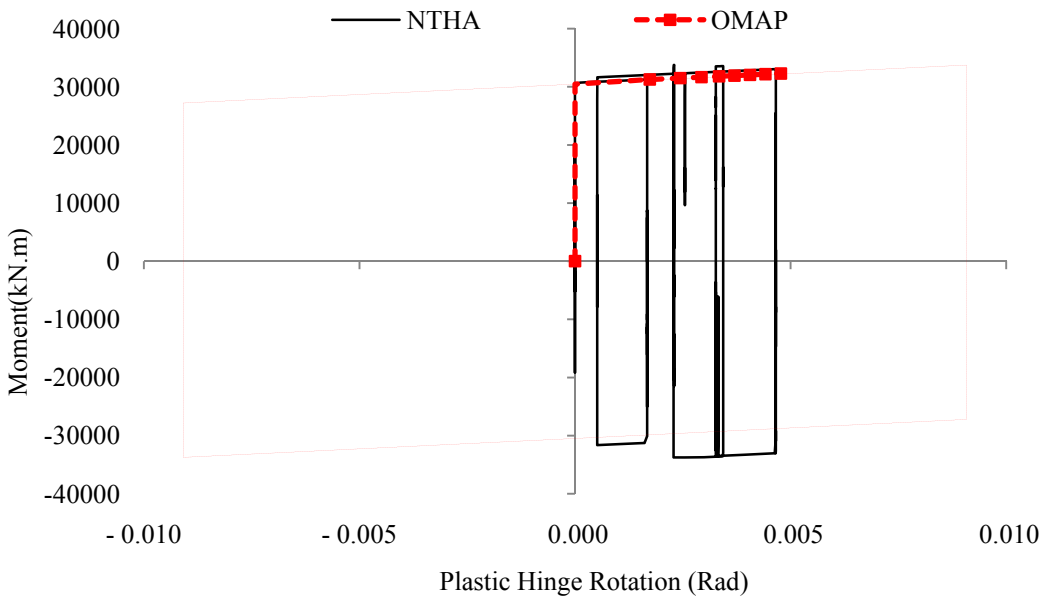

Fig. 3-13 Moment vs Plastic Hinge Rotation at the base

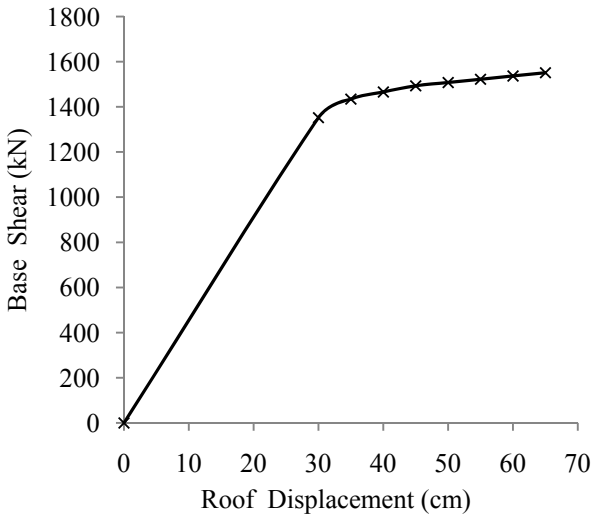

Fig. 3-14 Pushover curve (OMAP)

The OMAP procedure was applied to other case studies (W20/Erz, W30/Imp and W30/Erz). Another shear wall for 30 storys have been selected, the length of the wall is 6 m and the thickness is variable with the height. Table 3-4 summarizes the shear wall properties and Table3-5 summarizes the modal properties. The earthquake of Erzincan 1992 (Fig. 3-15) are applied for the two examples, 20 and 30 storys shear wall. Table 3-6 shows the structure references and the correspondent scale factors of the earthquake.

Table 3-4 Shear wall properties for 30–storey

Storey ID	Thickness (cm)	Longitudinal Reinforcement	Capacity Ratio* (Vertical Load)
1→5	35	2φ20/20cm	0.29
6→10	30	2φ18/20cm	0.29
11→15	28	2φ18/20cm	0.25
16→19	25	2φ14/20cm	0.22
20→21	20	2φ12/20cm	0.22
22→25	18	2φ12/20cm	0.21
26→28	15	2φ10/20cm	0.15
29→30	10	2φ10/20cm	0.14

* The capacity ratio concerns the first storey of each group

Table3-5. Modal properties for 30-storey shear wall

Mode	T (sec)	Γ	ξ%
1	4.91	22.86	5
2	0.86	12.71	2.6
3	0.33	7.86	5

4	0.19	0.00	8.4
5	0.17	5.64	9.1
6	0.11	4.38	14.3
7	0.08	3.67	20.5
8	0.07	0.00	22.4

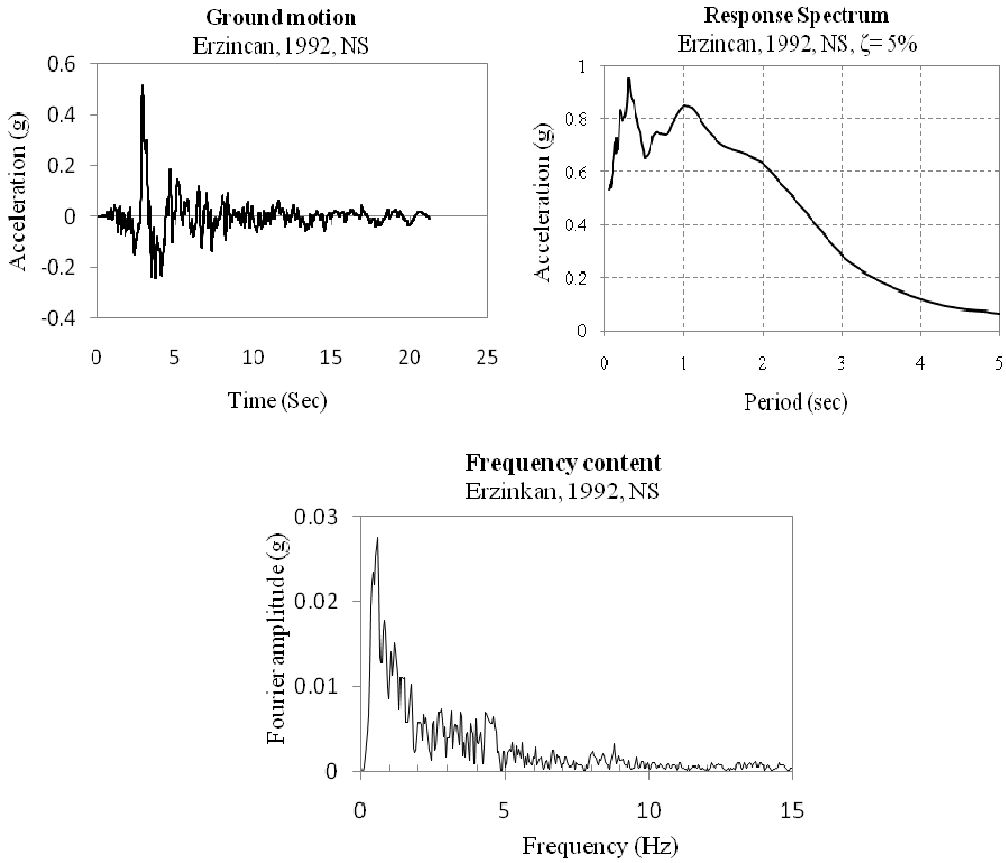

Fig. 3-15 Ground motions characteristics - Erzinkan, 1992, NS

Table 3-6 Structure references and correspondent scale factors of ground motions

Example	Structure Reference	No. of Storeys	Earthquake	Scale Factor
1	W20/Imp	20	Imperial Valley (1940)	2.5
2	W20/Erz	20	Erzincan (1992)	1.0
3	W30/Imp	30	Imperial Valley (1940)	1.5
4	W30/Erz	30	Erzincan (1992)	1.4

The adaptation effect is summarized in Fig. 3-16, Fig. 3-17, Fig. 3-18, Fig. 3-19. Results confirm the general trend observed for the first case study W20/Imp and

point out the great accuracy of the OMAP method with regard to the non-linear time history analysis.

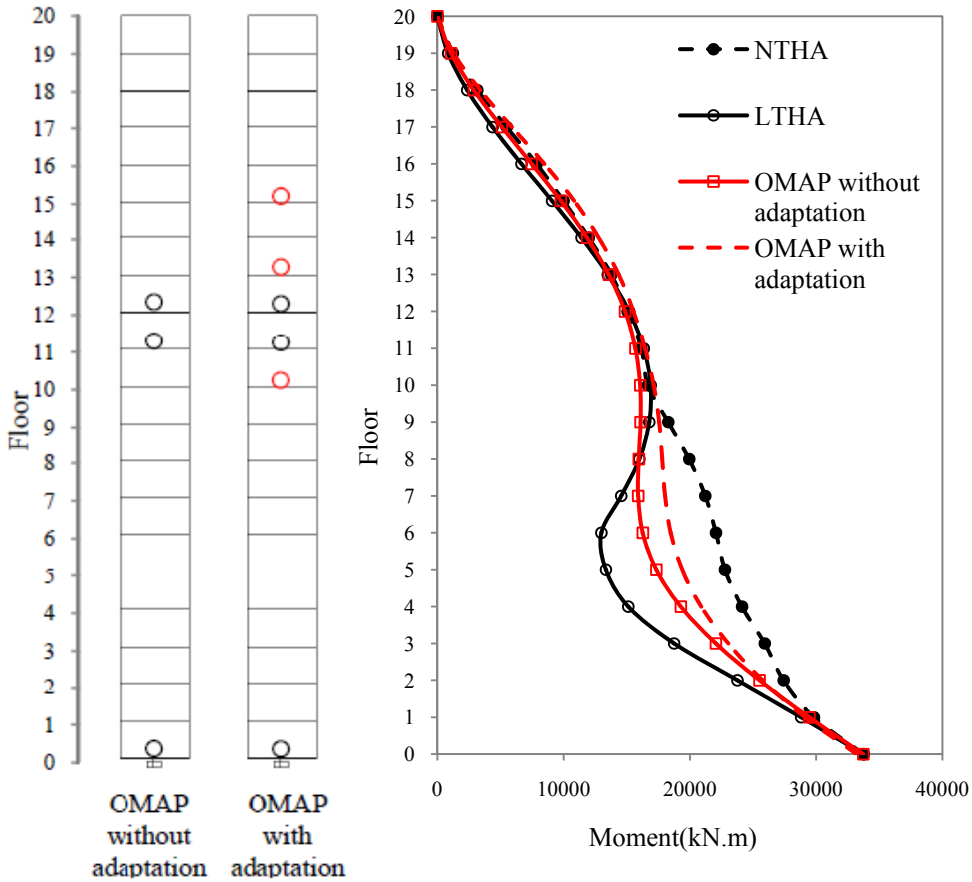

Fig. 3-16 Adaptation effect - Plastic hinge locations and corresponding moments (W20/Imp)

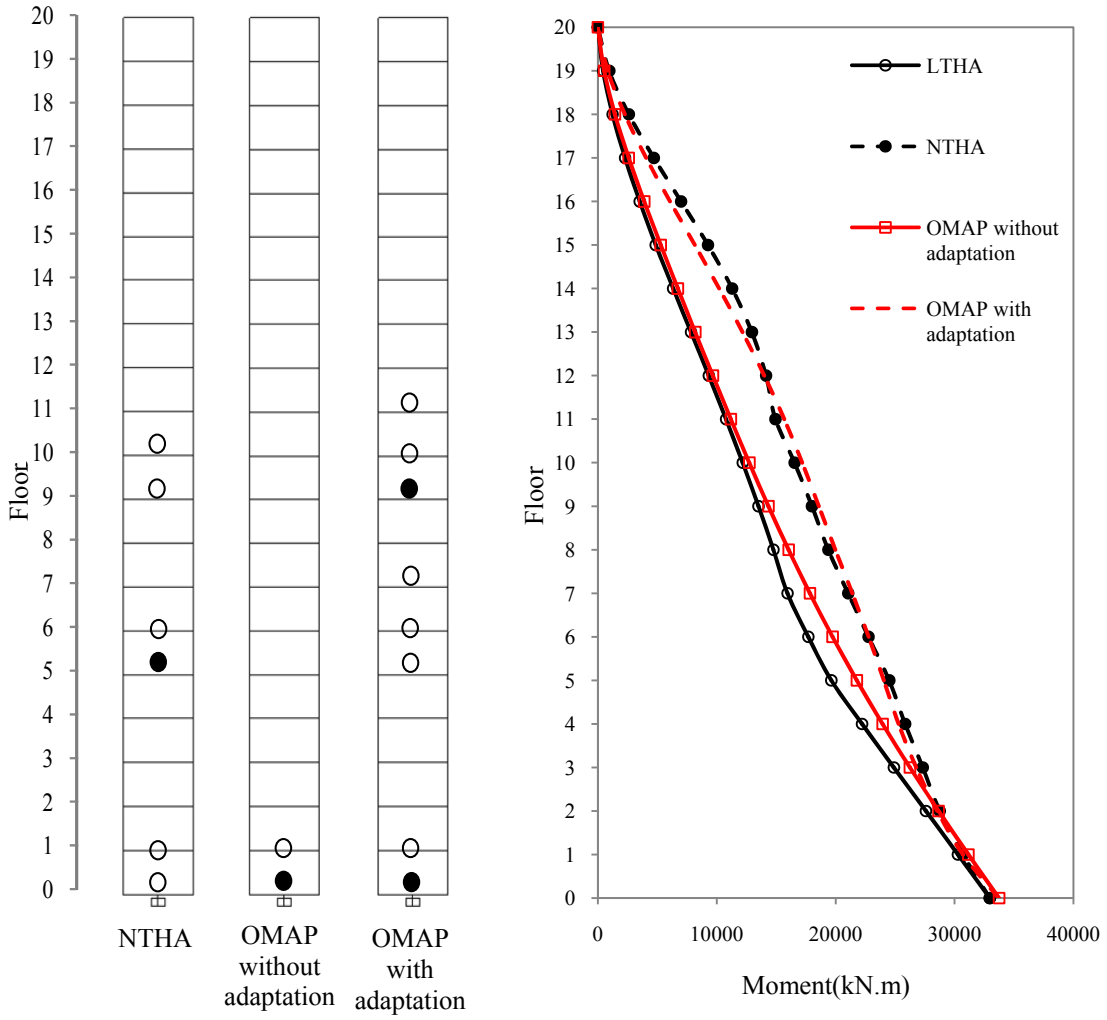

Fig. 3-17 Adaptation effect - Plastic hinge locations and corresponding moments (W20/Erz)

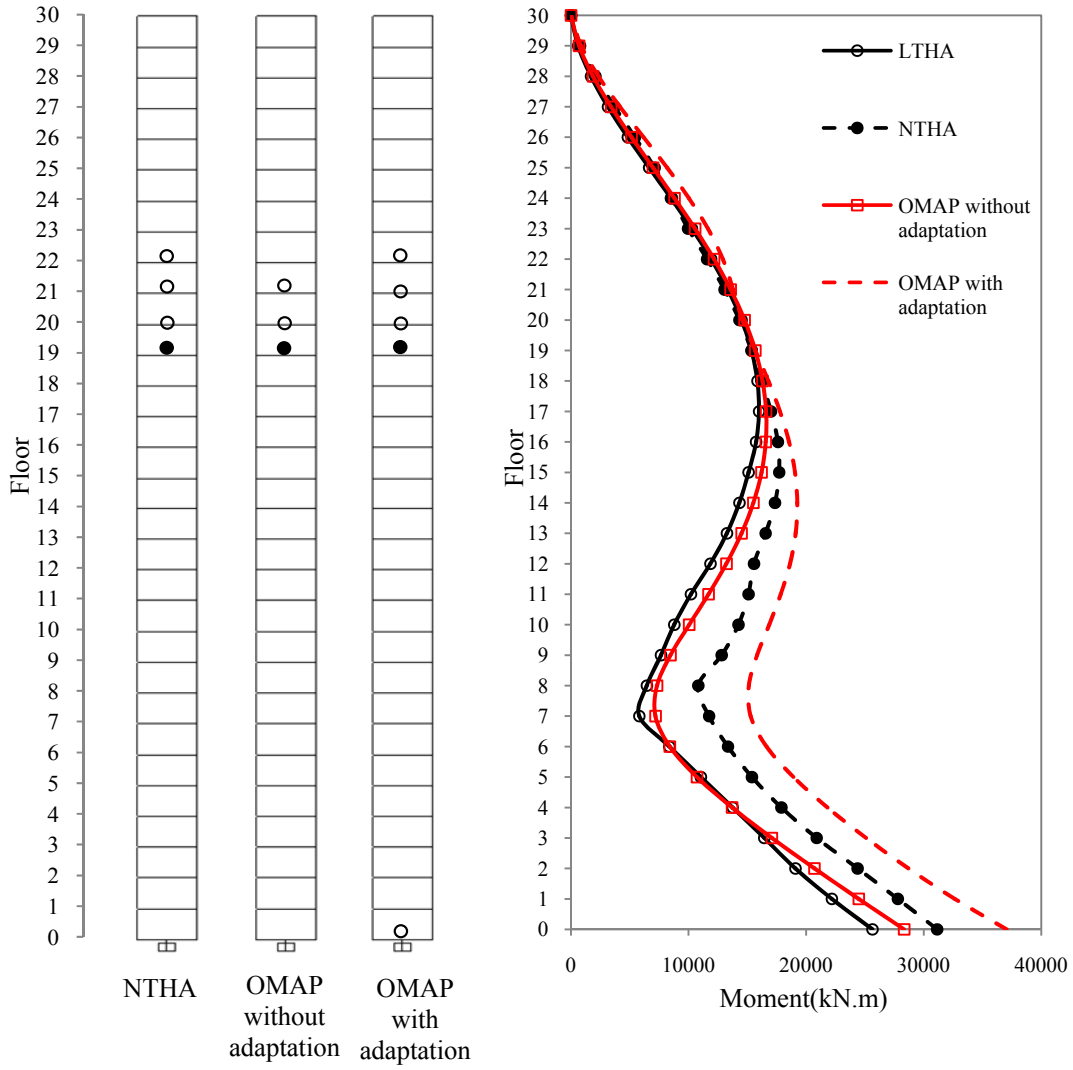

Fig. 3-18 Adaptation effect - Plastic hinge locations and corresponding moments (W30/Imp)

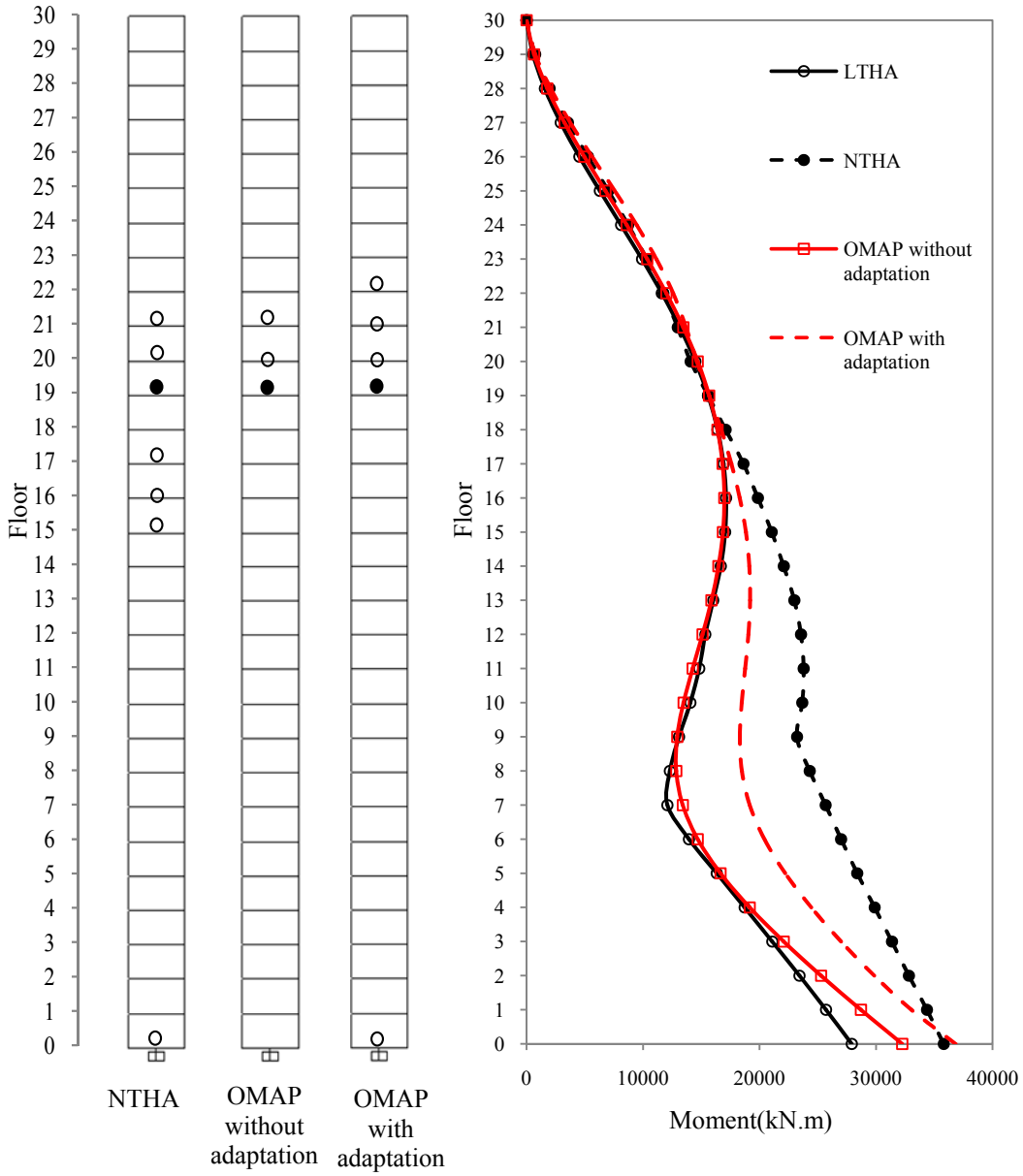

Fig. 3-19 Adaptation effect - Plastic hinge locations and corresponding moments (W30/Erz)

3.6 Conclusion

A new single-run adaptive pushover method "OMAP" is proposed to estimate the seismic response of shear wall structure. The load pattern is derived on the base of the overturning moment as recognition of the evidence that plasticity in the shear wall is mainly governed by this parameter. This method maintains the superiority of not decomposing the structure. At the same time, it avoids the pitfall which occurred in all

previous single-run adaptive pushover analyses in utilizing the modal combination for the applied loads instead of combining the response quantities induced by those loads in individual modes. The OMAP takes into account the progressive changes in the dynamic properties of the structure.

In order to illustrate its potential advantages, the results of the OMAP procedure have been compared to force-based and displacement-based procedures in addition to rigorous non linear time history analysis. The effect of both the base and the adaptation in the single-run adaptive pushover analysis are investigated. Results indicate that this method could predict the results of the nonlinear time history analysis appropriately, where the main advantage of this method consists in its easy implementation maintaining the principle of the adaptive response spectrum analysis.

The comparison between the non-adaptive form and the adaptive form of the proposed method emphasizes the importance of the adaptive feature to incorporate the progressive variation in dynamic and modal properties. The next chapter is concerned with the target displacement (performance point) which constitutes another major aspect of pushover analysis.

3.7 Appendix A : Incremental progressive variation in dynamic properties during the OMAP procedure

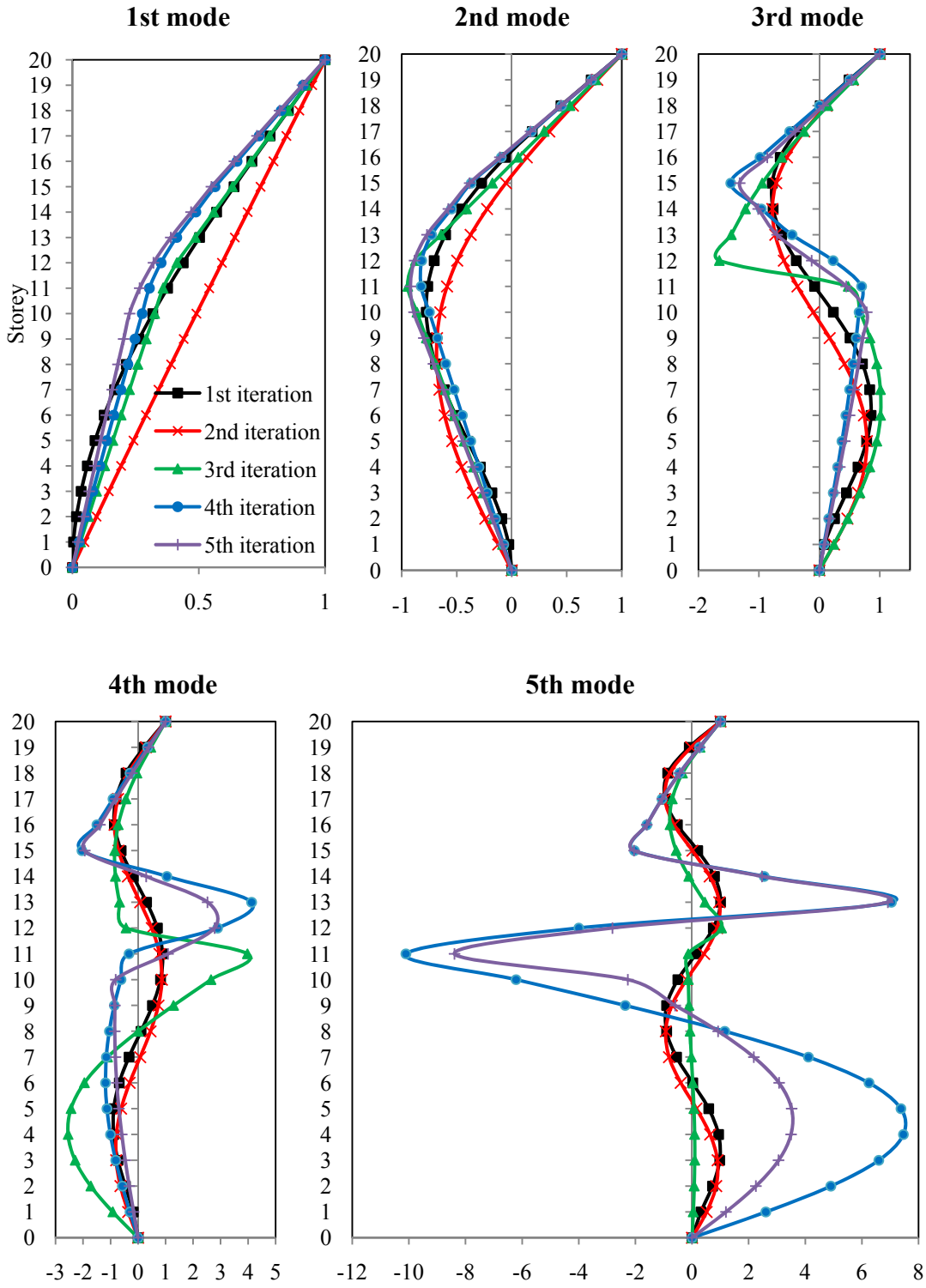

Fig. 3-20 Variation of the Modal shapes during the OMAP procedure

Table 3-7 Period

T (sec)	Iteration				
Mode	**1**	**2**	**3**	**4**	**5-8**
1	2.98	13.65	15.46	16.24	17.59
2	0.54	0.74	3.88	4.75	5.03
3	0.20	0.24	0.39	1.06	1.28
4	0.11	0.12	0.19	0.36	0.48
5	0.07	0.08	0.12	0.21	0.22

Table3-8 Damping ratio

ξ%	Iteration				
Mode	**1**	**2**	**3**	**4**	**5-8**
1	5.01	21.52	24.35	25.58	27.70
2	2.61	2.44	6.34	7.67	8.09
3	4.99	4.28	3.05	2.56	2.75
4	8.75	7.86	5.24	3.17	2.73
5	13.49	12.52	8.20	4.86	4.69

Table3-9 Modal participating mass ratios

%	Iteration				
Mode	**1**	**2**	**3**	**4**	**5-8**
1	0.62	0.76	0.67	0.64	0.60
2	0.19	0.13	0.18	0.21	0.25
3	0.072	0.043	0.043	0.024	0.028
4	0.038	0.020	0.052	0.022	0.013
5	0.023	0.012	0.001	0.059	0.031

Table3-10 Spectral accelerations

Sa (m/sec^2)	Iteration				
Mode	**1**	**2**	**3**	**4**	**5-8**
1	0.862	0.007	0.005	0.005	0.004
2	7.352	0.635	0.033	0.015	0.013
3	5.450	0.906	0.586	0.352	0.200
4	4.352	0.711	0.497	0.531	0.579
5	3.735	0.515	0.484	0.476	0.442

3.8 References

Antoniou, S., Pinho, R. (2004a). Advantages and limitations of adaptive and non adaptive force-based pushover Procedures. Journal of Earthquake Engineering, Vol. 8, No 4, pp. 497-522.

Antoniou, S., Pinho, R. (2004b). Development and verification of a displacement-based adaptive pushover Procedure. Journal of Earthquake Engineering, Vol. 8, No. 5, pp. 643-661.

ATC. Seismic evaluation and retrofit of concrete buildings. Report ATC-40. Redwood City (CA): Applied Technology Council; 1996.

Aydinoğlu, M. N. (2003). An incremental response spectrum analysis procedure based on inelastic spectral displacements for multi-mode seismic performance evaluation. Bull Earthquake Eng, 1:3_36.

Aydinoğlu, M. N. (2004). An improved pushover procedure for engineering practice: Incremental response spectrum analysis procedure (IRSA). In: International workshop on performance-based seismic design: concept and implementation. Bled, Slovenia. PEER Report 2004/05, pp. 345-356.

Aydinoğlu, M. N. (2007). A response spectrum-based nonlinear assessment tool for practice: incremental response spectrum analysis (IRSA). ISET Journal of Earthquake Technology, Paper No. 481, Vol. 44, No. 1, pp. 169–192.

Baros DK, Anagnastopoulos SA (2008) An assessment of static nonlinear pushover analyses in 2-D and 3-D applications, In: Bento R, Pinho R (eds) 3D Pushover 2008—proceedings of nonlinear static methods for design/assessment of 3D structures. IST Press, Lisbon, pp 45–58

Building Seismic Safety Council (BSSC). Pre-standard and commentary for the seismic rehabilitation of buildings. FEMA-356, Washington (DC): Federal Emergency Management Agency ; 2000.

Casarotti, C., Pinho, R. (2007). An adaptive capacity spectrum method for assessment of bridges subjected to earthquake action. Bull Earthquake Eng, 5,pp. 377–390.

Charney, F. A. (2008). Unintended consequences of modelling damping in structures. J StructEng ASCE, 134(4), pp. 581–592.

Chopra A.K. (2007). Dynamics of Structures, third edition, Prentice Hall, New Jersey.

Chopra A.K., Goel R.K. (2001). A modal pushover analysis procedure to estimate seismic demands for buildings: Theory and Preliminary Evaluation. PEER Report 2001/03, Pacific Earthquake Engineering Center, University of California Berkeley.

Chopra, A. K., and Goel, R. K. (2002). A modal pushover analysis procedure for estimating seismic demands for buildings. Earthquake Eng. Struct. Dyn., 31(3), pp. 561-582.

Computers, Structures Incorporated (CSI). SAP 2000 NL. USA, CA: Berkeley; 2007.

Elnashai, A. S. (2001). Advanced inelastic static (pushover) analysis for earthquake applications. Structural Engineering and Mechanics 12(1), pp. 51-69.

Goel, R. K., and Chopra, A. K. (2005). Extension of Modal Pushover Analysis to Compute Member Forces. Earthquake Spectra 21:125-139

Gupta, B., and Kunnath, S. K. (2000). Adaptive spectra-based pushover procedure for seismic evaluation of structures. Earthquake Spectra, 16(2), pp. 367-391.

IBC. (2003). International Building Code.

Kalkan, E. and Kunnath, SK. (2006). Adaptive modal combination procedure for nonlinear static analysis of building structures. J StructEng ASCE, 132(11), pp. 1721-1731.

Newmark, N.M. and Hall, W.J. (1982). Earthquake Spectra and Design, monograph. Earthquake Engineering Research Institute (EERI), Berkeley, California. Print.

Shakeri, K., Shayanfar, MA. and Kabeyasawa, T. (2010). A story shear-based adaptive pushover for estimating seismic demands of buildings. Eng Struct,32, pp. 174–83.

Smyrou, E., Priestley, M.J.N. and Carr, A.J. (2011). Modelling of Elastic Damping in Nonlinear Time-history Analyses of Cantilever RC Walls. Bulletin of Earthquake Engineering,9,pp. 1559-1578 (DOI: 10.1007/s10518-011-9286-y)

http://peer.berkeley.edu/smcat/

Chapter 4: Capacity Spectrum Method for a Single-run Adaptive Pushover Analysis

(Seismic Evaluation of Shear Wall Structures by OMAP method)

4.1 Abstract

The capacity spectrum method (CSM) proposed in ATC-40 (1996) is widely used in structural engineering practice. The basic assumption used in this method is that the structure vibrates predominantly in a single mode. On the other hand, the single-run adaptive pushover procedures are considered as practical tools to integrate the effect of higher modes with full interaction between them. Using modal equivalent seismic loads to do one pushover analysis leads to the absence of the pushover curve for each mode. Consequently, the use of an equivalent single degree of freedom system, as in CSM, for estimating the peak response quantities becomes unavailable. This chapter proposes an innovative method for integrating the principle of single run adaptive pushover procedures in CSM. The rigorous analytical base of the proposed method can be considered as a consequence of avoiding the pitfall inherent in single-run adaptive pushover procedures as illustrated in the previous chapter.

4.2 Introduction:

Estimating the peak response quantities using single-run adaptive pushover procedures is considered as the main limitation related to this type of analyses, where the pushover curve obtained combines multi-mode effects. This reported that using an equivalent single degree of freedom system for estimating the peak response quantities becomes unavailable (Aydinoğlu, 2003). A lot of single-run adaptive pushover procedures propose directly a target displacement instead of being calculated value (Antoniou and Pinho, 2004a; Antoniou and Pinho, 2004b). An attempt to specify the performance point (target displacement) for a single-run adaptive pushover procedure was firstly proposed by Casarotti and Pinho (2007). They used the floor displacements as an equivalent mode for finding the equivalent single degree of freedom for the system. Although the method was developed for bridge application, it was mentioned that it can be applied to building as well. In fact,

the proposed method does not have a consistent theoretical base. This critic is included in the paper itself by saying "*The authors are happy to note, however, that such apparent theoretical inconsistency did not prevent the proposed method from producing very good response predictions of the bridge case-studies considered in this work*". Also, Shakeri et al (2010) proposed another single-run adaptive pushover procedure and they have adopted the same methodology as Casarotti and Pinho (2007) for specifying the performance point. Controversially, in the validation examples, the proposed methodology for estimating the performance point has not been used but the target displacement was directly computed through the non-linear time history analysis.

This paper proposes an innovative method for specifying the performance point with single-run adaptive pushover procedures. The rigorous analytical base of the proposed method can be considered as a consequence of avoiding the pitfall inherent to the single-run adaptive pushover procedures. This pitfall, as mentioned in the previous chapter, consists in the use of the modal combination in defining the applied loads instead of combining the response quantities induced by those loads in individual modes (Chopra 2007, p. 569; Aydinoğlu 2003, 2007).

In the proposed method, although a single-run adaptive pushover analysis is performed, the modal quantities are picked out at each increment. As a result, using equivalent single degree of freedom system for estimating the peak response quantities becomes available.

In the first part of this chapter and after an important description of the theoretical basis of pushover methods, the methods converting the capacity curve to a capacity spectrum are presented. The comparison between the conventional pushover analysis method and the energy-based formulation one demonstrates that for adaptive pushover procedures there is no difference between the two methods. Then a new method to convert the capacity curve to a capacity spectrum is developed. This method does not only have conceptual superiority but it also has easier numerical implementation.

4.3 Theoretical Basis of Pushover Methods

The theoretical basis of pushover analysis can be developed using the linear modal response history analysis (MRHA). Where in MRHA, the structure is loaded using the inertia force distribution for each mode independently, then any response quantity r(t) (e.g. displacements, internal element forces, or moments) may be calculated as a combination of each of the modal responses $r_n(t)$ due to the external applied force.

For an inelastic structure, many methods have been proposed in the literature to combine the modal responses as described in the previous chapter.

4.3.1 *Modal response history analysis (MRHA)*

4.3.1.1 Classical modal equations

The differential equation of the dynamic response of a linear elastic multi- degree of freedom structure subjected to a horizontal base excitation $\ddot{u}_g$ is:

$$\ddot{\mathbf{u}} + \mathbf{c}\dot{\mathbf{u}} + \mathbf{k}\mathbf{u} = -\mathbf{m}\mathbf{1}\ddot{u}_g(t) = \mathbf{p}_{eff}(t) \quad (1)$$

In the case of a multistory building, u is a vector of N components that represents the lateral displacements of the floors relative to the base, and **m**, **c** and **k** are the mass, damping and stiffness matrices of the structure. The vector **1** is a column vector with each component equal to 1, $\mathbf{p}_{eff}(t)$ is a vector of the effective forces.

The displacement vector, **u**, can be decomposed into components expressed in terms of the free vibration mode shapes (ϕ_n), where q_n is the nth modal coordinate.

$$u = \sum_{n=1}^{N} u_n(t) = \sum_{n=1}^{N} \phi_n q_n(t) \quad (2)$$

The expression of the displacement vector in terms of the mode shapes [Eq. (2)] allows the system of N coupled equations represented by Eq. (1) to be uncoupled in terms of the modal coordinates. Substitution of Eq. (2) into Eq. (1) and application of the properties of orthogonality of the free vibration mode shapes with respect to **m**, **c** and **k** result in:

$$M_n\ddot{q}_n(t) + C_n\dot{q}_n(t) + K_n q_n(t) = -\phi_n^T\mathbf{m}\mathbf{1}\ddot{u}_g(t)$$

Or, alternatively as

$$\ddot{q}_n(t) + 2\zeta_n\omega_n\dot{q}_n(t) + \omega_n^2 q_n(t) = -\Gamma_n\ddot{u}_g(t) \tag{3}$$

where ζ_n is the damping ratio, ω_n is the natural vibration frequency and Γ_n is the modal participation factor:

$$\Gamma_n = \frac{L_n}{M_n}\ , \quad M_n = \phi_n^T\mathbf{m}\phi_n, \quad L_n = \phi_n^T\mathbf{m1} \tag{4}$$

A further simplification can be achieved by setting $q_n(t) = \Gamma_n D_n(t)$, resulting in the following differential equation of motion for the SDOF system:

$$\ddot{D}_n(t) + 2\zeta_n\omega_n\dot{D}_n(t) + \omega_n^2 D_n(t) = -\ddot{u}_g(t) \tag{5}$$

The solution of Eq. (5) for the $D_n(t)$ corresponding to each mode is the basis of modal response history analysis (MRHA), for which the vector u is given by:

$$\mathbf{u}(t) = \sum_{n=1}^{N}\mathbf{u}_n(t) = \sum_{n=1}^{N}\phi_n\Gamma_n D_n(t) \tag{6}$$

4.3.1.2 Modal expansion of excitation vector **p**(t) = **s** p(t)

In our case the applied forces $\mathbf{p}(t) = \mathbf{p}_{eff}(t)$ have the same time variation $p(t) = -\ddot{u}_g(t)$, and their spatial distribution is defined by $\mathbf{s} = \mathbf{m1}$ independent of time.

In order to address the forces that act on the structure for each modal response, the effective force, $\mathbf{p}_{eff}(t)$ should be decomposed taking note of the orthogonality of the mode shapes with respect to the mass matrix, where any element of the vector space can be expressed uniquely as a finite linear combination of basis vectors.

$$\mathbf{s} = \sum_{n=1}^{N}\mathbf{s}_n = \sum_{n=1}^{N} a_n\mathbf{m}\phi_n \tag{7}$$

Premultiplying both sides of Eq. (8) by ϕ_n^T and utilizing the orthogonality property of modes gives:

$$a_n = \frac{\phi_n^T\mathbf{s}}{\phi_n^T\mathbf{m}\phi_n} \tag{8}$$

The contribution of the nth mode to **s** is

$$\mathbf{s}_n = a_n \mathbf{m} \phi_n \tag{9}$$

which is independent of how the modes are normalized. This should be clear from the structure of Eqs. (8) and (9).

For **s=m1** => $a_n = \Gamma_n$

$$\mathbf{s}_n = \Gamma_n \mathbf{m} \phi_n \tag{10}$$

The effective earthquake forces can then be expressed as

$$\mathbf{p}_{eff}(t) = \sum_{n=1}^{N} \mathbf{p}_{eff,n}(t) = \sum_{n=1}^{N} -\mathbf{s}_n \ddot{u}_g(t) \tag{11}$$

Substituting Eq. (2), Eq. (10) and Eq. (11) into Eq. (1), and multiplying both sides by ϕ_n^T results in

$$\phi_n^T \left(\sum_{n=1}^{N} m\phi_n \ddot{q}_n(t) + \sum_{n=1}^{N} c\phi_n \dot{q}_n(t) + \sum_{n=1}^{N} k\phi_n q_n(t) = -\sum_{n=1}^{N} \Gamma_n m\phi_n \ddot{u}_g(t) \right) \tag{12}$$

which indicates that only the $\mathbf{s}_n$ component of $\mathbf{p}_{eff}(t)$ results in a non-zero response in the nth mode, Thus, $\mathbf{p}_{eff,n}(t)$ can be expressed as:

$$\mathbf{p}_{eff,n}(t) = -\mathbf{s}_n \ddot{u}_g(t) = -\Gamma_n \mathbf{m} \phi_n \ddot{u}_g(t) \tag{13}$$

Thus, it is apparent that only $\mathbf{p}_{eff,n}(t)$ causes response in the nth mode.

4.3.1.3 Calculation the modal responses by introducing modal equivalent static forces

An equivalent static force $\mathbf{f}_n(t)$ can be associated with the nth mode displacement $\mathbf{u}_n(t)$. The equivalent static force $\mathbf{f}_n(t)$ is the statically applied force that results in a displacement equal to $\mathbf{u}_n(t)$:

$$\mathbf{f}_n(t) = \mathbf{k}\mathbf{u}_n(t) = \mathbf{k}\phi_n q_n(t) = \omega_n^2 \mathbf{m} \phi_n \Gamma_n D_n(t) = \mathbf{s}_n A_n(t) \tag{14}$$

where $A_n(t)$ is the pseudo-acceleration:

$$A_n(t) = \omega_n^2 D_n(t) \tag{15}$$

So it can be emphasized that the pseudo-acceleration provides the exact peak value of the equivalent static force (elastic force), while the 'true' acceleration is needed to determine the peak value of the sum of elastic and damping forces (The force transmitted to the base).

For the elastic response, any response quantity r(t) (e.g. storey drifts, internal element forces) may be calculated as a combination of each of the modal responses $r_n(t)$ in modal response history analysis (MRHA):

$$r(t) = \sum_{n=1}^{N} r_n(t) = \sum_{n=1}^{N} r_n^{st} A_n(t) \tag{16}$$

where r_n^{st} is the static response of quantity r_n due to the external force $\mathbf{s}_n$. r_n^{st} and $A_n(t)$ are shown schematically in Fig. 4-1

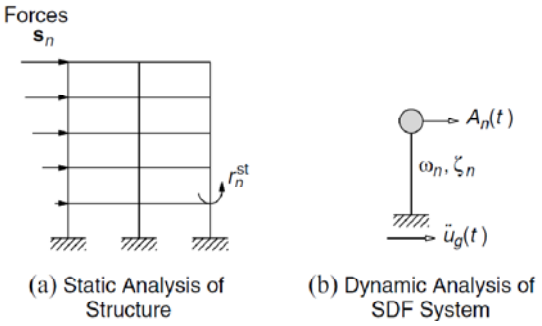

Fig. 4-1 Conceptual explanation of modal RHA of elastic MDF systems (Chopra and Goel 2002)

4.3.2 *Modal response spectrum analysis (RSA)*

The peak value of $r_n(t)$ for the nth mode is called r_{no}. Thus,

$$r_{no} = r_n^{st} A_n \tag{17}$$

where A_n is the ordinate of the pseudo-acceleration design (or response) spectra corresponding to the nth modal period. The peak value of the total response of the quantity r(t), given by r_o, can be estimated according to a combination rule such as CQC or SRSS. These rules combine the peak values obtained for each mode (Fig. 4-2).

$$\mathbf{s}_n = \Gamma_n \mathbf{m} \phi_n$$

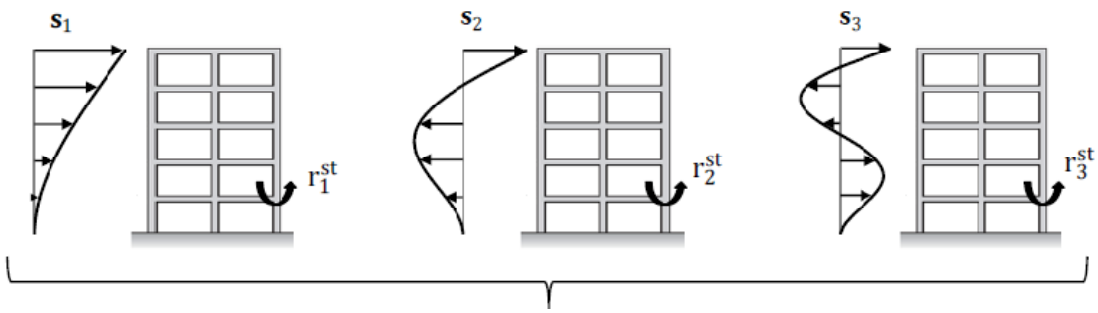

$$r_o \approx \sqrt{\sum_{n=1}^{N} r_{no}^2} = \sqrt{\sum_{n=1}^{N} (r_n^{st} A_n)^2}$$

Fig. 4-2 Conceptual explanation of modal RSA of elastic MDF systems

4.3.3 *Modal pushover analysis*

To develop a pushover analysis procedure consistent with RSA, we observe that static analysis of the structure subjected to lateral forces

$$\mathbf{f}_{no} = \mathbf{m}\boldsymbol{\phi}_n \Gamma_n A_n \tag{18}$$

will provide the same value of r_{no}, the peak nth-mode response as in Equation (17). Alternatively, this response value can be obtained by static analysis of the structure subjected to lateral forces distributed over the building height according to

$$\mathbf{s}_n^* = \mathbf{m}\phi_n$$

with the structure pushed to the roof displacement, u_{rno}, the peak value of the roof displacement due to the nth-mode, which from Equation (6) is

$$\mathbf{u}_{rno} = \phi_{rn} \Gamma_n D_n \tag{19}$$

The peak modal responses r_{no}, each determined by one pushover analysis, can be combined according to SRSS or CQC to obtain an estimate of the peak value r_o of the total response.

4.4 Capacity Spectrum Method to perform nonlinear analysis

The capacity spectrum method (CSM) was developed by Freeman (1975, 1998). It compares the capacity of a structure with the demands of earthquake ground motion on the structure for estimating the peak response quantities (Performance Point). The method is easy to understand, so it is adopted in this work to clarify how to estimate the peak response quantities of the structure using single-run adaptive pushover procedures. The basic assumption used in this method is that the structure vibrates predominantly in a single mode. Integrating the principle of single run adaptive

pushover procedures in this method allows in overcoming this limitation related to the higher modes of vibration.

Simplified nonlinear analysis procedures using pushover methods, such as the capacity spectrum method, require the determination of three primary elements: capacity, demand and performance.

Capacity is a representation of the structure's ability to resist the seismic demand. Structure capacity is usually represented by a pushover curve (capacity curve). The most convenient way to plot the force-displacement curve is by tracking the base shear force and the roof displacement. The base shear forces (V) and roof displacements (u_r) are converted to the spectral accelerations (A) and spectral displacements (D) of an equivalent Single-Degree-Of-Freedom (SDF) system, respectively (see Fig. 4-3). These spectral values define the capacity spectrum. Section 4.4.1 presents the methods generally used in the literature and the methodology proposed in this thesis to convert of the Capacity Curve to the Capacity Spectrum.

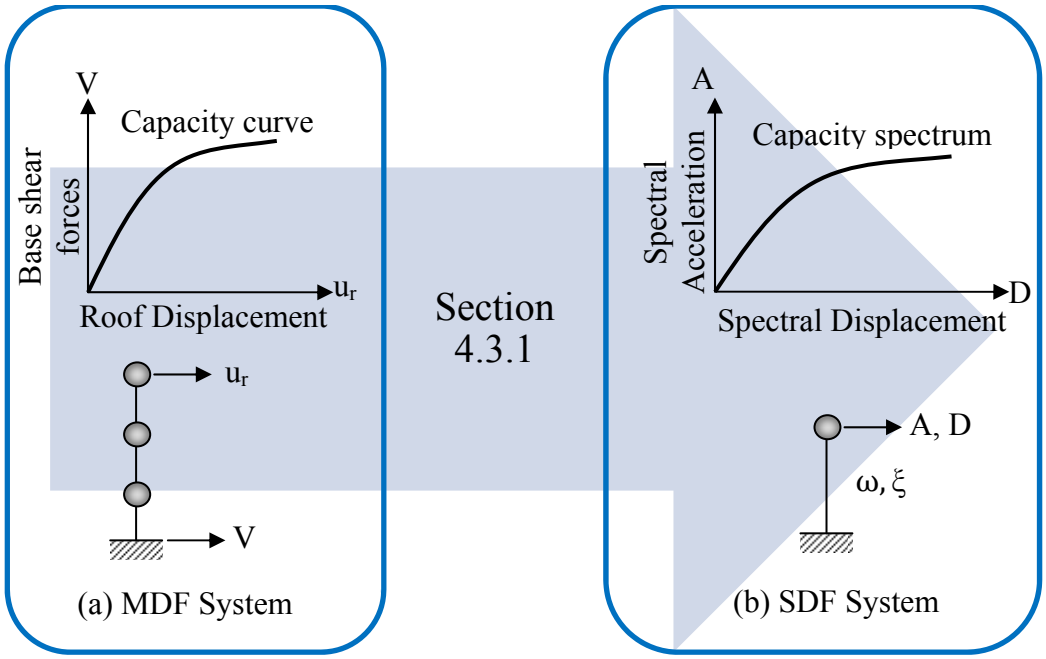

Fig. 4-3 Conversion of the Capacity Curve to the Capacity Spectrum

Demand (displacement) is an estimate of the maximum expected response of the building during the ground motion. Traditional linear analysis methods use lateral forces to represent a design condition. For nonlinear methods, it is easier and more direct to use a set of lateral displacements as a design condition. In CSM the demand curve is defined by highly damped elastic spectra reduced from the elastic design spectrum by using an approximate effective damping. The effective damping is calculated based on the shape of the capacity curve, the estimated displacement demand, and the resulting hysteresis loop. Section 4.4.2 presents how the effective damping could be calculated. The Acceleration-Displacement Response Spectrum (ADRS) format is used, in which spectral accelerations (Sa) are plotted against spectral displacements (Sd), with the periods represented by radial lines (see Fig. 4-4).

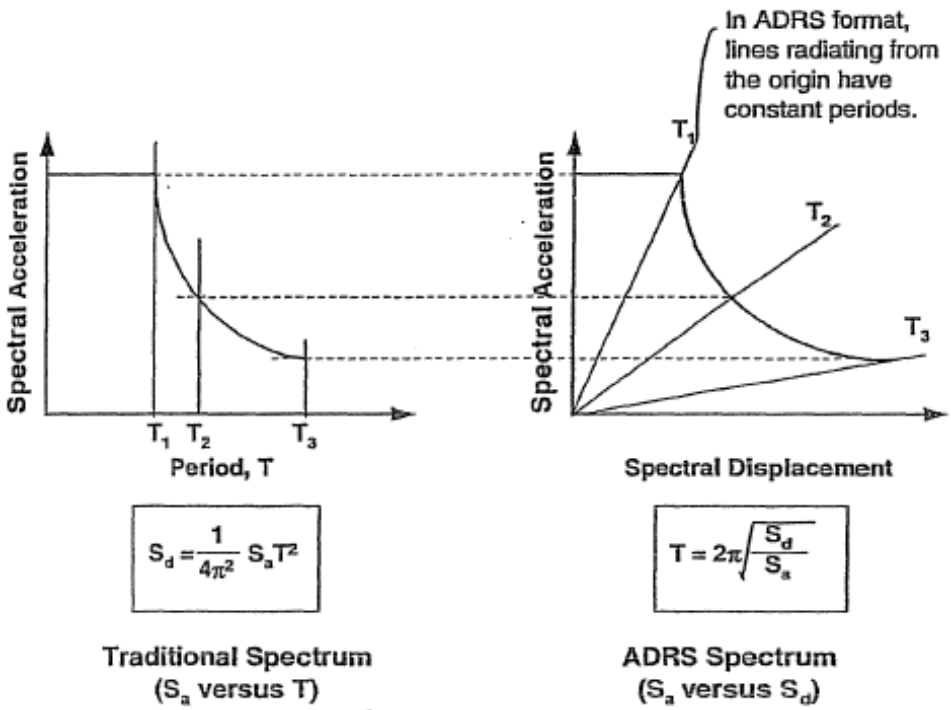

Fig. 4-4 Response spectra in Traditional andADRSFormats (ATC-40)

Performance is dependent on the manner that the capacity is able to handle the demand. The location of the Performance Point must satisfy two relationships: 1) The point must lie on the capacity spectrum curve in order to represent the structure at a given displacement, and 2) the point must lie on a spectral demand curve that represents the nonlinear demand at the same structural displacement. In other words,

the Performance Point is the point of the interaction between the capacity spectrum curve and the spectral demand curve.

4.4.1 *Conversion of the Capacity Curve to the Capacity Spectrum*

4.4.1.1 Conventional Method (ATC-40)

To use the capacity spectrum method proposed by ATC-40 (1996), it is necessary to convert the capacity curve, which is in terms of base shear and roof displacement to what is called a capacity spectrum, which is a representation of the capacity curve in Acceleration-Displacement Response Spectra (ADRS) format (i.e., D_n versus A_n). According to Eq. (19), the roof displacement for the mode n is $\mathbf{u}_{rn} = \phi_{rn}\Gamma_n D_n$ (In ATC-40, *n* is restricted to the first mode only). So,

$$D_n = \frac{\mathbf{u}_{rn}}{\phi_{rn}\Gamma_n} \tag{20}$$

The equation for the base shear, V_n, of the MDOF system is developed below, in order to identify the values to be plotted on the ordinate of the common representation. According to Eq. (18) :$f_n = \mathbf{m}\boldsymbol{\phi}_n\Gamma_n A_n$. So,

$$V_n = \mathbf{f}_n^T.\mathbf{1} = \phi_n^T\mathbf{m}.\mathbf{1}\Gamma_n A_n = L_n\Gamma_n A_n = \alpha_n A_n$$

$$A_n = \frac{V_n}{\alpha_n} \tag{21}$$

where α_n is the modal mass coefficient for the nth mode.

$$\alpha_n = L_n\Gamma_n = \frac{(\phi_n^T\mathbf{m}.\mathbf{1})^2}{\phi_n^T\mathbf{m}\phi_n} \tag{22}$$

4.4.1.2 Energy-Based Formulation of Modal Pushover Analysis (Hernandez-Montes et al. 2004)

As described before, the conventional pushover methods (e. g. ATC-40) of analysis establish the capacity curve of a structure with respect to the roof displacement. Disproportionate increases in the roof displacement, and even outright reversals in the case of higher mode pushover analyses (Goel and Chopra 2005), can distort the capacity curve of the "equivalent" SDOF system.

Hernandez-Montes et al. (2004) developed an energy based formulation to find the capacity spectrum. This method considers the energy absorbed (or the work

done) in the pushover analysis rather than viewing pushover analyses from the perspective of roof displacement. So, it avoids the arbitrary selection of a single floor (or roof) location as the parameter for representing the capacity curve, and may be used with single or multimode analysis procedures. The energy-based formulation is redeveloped below in order to compare it with our proposed method for adaptive modal pushover analysis (Section 4.4.1.3).

The equation of motion is often expressed as the dynamic equilibrium of force quantities [Eq. (1)], but it can equivalently be expressed in terms of energy quantities. The "absolute" energy form of Eq. (1), expressed in terms of the energy developed from the time that the excitation starts, can be obtained by integrating Eq. (1) with respect to displacement, as described by Uang and Bertero [1988]:

$$\frac{1}{2}\dot{\mathbf{u}}_t^T\mathbf{m}\dot{\mathbf{u}}_t + \int \dot{\mathbf{u}}^T\mathbf{c}d\mathbf{u} + \int \mathbf{f}_s^T d\mathbf{u} = \int(\sum_{i=1}^{ns} m_i\ddot{u}_{ti})du_g \tag{23}$$

Or in the relative formulations:

$$\frac{1}{2}\dot{\mathbf{u}}^T\mathbf{m}\dot{\mathbf{u}} + \int \dot{\mathbf{u}}^T\mathbf{c}d\mathbf{u} + \int \mathbf{f}_s^T d\mathbf{u} = -\int \mathbf{m1}\ddot{u}_g(t)d\mathbf{u} \tag{24}$$

where m_i is the lumped mass associated with the ith story and $\ddot{u}_{ti}$ is the absolute (or total) acceleration at the ith story, and f_s is the restoring force.

In both the "absolute" and "relative" energy formulations of the equation of motion, the absorbed energy, E_a is

$$E_a = \int \mathbf{f}_s^T d\mathbf{u} \tag{25}$$

As pointed out in the development of Eq. (14), the static force associated with the nth mode is fn(t). The restoring force is assumed to be equal to sum of the modal components $f_n(t)$. Following this assumption, the restoring force f_s can be represented in terms of its modal components:

$$\mathbf{f}_s(t) = \sum_{n=1}^{N} \mathbf{f}_n(t) = \sum_{n=1}^{N} \omega_n^2 \mathbf{m}\phi_n\Gamma_n D_n(t) \tag{26}$$

Due to the orthogonality of modes with respect to **k** the force $\mathbf{f}_n$ does work only for displacements in the nth mode. The work done by $\mathbf{f}_n$ on the differential modal displacements $d\mathbf{u}_r$ can be computed by substituting Eq. (14) for f_n and Eq. (2) for u_r:

$$\mathbf{f}_n^T(t)d\mathbf{u}_r = \phi_n^T\mathbf{k}\phi_r q_n(t)dq_r(t) \tag{27}$$

Where, $\phi_n^T\mathbf{k}\phi_r \neq 0$ for n=r and 0 otherwise

Thus, dE_n can be expressed as:

$$dE_n(t) = \mathbf{f}_n^T(t)d\mathbf{u}_n \tag{28}$$

In the elastic domain, the absorbed energy associated with the static force f_n going through an elastic displacement from 0 to u_n is:

$$E_n(t) = \int_{\mathbf{0}}^{\mathbf{u}_n} \mathbf{u}_n^T(t)\mathbf{k}d\mathbf{u}_n = \frac{1}{2}\mathbf{u}_n^T(t)\mathbf{k}\mathbf{u}_n(t) = \frac{1}{2}\mathbf{f}_n^T(t)\mathbf{u}_n \tag{29}$$

$$E_n(t) = \frac{1}{2}\mathbf{f}_n^T(t)\mathbf{u}_n = \frac{1}{2}\omega_n^2\phi_n^T\mathbf{m}\phi_n\Gamma_n^2D_n^2(t) = \frac{1}{2}\omega_n^2M_n\Gamma_n^2D_n^2(t) \tag{30}$$

The corresponding base shear associated with the nth mode pushover is:

$$V_n(t) = \mathbf{f}_n^T(t).\mathbf{1} = \omega_n^2\Gamma_n\phi_n^T\mathbf{m}.\mathbf{1}D_n(t) = \omega_n^2\Gamma_n^2M_nD_n(t) \tag{31}$$

Substituting Eq. (31) into Eq. (30), gives:

$$E_n(t) = \frac{1}{2}V_n(t)D_n(t) \tag{32}$$

More generally, for both the elastic and inelastic response, the work done by V_n in a differential displacement dD_n is dE_n:

$$dE_n(t) = \mathbf{f}_n^T(t)d\mathbf{u}_n = \omega_n^2\phi_n^T\mathbf{m}\phi_n\Gamma_n^2D_n(t)dD_n(t) = V_n(t)dD_n(t) \tag{33}$$

Using an incremental formulation, the terms ΔE_n and V_n can be computed for each step in the pushover analysis. Then, the corresponding increment in the energy-based displacement, ΔDn, may be calculated as

$$\Delta D_n = \frac{\Delta E_n}{V_n} \tag{34}$$

Where, $\Delta E_n = \mathbf{f}_n^T\,\Delta\mathbf{u}_n$, $V_n = \mathbf{f}_n^T\,\mathbf{1}$

The value of D_n corresponding to the base shear is determined by summation. Equation (34) is consistent with Eq. (32) in the elastic domain.

The possible influence of changes in the deformed shape from static forces associated with modes other than the nth mode is neglected in this formulation, because orthogonality of the load vector and the elastic mode shapes is assumed, as described earlier.

As with conventional pushover approaches, the mapping for the ordinate of the common representation can be obtained by Eq. (21): $A_n = \frac{V_n}{\alpha_n}$

4.4.1.3 Energy-Based Formulation of Adaptive Modal Pushover Analysis (*Kalkan and Kunnath (2006) and* ***Method Proposed in the present work***)

In order to incorporate the variation in dynamic properties associated to structural damages, Kalkan and Kunnath (2006) developed an adaptive modal procedure. Eigenvalue analysis is carried out at each load increment, then a static analysis is carried out based on instantaneous inertia force distribution across the height of the building for each mode independently. The energy-based formulation, Eq. (21) and Eq. (34), was utilized for representing the capacity curve at step (k).

$$\Delta D_n^{(k)} = \frac{\Delta E_n^{(k)}}{V_n^{(k)}} \tag{35}$$

$$D_n^{(k)} = D_n^{(k-1)} + \Delta D_n^{(k)} \tag{36}$$

$$A_n^{(k)} = \frac{V_n^{(k)}}{\alpha_n^{(k)}} \tag{37}$$

In fact, Eq. (21 or 37) is proposed instead of Eq. (15) for estimating the capacity pseudo-acceleration $A_{n,}$ because the natural frequency (ω_n) is unknown when the structure is plastic. But in adaptive procedures the natural frequency is calculated in each step, so the Eq. (15) can be utilized with an incremental formulation:

$$\Delta A_n^{(k)} = \left(\omega_n^{(k)}\right)^2 \Delta D_n^{(k)} \tag{38}$$

$$A_n^{(k)} = A_n^{(k-1)} + \Delta A_n^{(k)} \tag{39}$$

It can be obtained the same result of the Eq. (38) if the Eq. (37) is applied with an incremental formulation as follows:

$$\Delta A_n^{(k)} = \frac{\Delta V_n^{(k)}}{\alpha_n^{(k)}} \tag{40}$$

Where,

$$\frac{\Delta V_n^{(k)}}{\alpha_n^{(k)}} = \frac{\left(\omega_n^{(k)}\right)^2 (\mathbf{m}\phi_n^k \mathbf{1})\Gamma_n^k \Delta D_n(t)}{\alpha_n^{(k)}} = \left(\omega_n^{(k)}\right)^2 \Delta D_n^{(k)}$$

Also, it should be maintained that in adaptive methods there is no difference between the conventional and energy-based formulation for calculating the capacity displacement D_n. Where the Eq. 19 should be expressed with an incremental formulation as follows:

$$\Delta D_n^{(k)} = \frac{\Delta u_{rn}^{(k)}}{\phi_{rn}^{(k)} \Gamma_n^{(k)}} \tag{41}$$

4.4.2 *Calculation of the effective damping*

The damping that occurs when earthquake ground motion drives a structure into the inelastic range can be viewed as a combination of viscous damping that is inherent in the structure and hysteretic damping. Hysteretic damping can be represented as equivalent viscous damping. The most common method for defining equivalent viscous damping is to equate the energy dissipated in the vibration cycle to the energy dissipated in viscous damping. So, firstly the equation which gives the energy dissipated in viscous damping is developed in section 4.4.2.1. Also the graphical interpretation of the energy dissipated in viscous damping is presented in order to be used in section 4.4.2.2 to calculate the equivalent viscous damping of the hysteretic damping.

4.4.2.1 Energy dissipated in viscous damping

Consider the steady-state motion of an single degree of freedom system due to $p(t) = p_0 \sin \omega t$. The energy dissipated by viscous damping in one cycle of harmonic vibration is

$$E_D = \int f_D \, du = \int_0^{2\pi/\omega} (c\dot{u})\dot{u} \, dt = \int_0^{2\pi/\omega} c\dot{u}^2 dt$$

$$= c \int_0^{2\pi/\omega} [\omega u_0 \cos(\omega t - \phi) \ ]^2 dt = \pi \, c\omega u_0^2 = 2\pi \, \xi \frac{\omega}{\omega_n} k u_0^2 \tag{42}$$

In the steady-state vibration, the energy input to the system due to the applied force is dissipated in viscous damping. The external force p(t) inputs energy to the system, which for each cycle of vibration is:

$$E_I = \int p(t)\, du = \int_0^{2\pi/\omega} p(t)\dot{u}\, dt$$

$$= \int_0^{2\pi/\omega} [p_0 \sin \omega t][\omega u_0 \cos(\omega t - \phi)\ ]dt = \pi p_0 u_0 \sin \phi \tag{43}$$

This equation can be written as

$$E_I = 2\pi\, \xi \frac{\omega}{\omega_n} k u_0^2 \tag{44}$$

Equations (42) and (44) indicate that $E_I = E_D$.

So it can be noted that over each cycle of harmonic vibration the changes in potential energy and kinetic energy are zero. This can be confirmed as follows:

$$E_S = \int f_S\, du = \int_0^{2\pi/\omega} (ku)\dot{u}\, dt$$

$$= \int_0^{2\pi/\omega} k[u_0 \sin(\omega t - \phi)][\omega u_0 \cos(\omega t - \phi)]dt = 0$$

$$E_K = \int f_I\, du = \int_0^{2\pi/\omega} (m\ddot{u})\dot{u}\, dt$$

$$= \int_0^{2\pi/\omega} m[-\omega^2 u_0 \sin(\omega t - \phi)][\omega u_0 \cos(\omega t - \phi)]dt = 0$$

For the purpose to present a graphical interpretation for the energy dissipated in viscous damping, an equation relating the damping force f_D to the displacement u is derived:

$$f_D = c\dot{u}(t) = c\omega u_0\ \cos(\omega t - \phi)$$

$$= c\omega\sqrt{u_0^2 - u_0^2 \sin^2(\omega t - \phi)}$$

$$= c\omega\sqrt{u_0^2 - [u(t)]^2}$$

This can be rewritten as

$$\left(\frac{u}{u_0}\right)^2 + \left(\frac{f_D}{c\omega u_0}\right)^2 = 1 \tag{45}$$

Which is the equation of the ellipse shown in Fig. 4-5a. The area enclosed by the ellipse is $\pi(u_0)(c\omega u_0) = \pi\, c\omega u_0^2$, which is the same as Eq. (42). Thus the area within the hysteresis loop gives the dissipated energy.

The total (elastic plus damping) resisting force can be written as:

$$f_S + f_D = ku(t) + c\dot{u}(t)$$

$$= ku + c\omega\sqrt{u_0^2 - u^2} \tag{46}$$

A plot of $f_S + f_D$ against u is the ellipse of Fig. 4-5a rotated as shown in Fig. 4-5b because of the *ku* term in Eq. (46). The energy dissipated by damping is still the area enclosed by the ellipse because the area enclosed by the single-valued elastic force, $f_S = ku$, is zero.

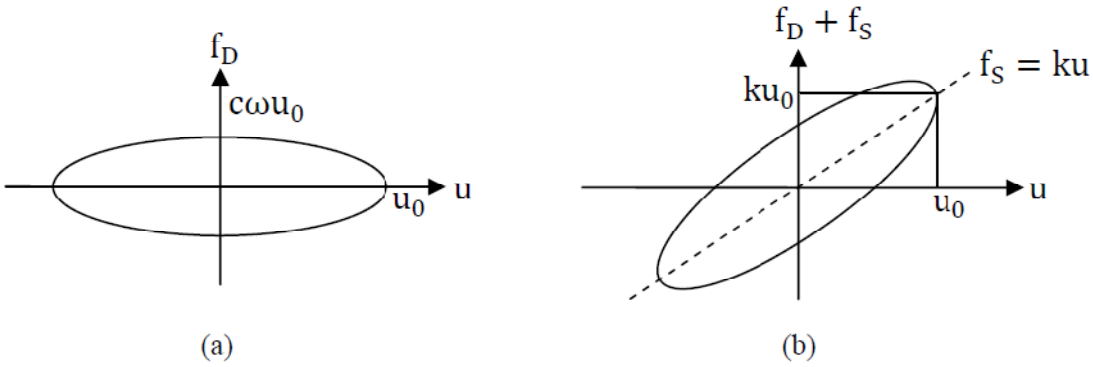

Fig. 4-5 Hysteresis loop for (a) viscous damper; (b) spring and viscous damper in parallel.

4.4.2.2 Equivalent viscous damping

For defining equivalent viscous damping the energy dissipated in the vibration cycle (the area E_D enclosed by the hysteresis loop) should be equated to the energy dissipated in viscous damping (Eq. (42)).

$$4\pi\, \xi_{eq} \frac{\omega}{\omega_n} E_{S0} = E_D \quad \text{or} \quad \xi_{eq} = \frac{1}{4\pi} \frac{1}{\omega/\omega_n} \frac{E_D}{E_{S0}} \tag{47}$$

Where, $E_{S0} = ku_0^2/2$

Eq. (47) shows that the damping ratio ξ_{eq} is related to the excitation frequency and natural frequency of the structure. For $\omega = \omega_n$ Eq. (47) becomes:

$$\xi_{eq(\omega=\omega_n)} = \frac{1}{4\pi}\frac{E_D}{E_{S0}} \tag{48}$$

The damping ratio ξ_{eq} determined at $\omega = \omega_n$ would not be correct at any another excitation frequency, but it would be a satisfactory approximation. This can be proved as follows:

For harmonic motion of a SDF system with damping ratio equals to ξ , the deformation response factor may be expressed as

$$R_d = \frac{u_0}{(u_{st})_0} = \frac{1}{\sqrt{[1-(\omega/\omega_n)^2]^2-[2\xi(\omega/\omega_n)]^2}} \tag{49}$$

Where $(u_{st})_0 = \frac{p_0}{k}$

For a damping ratio equals to $\frac{\xi}{\omega/\omega_n}$, the deformation response factor may be expressed as

$$R_d = \frac{u_0}{(u_{st})_0} = \frac{1}{\sqrt{[1-(\omega/\omega_n)^2]^2-[2\xi]^2}} \tag{50}$$

This result is obtained by modifying the viscous damping ratio in Eq. (49). In particular, ξ was replaced by $\frac{\xi}{\omega/\omega_n}$

Shown in Fig. 4-6 by dashed lines are plots of $u_0/(u_{st})_0$ as a function of the frequency ratio ω/ω_n for damping coefficient $\zeta = 0, 0.15$ and 0.3. The solid lines are for damping coefficient $\zeta = \frac{0}{\omega/\omega_n}, \frac{0.15}{\omega/\omega_n}$ and $\frac{0.3}{\omega/\omega_n}$.

From Fig. 4-6, it can be noted that ignoring the term $\frac{1}{\omega/\omega_n}$ in the Eq. (47) would be a satisfactory approximation.

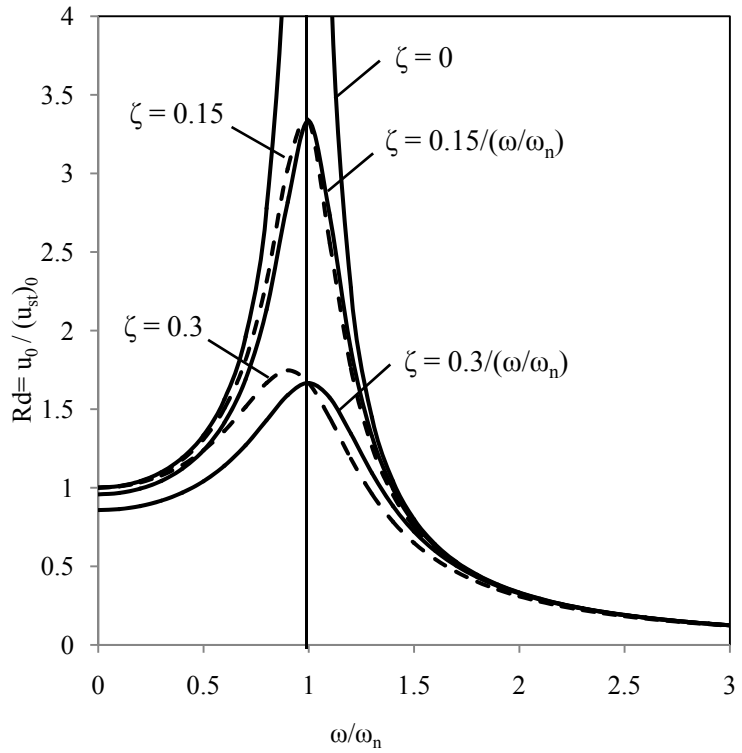

Fig. 4-6 The effect of ignoring [1/(ω/ω_n)] term in equivalent viscous damping on the deformation response factor

4.4.2.3 Effective damping

The effective viscous damping used to find the spectral demand curve, reduced from the elastic design spectrum, is defined by:

$$\xi_{eff} = k\xi_{eq} + \xi \tag{51}$$

Where,

k is the damping modification factor, which takes into account the effect of the divergence between the real hysteresis loop of the structure and the idealized one.

ξeq is the hysteretic damping, it can be calculated by using the Eq. (48) as follows:

$$\xi_{eq} = \frac{1}{4\pi}\frac{E_D}{E_{S0}} \tag{52}$$

Where,

E_D = energy dissipated by damping,

E_S = maximum strain energy;

The physical significance of the terms E_D and ES in Eq. (52) is illustrated in Fig. 4-7, where β_0 in the figure refers to $\xi_{eq,}$

ξ is the elastic viscous damping inherent in the structure. In ATC-40 (1996) it is assumed to be constant (5%). But in the proposed method there is a possibility of choosing different damping values for the mode(s), it allows incorporating different approaches of modeling damping in nonlinear time history analysis. The next paragraph gives an idea concerning this issue (section 4.5).

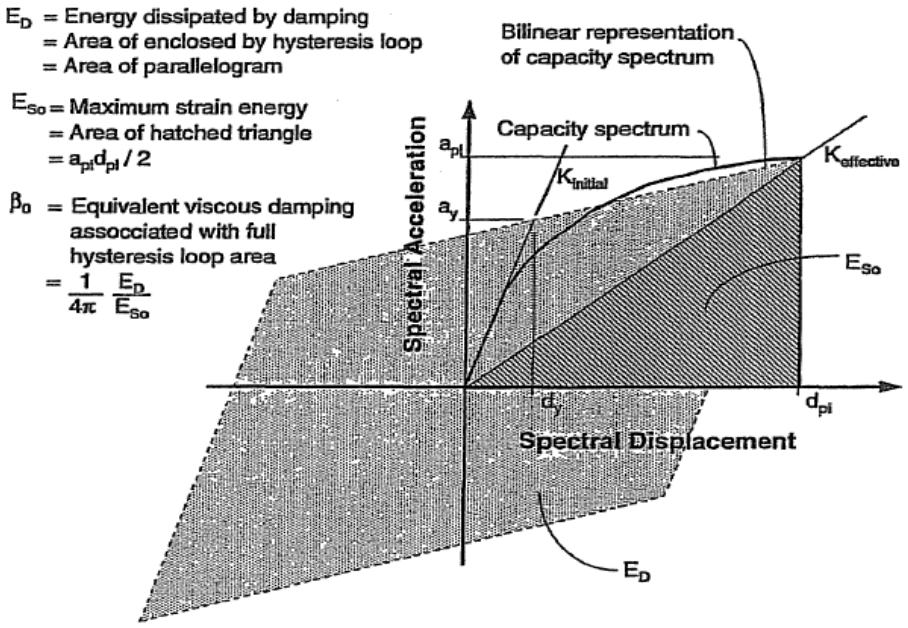

Fig. 4-7 Physical significance of the terms E_D and E_S (ATC-40, 1996)

4.5 Modeling of elastic damping in nonlinear response

4.5.1 *Conditions for classical damping*

It is knowen that the system has classical damping if the damping matrix **c** is diagonalized when transformed to undamped modal coordinates. Caughey (1960) showed that a damping matrix of the following form will always be classical:

$$\mathbf{c} = \mathbf{m}\sum_i a_i[\mathbf{m}^{-1}\mathbf{k}]^i \tag{53}$$

Where *i* can be anywhere in the range $-\infty<i<\infty$ and the summation may include as many terms as desired. With this form of the damping matrix it is possible to compute the damping coefficients necessary to provide uncoupling of a system having any

desired damping ratios in any specified number of modes. Given the coefficients, the damping ratio in each mode is obtained as follows:

$$\xi_n = \frac{1}{2\omega_n}\sum_i a_i \omega_n^{2i} \tag{54}$$

Eq. (54) may be used to determine the constants ai for any desired values of modal damping ratios corresponding to any specified numbers of modes.

One common approach is to limit the Caughey series to two terms, with i=0 and 1. Using Eq. (53), the resulting damping matrix is

$$\mathbf{c} = a_0\mathbf{m} + a_1\mathbf{k} \tag{55}$$

Damping as expressed in Eq. (55) is often referred to as Rayleigh damping. Given coefficients $a0$ and $a1$, the damping ratio in mode n can be determined from Eq. (59) as

$$\xi_n = \frac{a_0}{2\omega_n} + \frac{a_1\omega_n}{2} \tag{56}$$

The coefficients a_0 and a_1 are determined by specifying damping ratios in any two modes and writing Eq. (56) for each mode.

4.5.2 *Using Rayleigh Damping in nonlinear time history analysis*

When Rayleigh proportional damping is used, the analyst has three basic approaches to deal with the inelastic response (Charney 2008).

Approach A:

The damping matrix is computed on the basis of the initial stiffness. Hence, the damping matrix used for each step in the analysis is

$$\mathbf{c}(t) = a_0\,\mathbf{m} + a_1\,\mathbf{k} \tag{57}$$

This damping matrix is constant throughout the analysis. At any step of the analysis in which the tangent stiffness is not equal (or proportional) to the elastic stiffness, the damping matrix will be nonclassical because the current mode shapes (based on the instantaneous tangent stiffness) will not diagonalize ***k***.

Approach B:

The $a0$ and $a1$ proportionality terms are computed on the basis of the initial stiffness, and the damping matrix is updated each time the tangent stiffness changes. The damping matrix is

$$\mathbf{c}(t) = a_0\,\mathbf{m} + a_1\,\mathbf{k_t} \tag{58}$$

where the subscript t on the $\boldsymbol{k}$ term represents the tangent stiffness. In this case, the damping matrix will be classical at each step in the analysis because the current mode shapes will diagonalize $\boldsymbol{k}_t$.

Approach C:

The $a0$ and $a1$ terms are recomputed each time the stiffness changes, and the damping matrix is reformed on this basis (assuming that the damping ratios in the specified modes, two modes in Rayleigh damping, do not change regardless of modal frequency). In this case, the damping matrix is given by

$$\mathbf{c}(t) = a_{0t}\,\mathbf{m} + a_{1t}\,\mathbf{k_t} \tag{59}$$

where the added subscript t on the a0 and a1 terms in Eq. (59) indicates that these are based on the tangent stiffness. As with approach B, the damping matrix will be classical. It is noted that a principal disadvantage of approach C is that the two modal frequencies ωk and ωm on which a0t and a1t are based [see Eq. (59)] must be recomputed with each change in stiffness. This implies the need for an eigenanalysis each time the system stiffness changes.

4.5.3 *Using Rayleigh damping in adaptive pushover analysis*

Given any damping matrix, classical or nonclassical, the damping ratios in each mode may be found by the modal strain energy approach (Johnson and Kienholz, 1982), shown in Eq. (60):

$$\zeta_n = \frac{\phi_n^T \mathbf{c} \phi_n}{2\omega_n \phi_n^T \mathbf{m} \phi_n} \tag{60}$$

For classically damped systems, the resulting damping ratios are exact, and for nonclassically damped systems, they are approximate (Warburton and Soni 1977).

Eq. (60) is applied to the different Approaches for using Rayleigh damping in nonlinear time history analysis. The results obtained are as follows:

Modal damping ratio corresponding to the Approach A:

$$\zeta_{n,t} = \frac{\phi_{n,t}^{T}\mathbf{c}\phi_{n,t}}{2\omega_{n,t}\phi_{n,t}^{T}\mathbf{m}\phi_{n,t}} \tag{61}$$

Where the subscript *t* refers to the tangent stiffness

Modal damping ratio corresponding to the Approach B:

$$\xi_{n,t} = \frac{a_0}{2\omega_{n,t}} + \frac{a_1\omega_{n,t}}{2} \tag{62}$$

Where,

$$a_0 = \frac{2\omega_i\omega_j(\omega_i\xi_j - \omega_j\xi_i)}{\omega_i^2 - \omega_j^2} \tag{63}$$

$$a_1 = \frac{2(\omega_i\xi_i - \omega_j\xi_j)}{\omega_i^2 - \omega_j^2} \tag{64}$$

i and j refer to the mode number of the two selected modes for specifying the Rayleigh damping coefficients

Modal damping ratio corresponding to the Approach C:

$$\xi_{n,t} = \frac{a_{0,t}}{2\omega_{n,t}} + \frac{a_{1,t}\omega_{n,t}}{2} \tag{65}$$

$$a_{0,t} = \frac{2\omega_{i,t}\omega_{j,t}(\omega_{i,t}\xi_j - \omega_{j,t}\xi_i)}{\omega_{i,t}^2 - \omega_{j,t}^2} \tag{66}$$

$$a_{1,t} = \frac{2(\omega_{i,t}\xi_i - \omega_{j,t}\xi_j)}{\omega_{i,t}^2 - \omega_{j,t}^2} \tag{67}$$

For n=i or n=j , $\xi_{n,t}$ is constant during the adaptive pushover analysis

4.6 Capacity Spectrum Method to perform Single-run Adaptive Pushover Analysis *(Description of the proposed method)*

The single-run adaptive pushover method proposed in the previous chapter, OMAP method, is chosen to perform the pushover analysis. In the previous chapter just the form of the external applied loads has been discussed. In this chapter, the proposed method (OMAP) is extended to calculate the performance point by using the capacity spectrum method. The extended OMAP algorithm includes the following basic steps:

1. Defining the elastic response spectrum (Pseudo-accelerations vs. Periods) with the corresponding damping ratio.

2. Performing an eigenvalue analysis of the structure to compute periods (T_n), mode shapes (Φ_{in}) and modal participation factors (Γ_n) for the (n) desirable modes, where "i" is the story number and "n" is the mode number;

3. Choosing the modal elastic damping ratio of the structure ξ_n;

4. Computing the pseudo-spectral acceleration for each considered mode (S_{a_n}); if the damping ratio of the nth mode is different from that of the used response spectrum, this latter is adjusted using the following formula (Newmark and Hall, 1982):

$$A_2 = A_1 \frac{(2.31 - 0.41 * \ln \beta_2)}{(2.31 - 0.41 * \ln \beta_1)} \tag{68}$$

   where:

   A_1 = Acceleration corresponding to damping ratio β_1;

   A_2 = Acceleration corresponding to damping ratio β_2;

   $0 < \beta_1 < 100$ (percentage);

   $0 < \beta_2 < 100$ (percentage); and

   ln = natural logarithm (base e).

5. Computing the load factor (λ) for this iteration as follows:

a) Determine the roof displacement before the scaling (u_r) by quadratic combination rule to the peak modal floor displacements

$$u_r = \sqrt{\sum_{n=1}^{Nm} {u_{rn}}^2} \tag{69}$$

$$u_{rn} = \Gamma_n \Phi_{rn} S_{d_n} \tag{70}$$

Where,

u_{rn} is the peak modal floor displacement at the roof for n^{th} mode before the scaling.

$$S_{d_n} = \frac{S_{a_n}}{{\omega_n}^2} \tag{71}$$

ω_n is the nth natural frequency

b) Determine the load factor (λ)

$$\lambda = \frac{\Delta u_{roof}}{u_r} \tag{72}$$

Where, Δu_{roof} is the desirable incremental floor displacement for this iteration.

6. Computing the peak modal responses for the (n) modes as follows:

$$\Delta f_{in} = \lambda \Gamma_n \Phi_{in} m_i S_{a_n} \tag{73}$$

$$\Delta SS_{in} = \sum_{k=i}^{Ns} \Delta f_{kj} \tag{74}$$

$$\Delta OM_{in} = \sum_{k=i}^{Ns} \Delta SS_{kn} * h_k \tag{75}$$

$$\Delta u_{in} = \lambda \Gamma_n \Phi_{in} S_{d_n} \tag{76}$$

$$\Delta \delta_{in} = \Delta u_{in} - \Delta u_{(i-1)n} \tag{77}$$

where:

m_i is the mass of ith story

Δf_{in} is the incremental lateral floor force at i^{th} floor for n^{th} mode

ΔSS_{in} is the incremental modal story shear at i^{th} story for n^{th} mode

ΔOM_{in} is the incremental modal overturning moment at i^{th} floor for n^{th} mode

h_i is the height of the ith story

Ns is the number of stories or floors.

Δu_{in} is the incremental floor displacement at i^{th} floor for n^{th} mode

$\Delta\delta_{in}$ is the incremental story drift at i^{th} story for n^{th} mode

7. Calculating the incremental capacity displacement and pseudo-acceleration For calculating the incremental capacity pseudo-acceleration, Eq. (41) can be used:

$$\Delta D_n = \frac{\Delta \mathbf{u}_{rn}}{\Phi_{rn}\Gamma_n} = \frac{\lambda\Gamma_n\Phi_{rn}S_{a_n}/\omega_n{}^2}{\Phi_{rn}\Gamma_n} = \lambda S_{d_n} \tag{78 a}$$

Or by using the energy-based formulation [Eq. (35)]

$$\Delta D_n = \frac{\Delta E_n}{V_n} = \frac{\mathbf{f}_n^T\,\Delta\mathbf{u}_n}{\mathbf{f}_n^T\,\mathbf{1}} = \frac{\Delta\mathbf{f}_n^T\,\Delta\mathbf{u}_n}{\Delta\mathbf{f}_n^T\,\mathbf{1}} = \frac{\sum_{k=i}^{Ns}(\lambda\Gamma_n\Phi_{in}m_iS_{a_n})(\lambda\Gamma_n\Phi_{in}S_{d_n})}{\sum_{k=i}^{Ns}\lambda\Gamma_n\Phi_{in}m_iS_{a_n}} =$$

$$\lambda\Gamma_nS_{d_n}\frac{\sum_{k=i}^{Ns}\Phi_{in}m_i\Phi_{in}}{\sum_{k=i}^{Ns}\Phi_{in}m_i} = \lambda S_{d_n} \tag{78b}$$

For calculating the incremental capacity pseudo-acceleration, Eq. (38) can be used:

$$\Delta A_n = (\omega_n)^2\Delta D_n = (\omega_n)^2\lambda S_{d_n} = \lambda S_{a_n} \tag{79a}$$

Or by using the energy-based formulation [Eq. (40)]

$$\Delta A_n = \frac{\Delta V_n}{\alpha_n} = \frac{\sum_{k=i}^{Ns}\lambda\Gamma_n\Phi_{in}m_iS_{a_n}}{L_n\Gamma_n} = \lambda S_{a_n} \tag{79b}$$

8. Plot the modal capacity spectrum (i.e., ΔD_n vs A_n) by using the Eq.36 and Eq.39

9. Calculating the effective viscous damping:

$$\xi_{eff_n} = k\xi_{eq_n} + \xi_n \tag{80}$$

10. Plot the reduced response spectrum for each mode by utilizing the equivalent viscous damping calculated in Step 9. The relationships developed by Newmark and Hall (1982) can be used.

11. Calculating the desirable incremental combined peak responses Δr_i by quadratic combination rule for this iteration and add these to the same from the previous iteration:

$$\Delta r_i = \sqrt{\sum_{n=1}^{Nm} \Delta r_{in}{}^2} \tag{81}$$

For example, the combined overturning moment and shear force at i^{th} floor are given respectively as follow:

$$\Delta OM_i = \sqrt{\sum_{n=1}^{Nm} \Delta OM_{in}{}^2}$$

$$\Delta SS_i = \sqrt{\sum_{n=1}^{Nm} \Delta SS_{in}{}^2}$$

12. Calculating the equivalent lateral forces which give the combined overturning moment:

$$F_i = \frac{OM_i - OM_{i+1}}{h_i} - \frac{OM_{i+1} - OM_{i+2}}{h_{i+1}}; i = 1,2, \dots, (Ns - 1)$$

$$F_{Ns} = \frac{OM_{Ns}}{h_{Ns}}; i = Ns \tag{82}$$

13. Performing the pushover analysis by using the equivalent lateral forces computed in Step (12) and starting from state at end of the previous iteration.

14. If there is not an intersection between the capacity spectrum for the first mode and its reduced response spectrum, additional iteration must be made by returning to step 2.

From the above, it can be noted that although a single-run adaptive pushover analysis is performed, the modal quantities are picked out at each increment. As a result, using equivalent single degree of freedom system for estimating the peak response quantities becomes available.

4.7 Illustrative examples:

The examples used in the previous chapter are selected in the evaluation of the efficiency of the OMAP against the NTHA. The walls are modeled as beam elements

considering inelastic fibers in order to omit the inaccuracy related to using the simplified multilinear model in previous chapter (See Fig. 3-13). Fig. 4-8 shows the material stress-strain curve for the steel and the concrete. The nonlinear behavior is simulated via discrete hinges defined in the lower end of each storey. The plastic hinge length is set equal to 0.5 times the flexural depth of the shear wall (FEMA-356); lp = 0.5*0.9*6=2.7 m. In this simulation the cyclic stiffness degradation of structural elements is ignored when the NTHA is performed. The aim of this simplification is to eliminate the difference between the monotonic behavior and the cyclic behavior (see Fig. 4-9), so the damping modification factor (k) is equated to 1. The incremental roof displacement is specified as 10 cm for the first iteration and 5 cm for the rest.

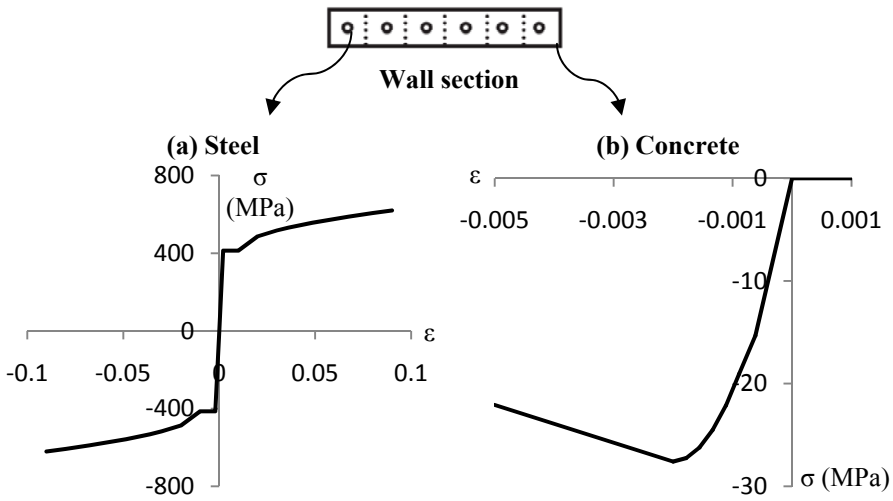

Fig. 4-8 Material stress-strain curve

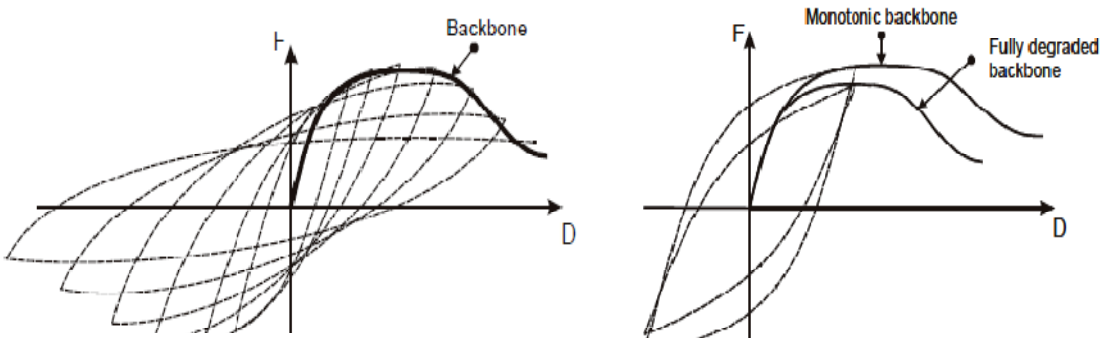

(a) Without cyclic stiffness degradation **(b)** With cyclic stiffness degradation

Fig. 4-9 Monotonic and Cyclic behavior

A damping ratio of 5% is considered for the first and third modes of vibration, in order to specify the mass and stiffness-proportional damping coefficients where, the Rayleigh damping matrix is defined as the Approach B for both the time history and pushover analysis. Table 4-1 shows the structure references and the corresponding scale factors of the earthquake.

Table 4-1 Structure references and corresponding scale factors of ground motions

Example	Structure Reference	No. of Storeys	Earthquake	Scale Factor
1	W20/Imp	20	Imperial Valley (1940)	2.5
2	W20/Erz	20	Erzincan (1992)	1.0
3	W30/Imp	30	Imperial Valley (1940)	2.5
4	W30/Erz	30	Erzincan (1992)	1.0

4.8 Results and Discussion

Firstly, the results for the case of **W20/Imp** are presented.

a- capacity spectrum

As explained before, this work does not only propose an innovative method for specifying the performance point for a single-run adaptive pushover analysis but also it develops a new method to convert the capacity curve to a capacity spectrum. Fig. 4-10 shows a comparison between the capacity spectrum calculated by the conventional energy-based formulation of adaptive modal pushover [Eq. (37)] and the proposed method [Eq. (39)]. For the proposed method, the slope of the curve is always positive and equals to $\left(\omega_n^{(k)}\right)^2$ at the step (k). This is not always the case for the conventional energy-based method (Kalkan and Kunnath 2006) especially at advanced plasticity state.

b- Performance point:

Normally just the first mode is demanded to specify the performance point, however, other modes (the second and the third) are plotted with their corresponding demand spectrum to give an idea about the amount of the plasticity in the higher modes. Fig. 4-11 shows the capacity spectrum and the demand spectrum (for the three first modes) corresponded to the performance point.

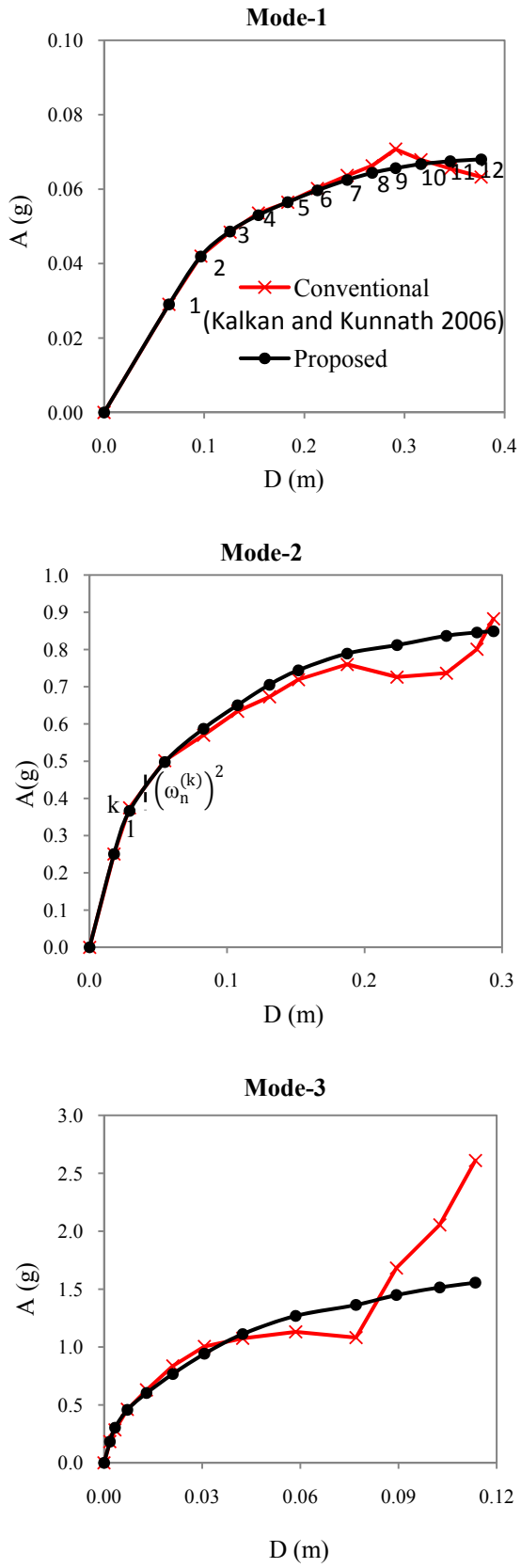

Fig. 4-10 Capacity spectrum (W20/Imp)

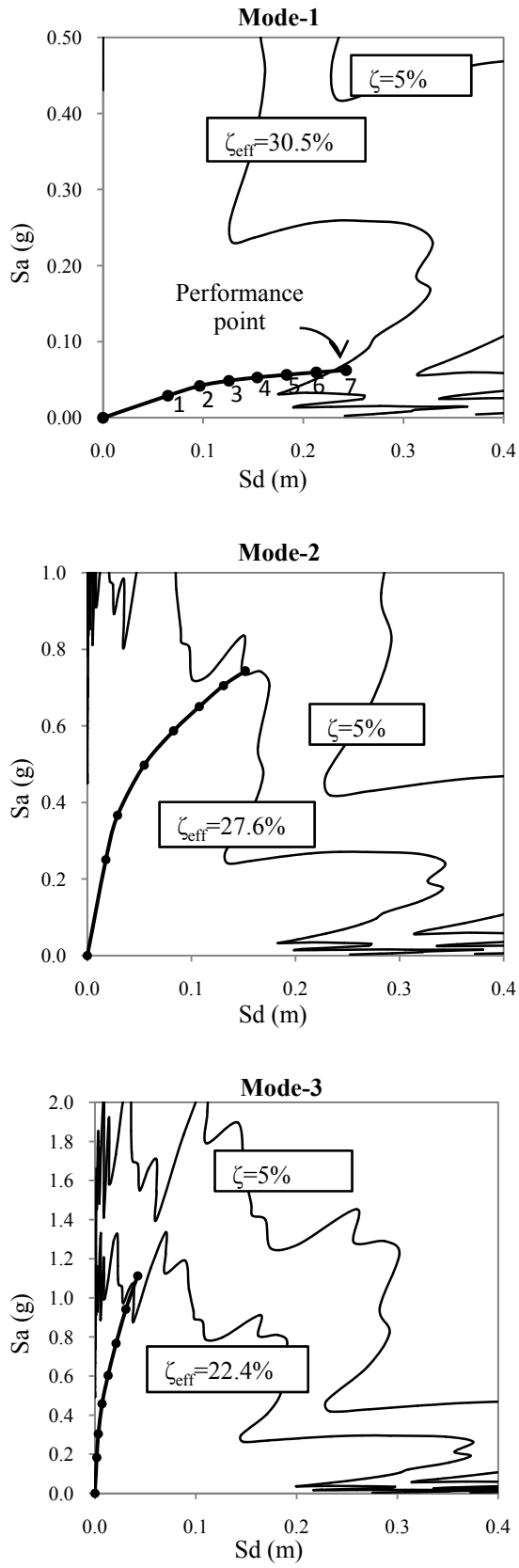

Fig. 4-11 Performance point(W20/Imp)

c- Hinge rotations:

The discretization of the shear wall section using inelastic fibers allows computing not only the plastic hinge rotations but also the elastic ones. This is not the case when the hinge properties are used for the gross section as in the previous chapter. Fig. 4-12 shows the total hinge rotations at each story. The hinge rotation versus the moment is detailed at the base of the shear wall.

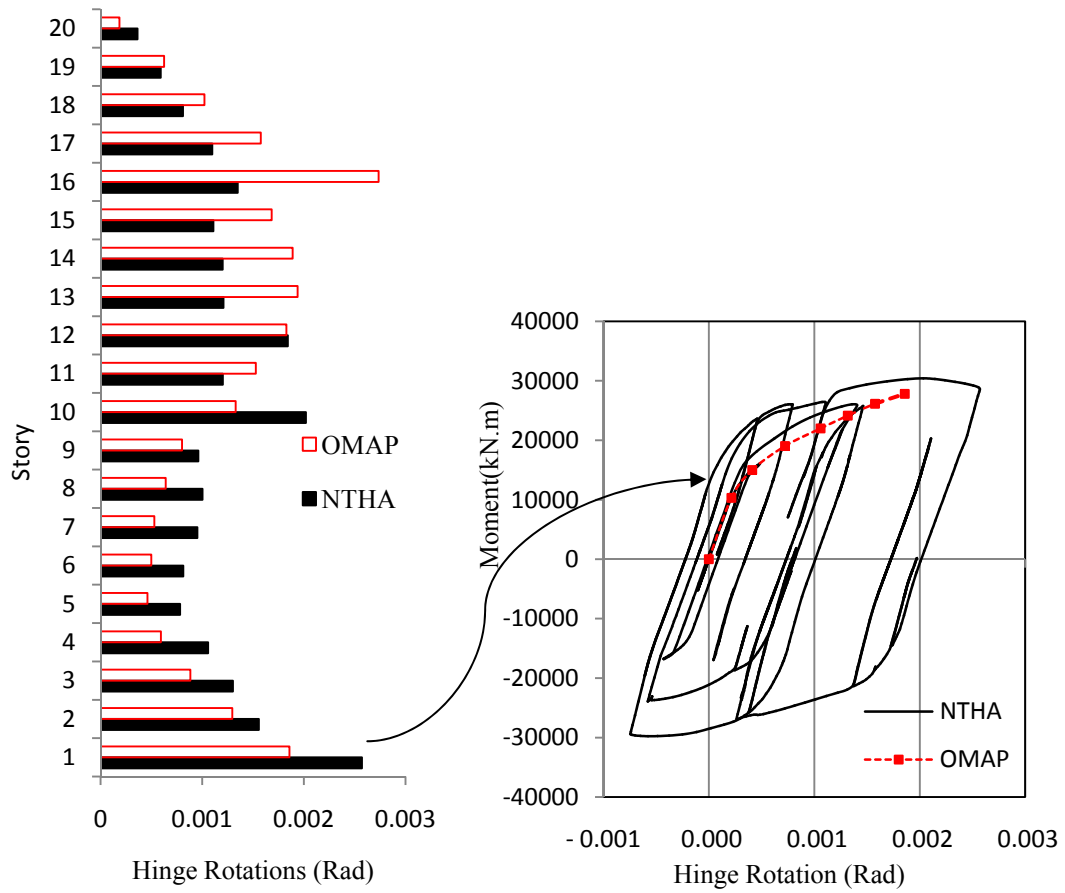

Fig. 4-12 Hinge Rotations (W20/Imp)

d- Other response quantities:

Fig. 4-13 shows the floor displacements and the story drifts estimated by OMAP and NTHA. Similarly, Fig. 4-14 shows the moments and story shears. It can be noted that OMAP procedure estimates the response quantities and the member forces with a reasonable accuracy.

Similarly Fig. 4-15, Fig. 4-16, Fig. 4-17, Fig. 4-18 and Fig. 4-19 show the results for the case study (W20/Erz). Fig. 4-20, Fig. 4-21, Fig. 4-22, Fig. 4-23 and Fig. 4-24 show the results for the case study (W30/Imp). Fig. 4-25, Fig. 4-26, Fig. 4-27, Fig. 4-28 and Fig. 4-29 show the results for the case study (W30/Erz).

The results confirm the general trend observed for the first case study W20/Imp and point out the reasonable accuracy of the OMAP method with regard to the non-linear time history analysis.

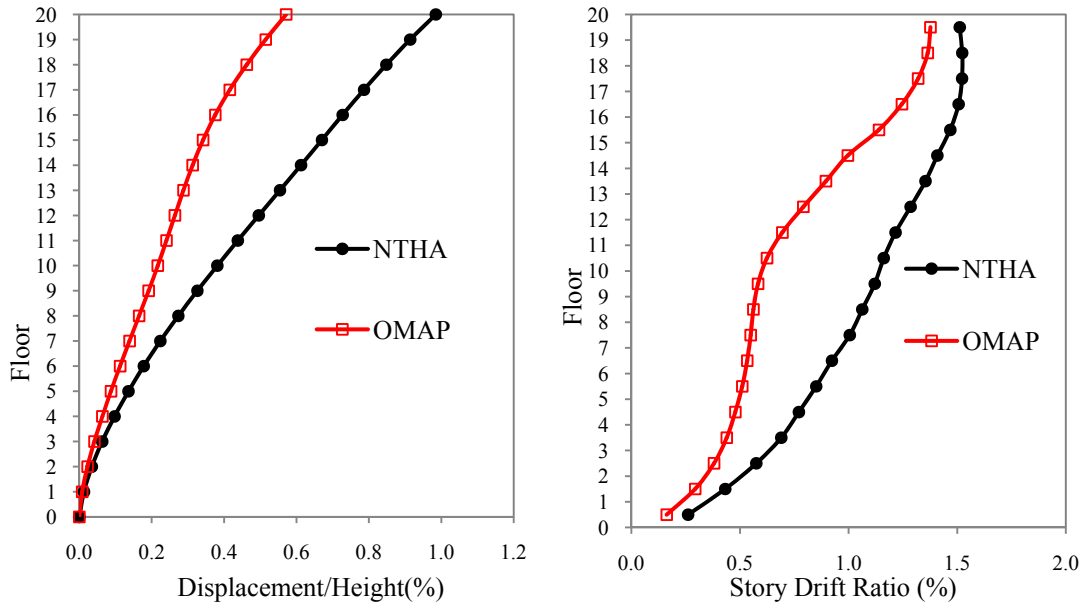

Fig. 4-13 Floor displacement and Story drift (OMAP vs NTHA) (W20/Imp)

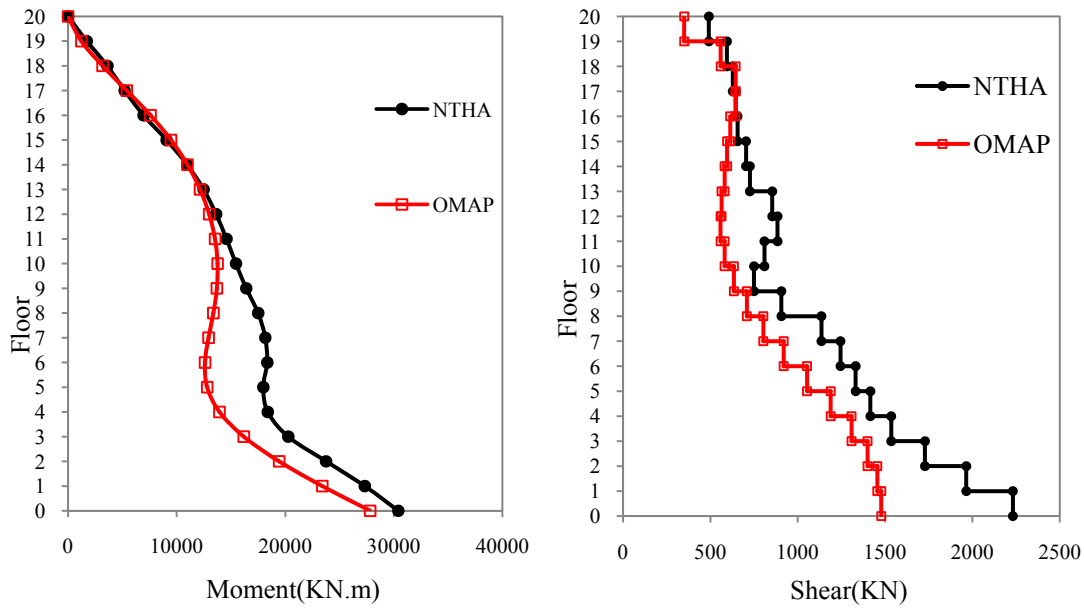

Fig. 4-14 Moment and Story shear (OMAP vs NTHA) (W20/Imp)

Example: W20/Erz

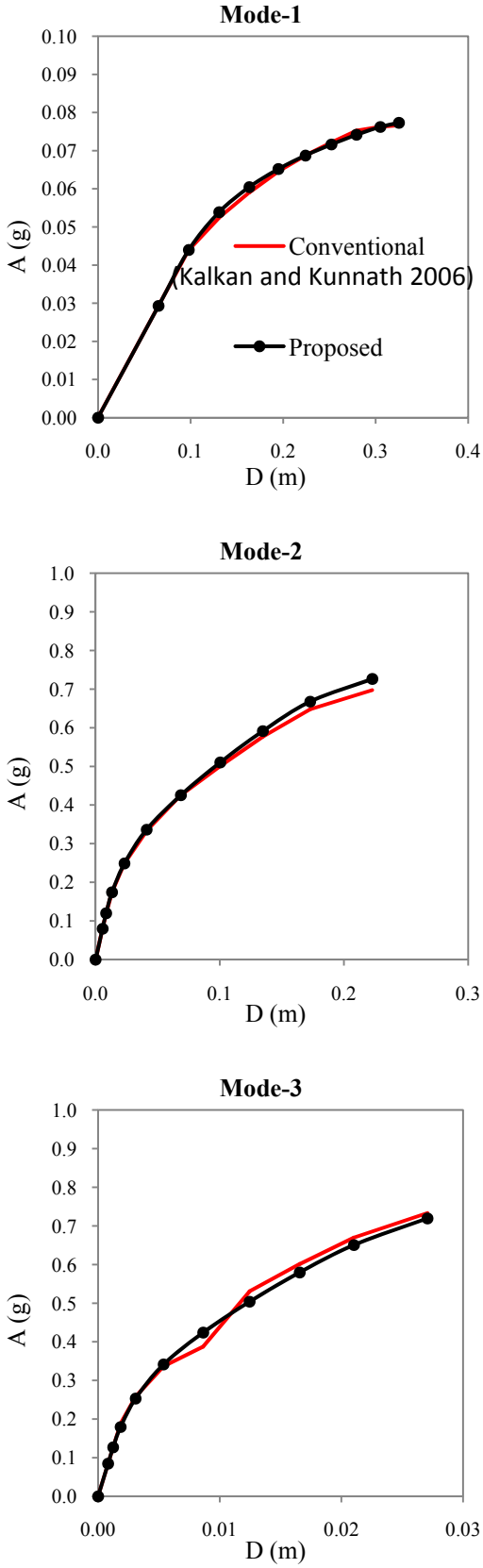

Fig. 4-15 Capacity spectrum (W20/Erz)

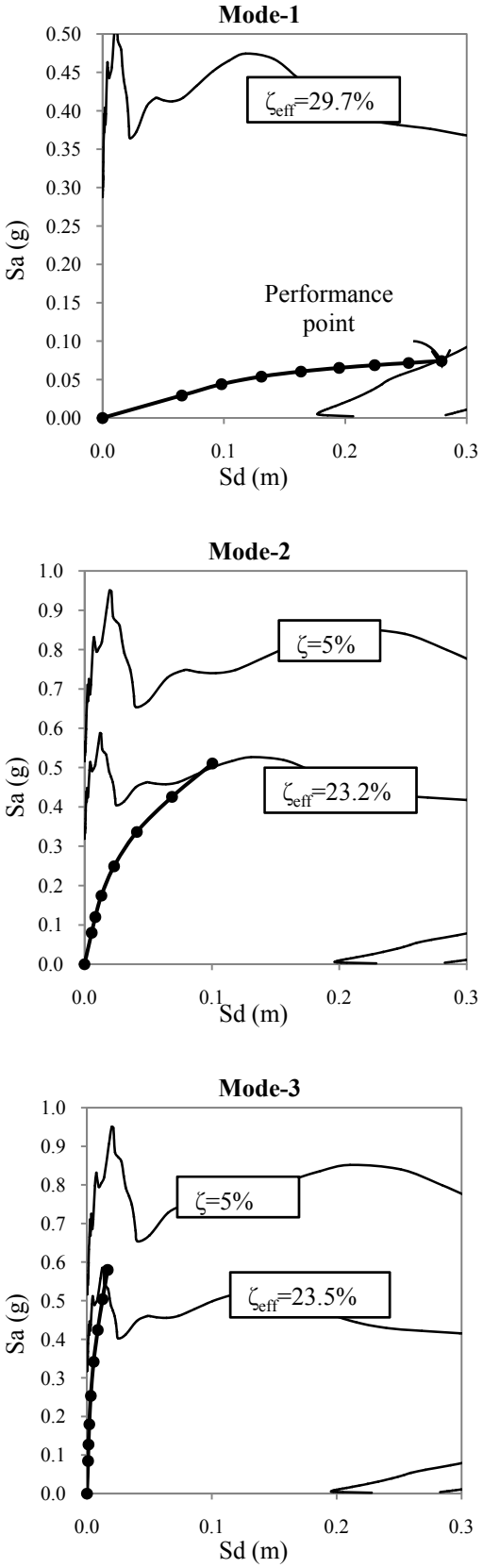

Fig. 4-16 Performance point (W20/Erz)

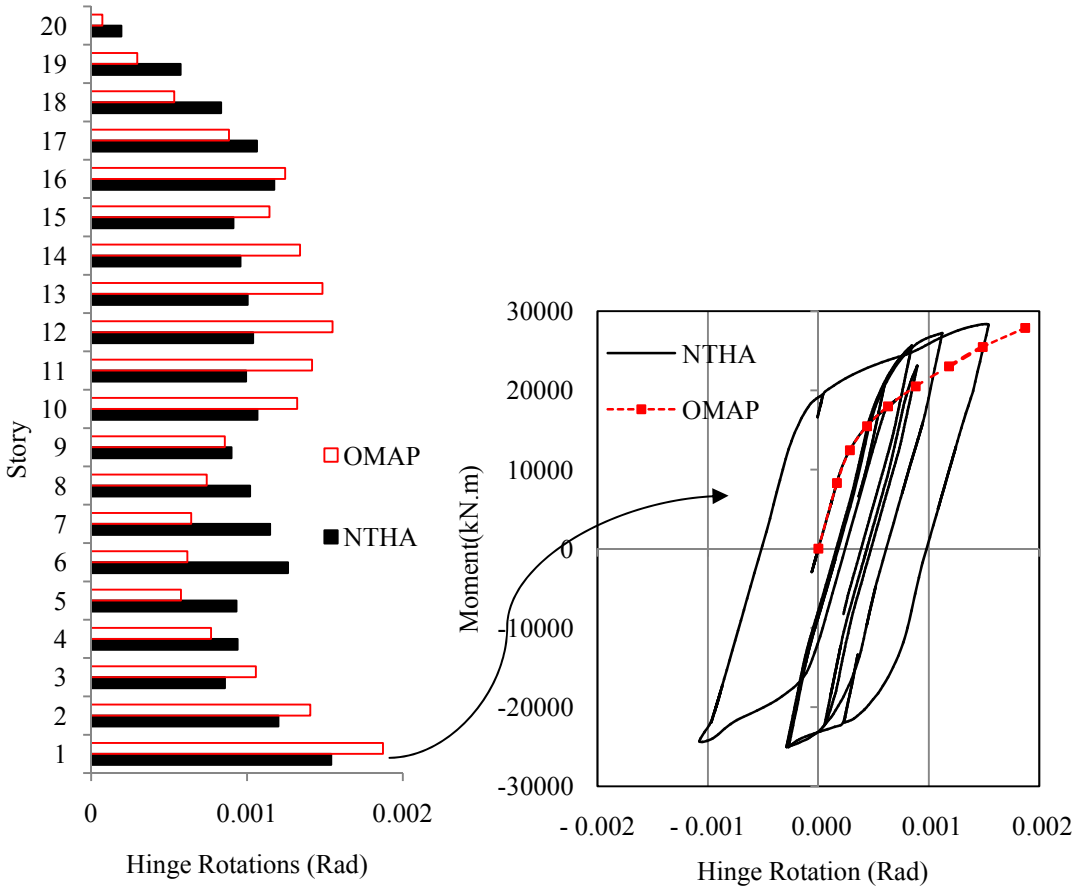

Fig. 4-17 Hinge Rotations (W20/Erz)

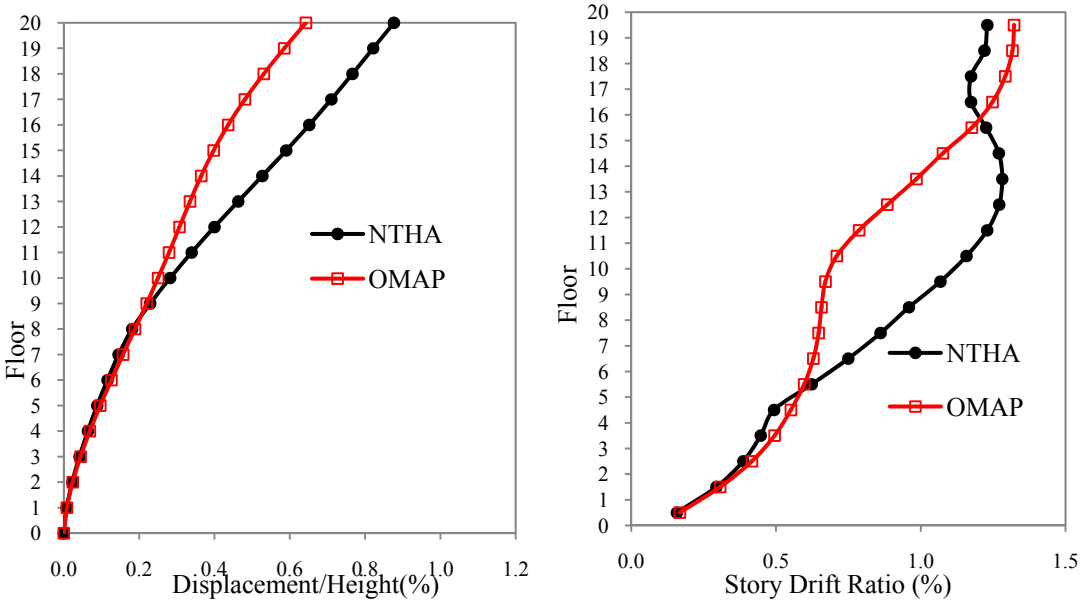

Fig. 4-18 Floor displacement and Story drift (OMAP vs NTHA) (W20/Erz)

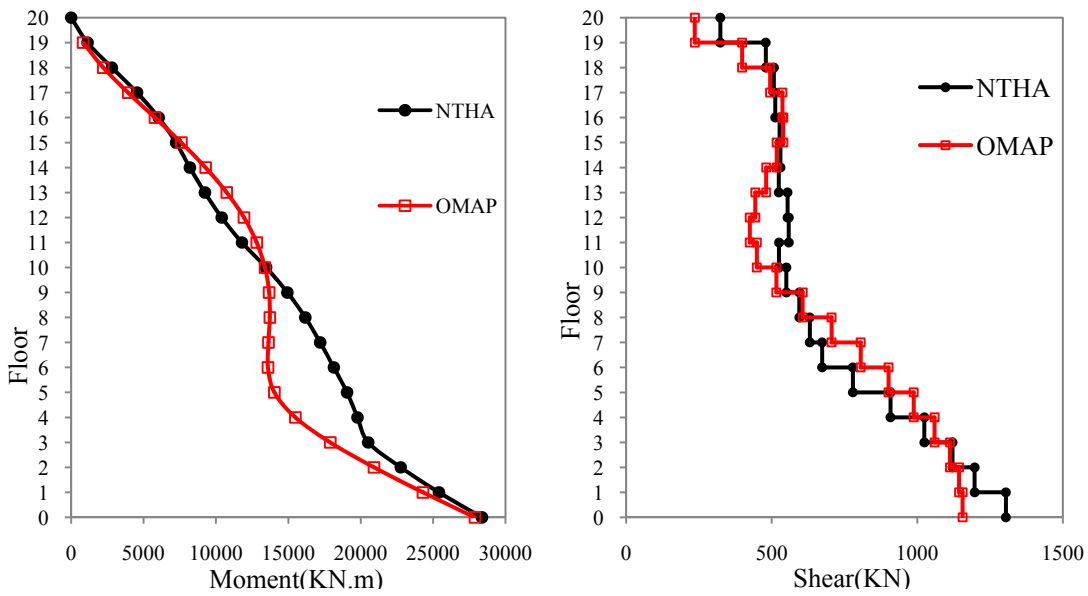

Fig. 4-19 Moment and Story shear (OMAP vs NTHA) (W20/Erz)

Example: W30/Imp

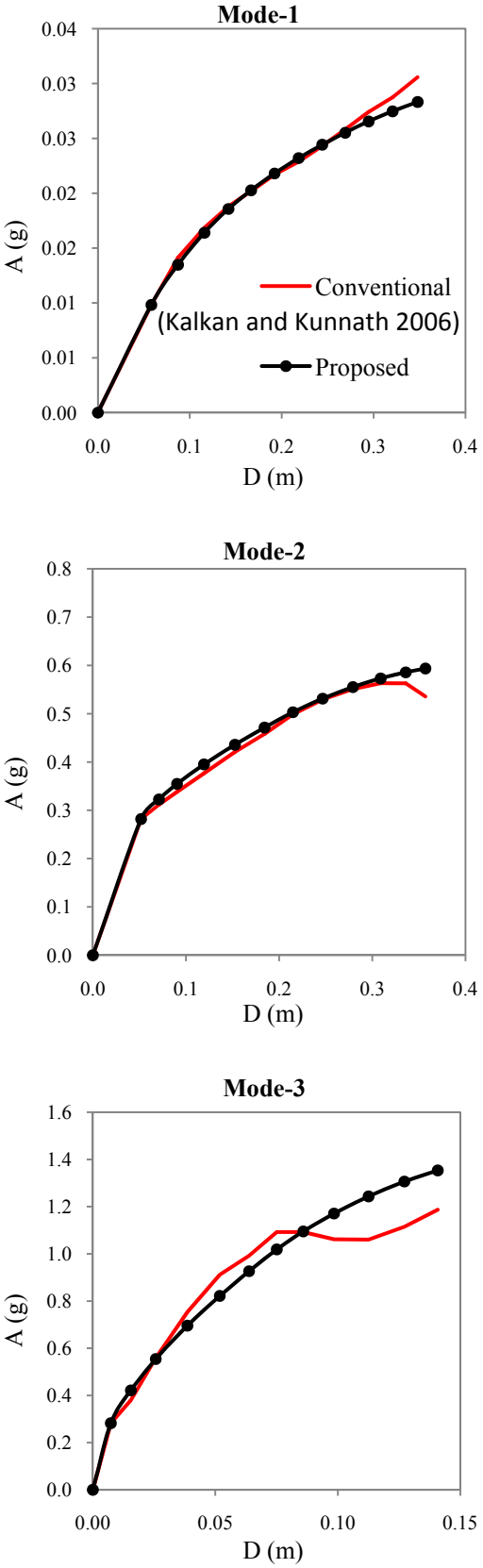

Fig. 4-20 Capacity spectrum (W30/Imp)

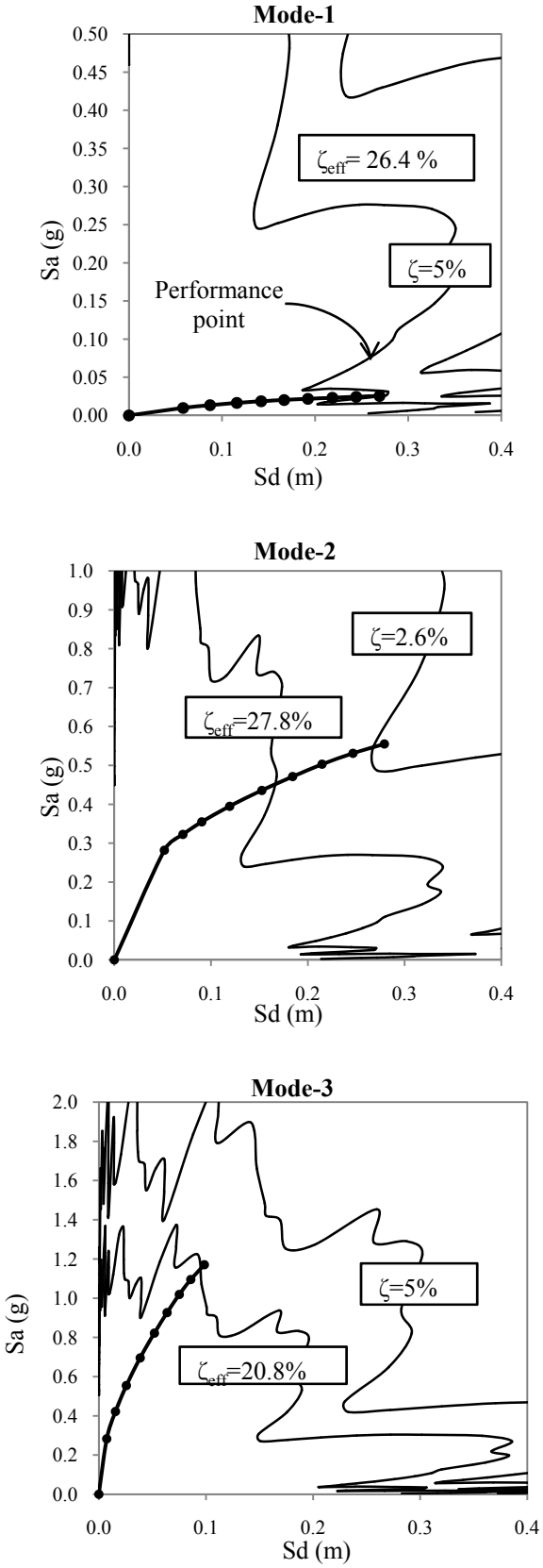

Fig. 4-21 Performance point (W30/Imp)

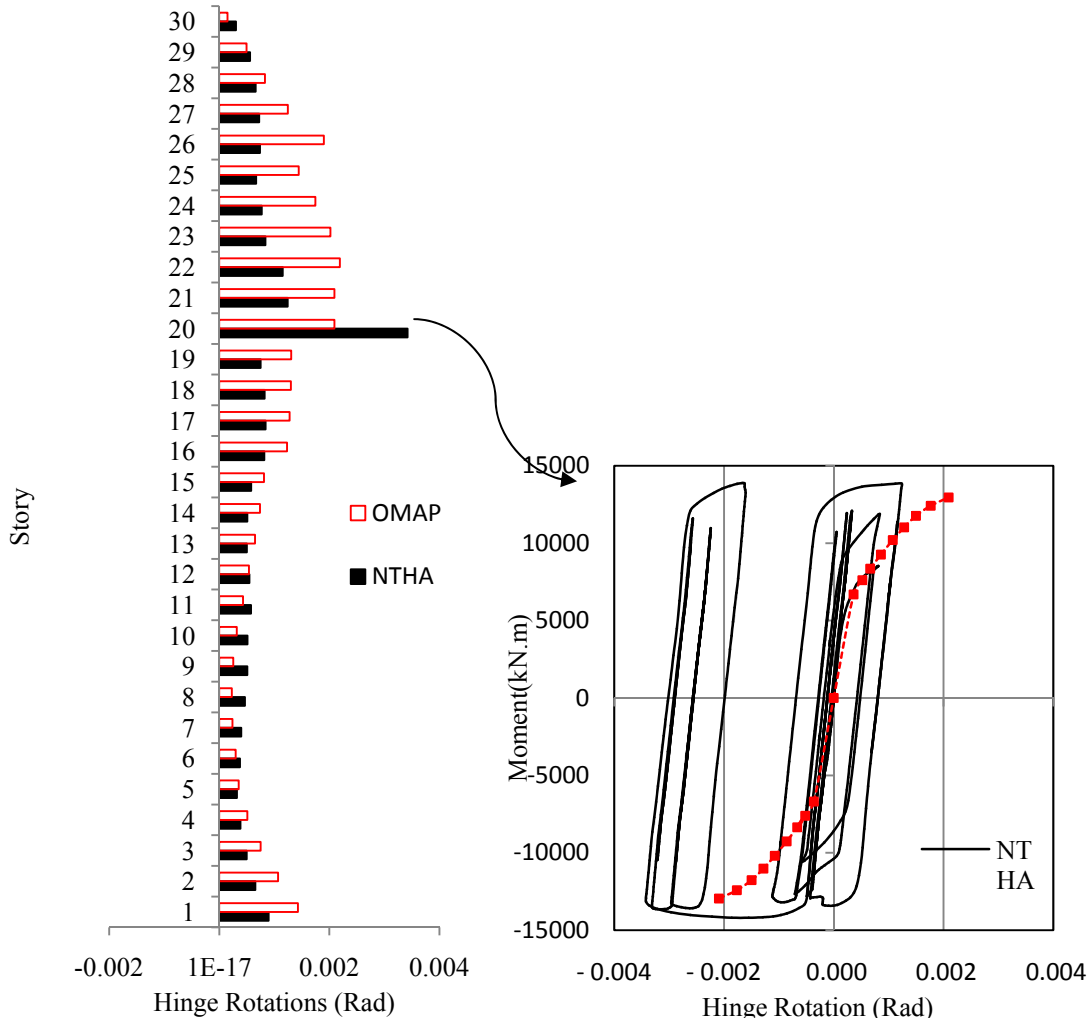

Fig. 4-22 Hinge Rotations (W30/Imp)

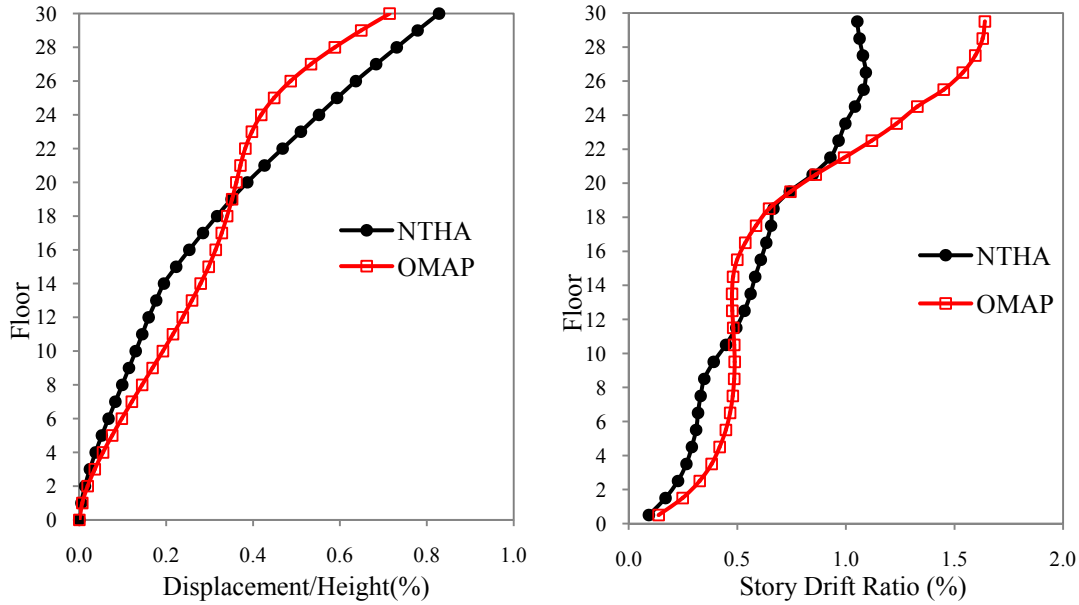

Fig. 4-23 Floor displacement and Story drift (OMAP vs NTHA) (W30/Imp)

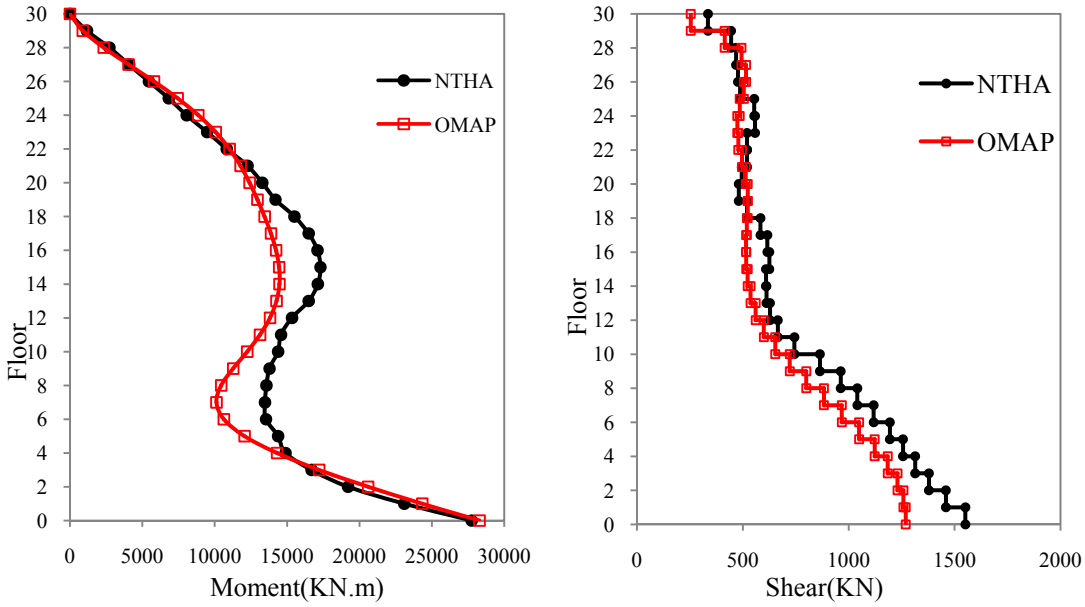

Fig. 4-24 Moment and Story shear (OMAP vs NTHA) (W30/Imp)

Example: W30/Erz

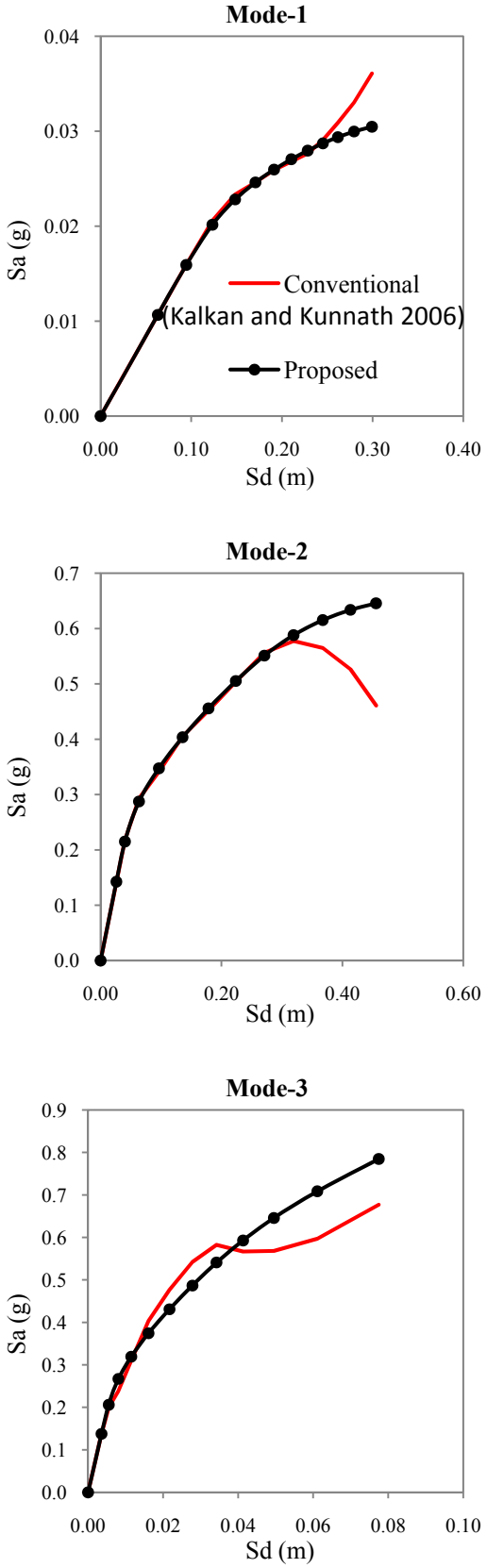

Fig. 4-25 Capacity spectrum (W30/Erz)

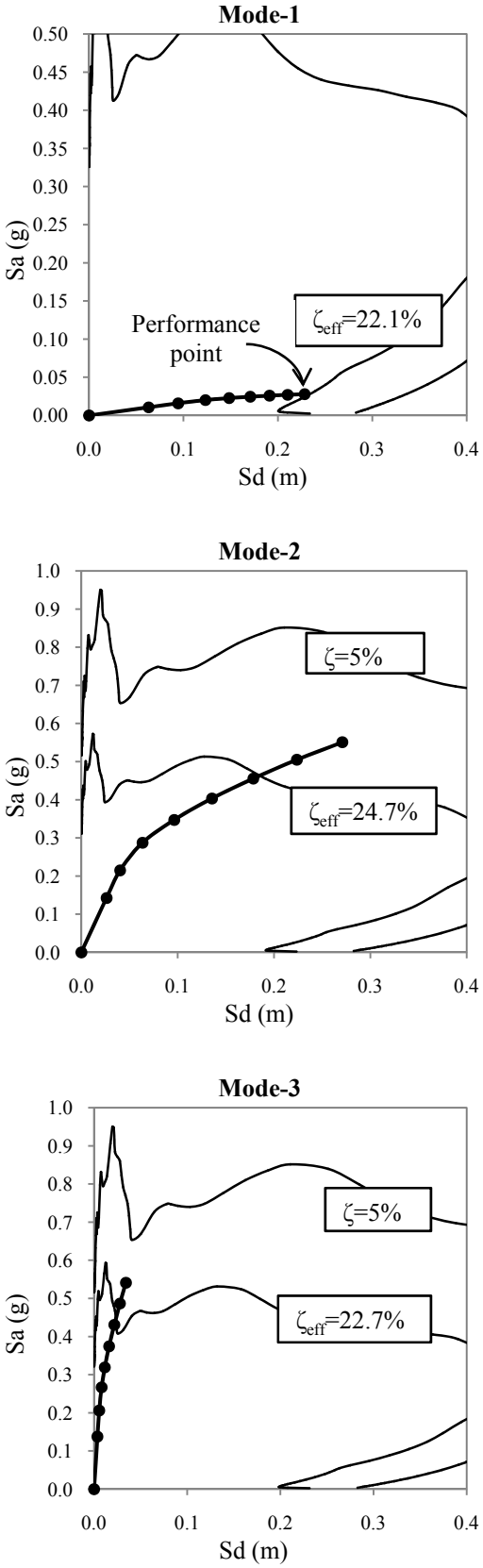

Fig. 4-26 Performance point (W30/Erz)

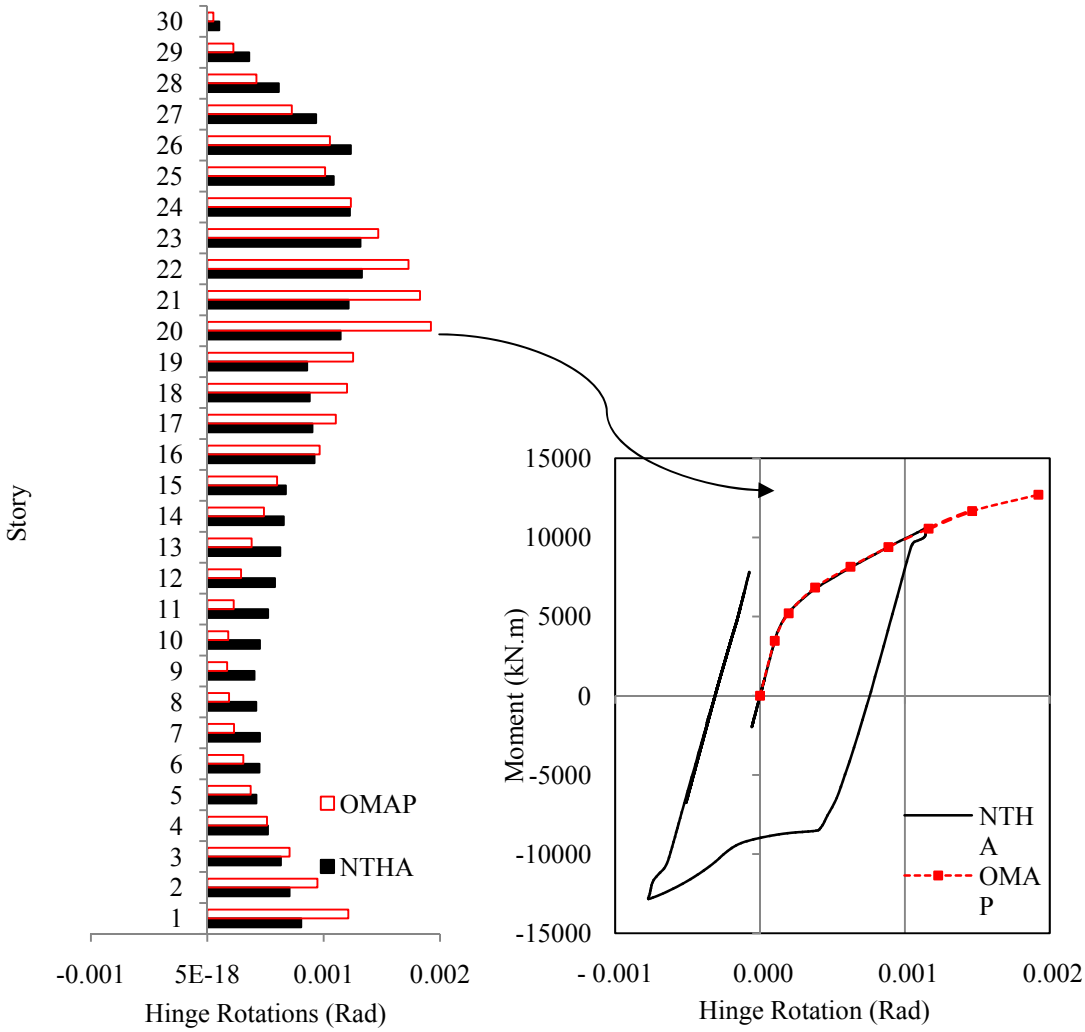

Fig. 4-27 Hinge Rotations (W30/Erz)

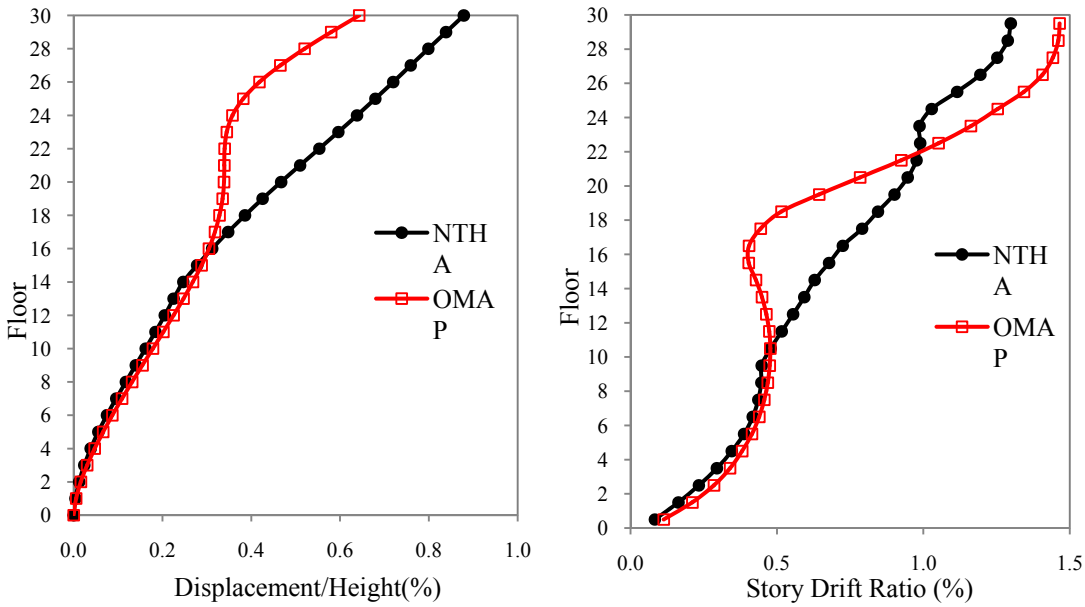

Fig. 4-28 Floor displacement and Story drift (OMAP vs NTHA) (W30/Erz)

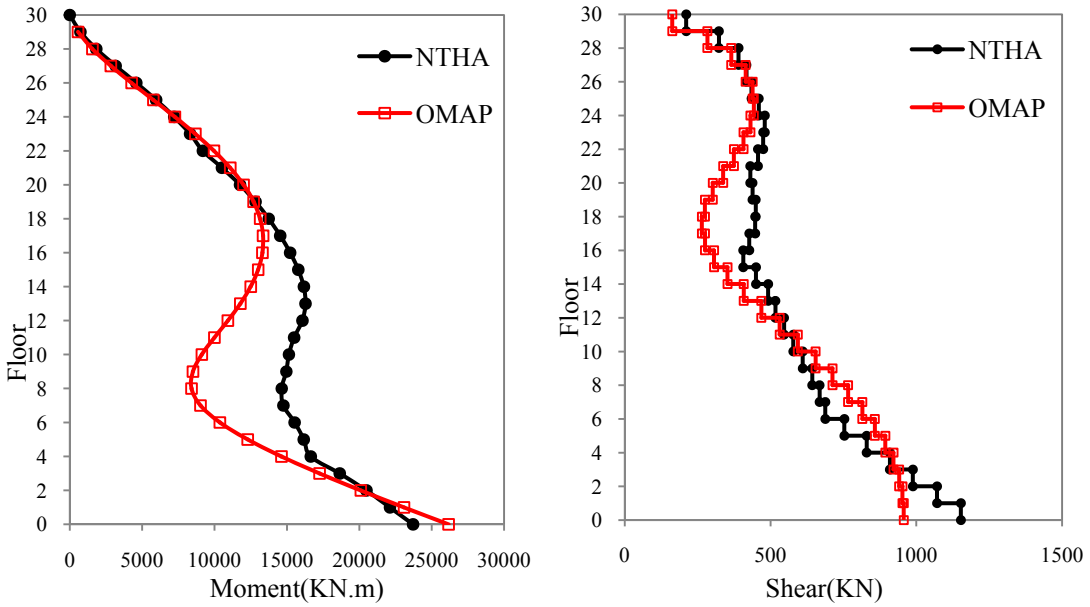

Fig. 4-29 Moment and Story shear (OMAP vs NTHA) (W30/Erz)

4.9 Conclusion

An innovative method for specifying the performance point for single-run adaptive pushover procedures is proposed. Where, the principle of the single-run adaptive pushover procedures is integrated with the capacity spectrum method proposed by ATC-40 (1996). The rigorous analytical base of the proposed method can be considered as a consequence of avoiding the pitfall inherent to single-run adaptive pushover procedures available in the literature. Where, although a single-run adaptive pushover analysis is performed, the modal quantities are picked out at each increment. As a result, using an equivalent single degree of freedom system for estimating the peak response quantities becomes available.

At the same time, the proposed method developed a new technique to convert the capacity curve to a capacity spectrum. By adopting this technique, the capacity displacement can be calculated either by the conventional formulation (ATC, 1996) or by the energy-based formulation (Hernandez-Montes et al, 2003). On the other side, the proposed technique calculates the capacity acceleration by using an incremental formulation. This technique does not only have conceptual superiority over the conventional and energy-based formulation but it also has easier numerical implementation.

The results of the proposed method have been compared to the non linear time history analysis. They indicate that this method could predict the results of the nonlinear time history analysis appropriately, where the main advantage of proposed method consists in its easy implementation maintaining the possibility of using an equivalent single degree of freedom system for estimating the performance point.

Another work will discuss the possibility of integrating single-run adaptive pushover procedures with other methods as the displacement coefficient method (e.g., FEMA-273; ASCE-41) and the N2 method which was developed by Fajfar (1999,2000) and it has been implemented in Eurocode 8 (2004).

4.10 References

Antoniou, S., Pinho, R. (2004a). Advantages and limitations of adaptive and non adaptive force-based pushover Procedures. Journal of Earthquake Engineering, Vol. 8, No 4, pp. 497-522.

Antoniou, S., Pinho, R. (2004b). Development and verification of a displacement-based adaptive pushover Procedure. Journal of Earthquake Engineering, Vol. 8, No. 5, pp. 643-661.

ASCE/SEI Standard 41-06. Seismic Rehabilitation of Existing Buildings. prepublication edition. Structural Engineering Institute, American Society of Civil Engineers; 2006.

ATC. Seismic evaluation and retrofit of concrete buildings. Report ATC-40. Redwood City (CA): Applied Technology Council; 1996.

Aydinoğlu, M. N. (2003). An incremental response spectrum analysis procedure based on inelastic spectral displacements for multi-mode seismic performance evaluation. Bull Earthquake Eng, 1:3_36.

Aydinoğlu, M. N. (2004). An improved pushover procedure for engineering practice: Incremental response spectrum analysis procedure (IRSA). In: International workshop on performance-based seismic design: concept and implementation. Bled, Slovenia. PEER Report 2004/05, pp. 345-356.

Aydinoğlu, M. N. (2007). A response spectrum-based nonlinear assessment tool for practice: incremental response spectrum analysis (IRSA). ISET Journal of Earthquake Technology, Paper No. 481, Vol. 44, No. 1, pp. 169–192.

Baros DK, Anagnastopoulos SA (2008) An assessment of static nonlinear pushover analyses in 2-D and 3-D applications, In: Bento R, Pinho R (eds) 3D Pushover 2008—proceedings of nonlinear static methods for design/assessment of 3D structures. IST Press, Lisbon, pp 45–58

Building Seismic Safety Council (BSSC), NEHRP guidelines for the seismic rehabilitation of buildings, FEMA-273, developed by ATC for FEMA, Washington, D.C., 1997.

Building Seismic Safety Council (BSSC). Pre-standard and commentary for the seismic rehabilitation of buildings. FEMA-356, Washington (DC): Federal Emergency Management Agency ; 2000.

Casarotti, C., Pinho, R. (2007). An adaptive capacity spectrum method for assessment of bridges subjected to earthquake action. Bull Earthquake Eng, 5, pp. 377–390.

CEN. Eurocode 8: design of structures for earthquake resistance. Part 1: general rules seismic actions and rules for buildings. EN 1998-1, CEN, Brussels, December 2004.

Charney, F. A. (2008). Unintended consequences of modelling damping in structures. J Struct Eng ASCE, 134(4), pp. 581–592.

Caughey, T. K. (1960). Classical normal modes in damped linear systems. J. Appl. Mech., 27, 269–271.

Chopra A.K. (2007). Dynamics of Structures, third edition, Prentice Hall, New Jersey.

Chopra A.K., Goel R.K. (2001). A modal pushover analysis procedure to estimate seismic demands for buildings: Theory and Preliminary Evaluation. PEER Report 2001/03, Pacific Earthquake Engineering Center, University of California Berkeley.

Chopra, A. K., and Goel, R. K. (2002). A modal pushover analysis procedure for estimating seismic demands for buildings. Earthquake Eng. Struct. Dyn., 31(3), pp. 561-582.

Computers, Structures Incorporated (CSI). SAP 2000 NL. USA, CA: Berkeley; 2007.

Elnashai, A. S. (2001). Advanced inelastic static (pushover) analysis for earthquake applications. Structural Engineering and Mechanics 12(1), pp. 51-69.

Fajfar P. Capacity spectrum method based on inelastic demand spectra. Earthquake Engineering and Structural Dynamics 1999; 28(3):979–993.

Fajfar P. A nonlinear analysis method for performance-based seismic design. Earthquake Spectra 2000; 16(3): 573–592.

Freeman S. A., Nicoletti J.P. and Tyrell J.V. (1975). Evaluations of existing buildings for seismic risk} A case study of Puget Sound Naval Shipyard, Bremerton, Washington', Proc. 1st ;.S. National Conf. Earthquake Engng., EERI, Berkeley, pp. 113-122.

Freeman S.A. Development and use of capacity spectrum method. In: Proceedings of the 6 US national conference on earthquake engineering, 1998.

Goel R, Chopra AK. Role of higher-'mode' pushover analyses in seismic analysis of buildings. Earthquake Spectra 2005: 21(4):1027–1041.

Gupta, B., and Kunnath, S. K. (2000). Adaptive spectra-based pushover procedure for seismic evaluation of structures. Earthquake Spectra, 16(2), pp. 367-391.

Hernandez-Montes, E., Kwon, O. S., and Aschheim, M. A. (2004). "An energy based formulation for first and multiple-mode nonlinear static (Pushover) analyses." *J. Earthquake Eng.*, 8(1), 69–88.

Johnson, C.D. and Kienholz, D.A. (1982), "Finite Element Prediction of Damping in Structures with Constrained Viscoelastic Layers", AIAA Journal, 20(9), pp.1284-1290.

Kalkan, E. and Kunnath, SK. (2006). Adaptive modal combination procedure for nonlinear static analysis of building structures. J Struct Eng ASCE, 132(11), pp. 1721-1731.

Newmark, N.M. and Hall, W.J. (1982). Earthquake Spectra and Design, monograph. Earthquake Engineering Research Institute (EERI), Berkeley, California. Print.

Shakeri, K., Shayanfar, MA. and Kabeyasawa, T. (2010). A storey shear-based adaptive pushover for estimating seismic demands of buildings. Eng Struct,32, pp. 174–83.

Smyrou, E., Priestley, M.J.N. and Carr, A.J. (2011). Modelling of Elastic Damping in Nonlinear Time-history Analyses of Cantilever RC Walls. Bulletin of Earthquake Engineering,9,pp. 1559-1578 (DOI: 10.1007/s10518-011-9286-y)

Uang, C.-M. and Bertero, V. V. (1988) Use of Energy as a Design Criterion in Earthquuake-Resistant Design, Report No. UCB/EERC-88/18, Earthquake Engineering Research Centre, University of California, Berkeley, November.

Warburton, G. B., and Soni, S. R. _1977_. "Errors in response calculations for non-classically damped structures." Earthquake Eng. Struct. Dyn., 5, 365–376.

Chapter 5: General conclusion and perspectives

In this work, the seismic performance of the reinforced concrete high rise buildings has been investigated. Three steps toward this objective have been achieved. These steps are organized in three parts:

The first part (second chapter) included a linear analysis of the behavior of curtailed wall-frame structures. The continuum model proposed by Nollet and Stafford Smith (1993) to determine the optimum level of wall curtailment has been revisited. Results show that the continuum model is a simple and efficient tool but should be used carefully. It is highly sensitive to the calculation precision because the use of hyperbolic functions that need high calculation precision for high values of the variables. Using high calculation precision modified the values given by Nollet and Stafford Smith (1993). An important result is obtained "The optimum level of curtailment lies always between the point of inflection and the zero wall shear in the corresponding full-height wall structure". This result is very useful when searching for the optimum level of curtailment. The effect of curtailment height on the resulting internal forces is also discussed. It is shown that "The optimum level of curtailment which results in the minimum top deflection of the structure eliminates at the same time the negative moments and negative shear forces in the wall". It corresponds to a zero shear force at the top of the wall which presents a simpler alternative to determine the optimum level of curtailment.

In the second part, an overview of the main adaptive pushover procedures is presented. After an in-depth description of the principle of single run adaptive pushover procedures, it is found that there is a relationship between the base selected for performing a single run adaptive pushover analysis and the type of structure. A new single-run adaptive pushover method "OMAP" is proposed to estimate the seismic response of shear wall structure. The load pattern is derived on the base of the overturning moment as recognition of the evidence that plasticity in the shear wall is mainly governed by this parameter. This method maintains the superiority of not decomposing the structure. At the same time, it avoids the pitfall which occurred in all

previous single-run adaptive pushover analyses that use the modal combination for the applied loads instead of combining the response quantities induced by those loads in individual modes. The OMAP takes into account the progressive changes in the dynamic properties of the structure. In order to illustrate its potential advantages, the results of the OMAP procedure have been compared to force-based and displacement-based procedures in addition to rigorous non linear time history analysis. The effect of both the base and the adaptation in the single-run adaptive pushover analysis are investigated. Results indicate that this method could predict the results of the nonlinear time history analysis appropriately, where the main advantage consists in its easy implementation maintaining the principle of the adaptive response spectrum analysis. The comparison between the non-adaptive form and the adaptive form of the proposed method emphasizes the importance of the adaptive feature to incorporate the progressive variation in dynamic and modal properties.

The third part is concerned with the performance point (target displacement) which is another major aspect of the pushover analysis. It presents an innovative method for specifying the performance point using single-run adaptive pushover procedures. Where, although a single-run adaptive pushover analysis is performed, the modal quantities are picked out at each increment. As a result, using an equivalent single degree of freedom system for estimating the peak response quantities becomes available. At the same time, the proposed method developed a new technique to convert the capacity curve to a capacity spectrum. By adopting this technique, the capacity displacement can be calculated either by the conventional formulation (ATC, 1996) or by the energy-based formulation (Hernandez-Montes et al, 2003). On the other side, the proposed technique calculates the capacity acceleration using an incremental formulation. This technique does not only have conceptual superiority over the conventional and energy-based formulation but it also has easier numerical implementation. The results of the proposed method have been compared to the non linear time history analysis. The prediction of the deformed shapes as well as shear/moment distributions, proved to be very effective.

The present work provides an interesting nonlinear static method to predict the nonlinear seismic response of shear wall structures. It opens up new lines to work on:

- Adaptation of the method to frame structures and then to wall-frame structures.
- Introducing the effect of the soil structure interaction and the p-delta effect in the proposed method.
- Performing the single-run adaptive pushover analysis for shear wall structures based on inelastic spectrum method.